

12:5

THE SPHERICAL HARMONICS METHOD  
FOR CRITICAL SPHERES

by

655  
JAMES DONALD CALLEN

B. S., Kansas State University, 1962

---

A MASTER'S THESIS

submitted in partial fulfillment of the

requirements for the degree

MASTER OF SCIENCE

Department of Nuclear Engineering

KANSAS STATE UNIVERSITY  
Manhattan, Kansas

1964

Approved by:

*John O. Mingle*  
\_\_\_\_\_  
Major Professor

LD  
2668  
T4  
1964  
C15  
C.2  
Document

CONTENTS

1.0	INTRODUCTION.....	1
2.0	THEORY OF NEUTRON TRANSPORT.....	3
2.1	The Spherical Harmonics Approximations.....	3
2.2	The Spherical Geometry Solution.....	9
2.3	The General Theory of Boundary Conditions.....	13
2.4	Formulation of Boundary Conditions.....	21
3.0	DISCUSSION AND RESULTS.....	28
3.1	General Discussion.....	28
3.2	Results of Numerical Calculations for Bare Spherical Reactors.....	32
3.3	Results of Numerical Calculations for Reflected Spherical Reactors.....	50
3.4	Conclusions.....	60
4.0	SUGGESTIONS FOR FURTHER STUDY.....	62
	ACKNOWLEDGMENT.....	64
	LITERATURE CITED.....	65
	APPENDICES.....	67
	APPENDIX A: The $Q_{\frac{1}{2}}(x)$ and $C_{\frac{1}{2}}(x)$ Functions.....	68
	APPENDIX B: Variational Boundary Conditions.....	71
	APPENDIX C: Description and Explanation of Computer Programs.....	79

## LIST OF TABLES

I.	Weighting factors for Eq. (64).....	30
II.	Calculated results for a bare spherical reactor in which $c$ is 1.05. The exact critical radius is 7.2772 mean free paths.....	33
III.	Calculated results for a bare spherical reactor in which $c$ is 1.02. The exact critical radius is 12.0270 mean free paths.....	44
IV.	Calculated results for a bare spherical reactor in which $c$ is 1.40. The exact critical radius is 1.9854 mean free paths.....	46
V.	Reflected reactor cases to be considered.....	50
VI.	Calculated results for case 1 (reflected reactor) in which $c$ is 1.05.....	52
VII.	Calculated results for case 2 (reflected reactor) in which $c$ is 1.05.....	52
VIII.	Calculated results for case 3 (reflected reactor) in which $c$ is 1.05.....	53
IX.	Calculated results for case 4 (reflected reactor) in which $c$ is 1.05.....	53
X.	Calculated results for case 5 (reflected reactor) in which $c$ is 1.05.....	55
XI.	Calculated results for case 6 (reflected reactor) in which $c$ is 1.05.....	55
XII.	Calculated results for case 5 (reflected reactor) in which $c$ is 1.02.....	56
XIII.	Calculated results for case 5 (reflected reactor) in which $c$ is 1.40.....	56
B-I.	Constants for variational boundary conditions (right hand boundary).....	76
C-1.	Input data.....	80
C-II.	Sample page of output.....	81
C-III.	Sense switches.....	82
C-IV.	Control cards used by PLOT.....	93

## LIST OF FIGURES

1. Geometrical interpretation of the variable $s$ .....	5
2. The spatial dependence of the total neutron flux for a two region problem with an interfacial boundary at $R$ .....	16
3. Convergence graph for a bare spherical reactor in which $c$ is 1.05 using Marshak's boundary conditions.....	36
4. Convergence graph for a bare spherical reactor in which $c$ is 1.05 using Mark's boundary conditions.....	38
5. Convergence graph for a bare spherical reactor in which $c$ is 1.05 using the infinite black reflector boundary conditions.....	40
6. Convergence graph for a bare spherical reactor in which $c$ is 1.05 using the variational boundary conditions.....	41
7. Angular flux at the vacuum interface as a function of $\cos\theta$ from a $P_3$ approximation.....	43
8. Angular flux at the core-reflector interface as a function of $\cos\theta$ for a $P_4$ approximation.....	58

## NOMENCLATURE

$A_0$	Constant associated with zero root
$A_0^*$	Modified constant associated with zero root
$A_k$	Constants in the core region determined from boundary conditions
$\bar{A}_k$	Constants in the reflector region determined from boundary conditions
$b_{i,j}$	Elements of boundary condition matrix
$c$	Mean number of secondaries per interaction in the core region
$\bar{c}$	Mean number of secondaries per interaction in the reflector region
$D$	Diffusion theory diffusion coefficient
$E$	Energy
$dE$	Differential energy element
$f(\underline{r}, E, \underline{\Omega}, t), f(r, \mu)$	Angular flux
$f_l(r)$	Spherical harmonics component of the angular flux
$G_l(\lambda_k)$	Elements of solution vectors
$i, j, k, l, m, n$	Summation indices
$L$	Order of spherical harmonics approximation
$P_l(\mu)$	Legendre polynomial
$r$	Radial distance from the origin
$\underline{r}$	Field position vector
$d\underline{r}$	Differential volume element
$R$	Critical radius, interface between two media
$R_0$	Reflector thickness
$R_L$	Critical radius determined using an $L^{\text{th}}$ order approximation
$s$	Distance laid off along $\underline{\Omega}$

$S(\underline{r}, E, \underline{\Omega}, t), S(\underline{r})$	Neutron source
T	Matrix containing coefficients of $A_k$ and $\bar{A}_k$ as required by the boundary conditions
$t_{jk}$	Elements of T
v	Neutron speed
$w_L$	Weighting factor to be applied to $L^{\text{th}}$ order approximation result
$W_{\ell}(x)$	Non-singular part of the Legendre polynomials of the second kind
X	Column matrix containing $A_k$ and $\bar{A}_k$
$x_k$	Elements of X
$\delta_{\ell m}$	Kronecker delta, $\delta_{\ell m} = \begin{cases} 1, & \ell = m \\ 0, & \ell \neq m \end{cases}$
$\Delta(r)$	Unit pulse function, $\Delta(r) = \begin{cases} 1, & r = 0 \\ 0, & r \neq 0 \end{cases}$
$\theta$	Angle between $\underline{\Omega}$ and the extension of r
$\kappa^{-1}$	Diffusion length
$\lambda_0$	Zero root relaxation constant
$\lambda_k$	Relaxation constant root in the core region
$\bar{\lambda}_k$	Relaxation constant root in the reflector region
$\mu$	$\cos \theta$
v	Mean number of secondary neutrons resulting from a fission type interaction
$\Sigma$	Total macroscopic cross section in the core region
$\bar{\Sigma}$	Total macroscopic cross section in the reflector region
$\Sigma_a$	Macroscopic absorption cross section in the core region
$\bar{\Sigma}_a$	Macroscopic absorption cross section in the reflector region
$\Sigma_f$	Macroscopic fission cross section
$\Sigma_s$	Macroscopic scattering cross section

$\phi$	Azimuthal angle which $\underline{\Omega}$ makes with the extension of $r$
$\phi(\underline{r}), \phi(r)$	Total neutron flux
$\underline{\Omega}$	Unit vector in the direction of neutron motion
$d\underline{\Omega}$	Differential solid angle

## 1.0 INTRODUCTION

In the design of a nuclear reactor the critical size of the reactor is a very important quantity. A convenient method of analytically solving the monoenergetic Boltzmann neutron transport equation for the critical size is the spherical harmonics method. Because the even order approximations are difficult to formulate, most of the usage of the spherical harmonics method has been restricted to the odd order approximations.

Rumyantsev (18) was one of the first to suggest that the use of the even order approximations could result in improvements in accuracy over the odd order approximations. Mingle (13,14) has found that for the disadvantage factor problem the even and odd order approximations counterconverge to the correct result, i.e., both the even and odd order approximations converge to the exact answer with one set of approximations yielding an upper bound while the other set provides a lower bound. Dawson (4) has modified the  $P_2$  solutions to the Boltzmann neutron transport equation to obtain solutions which lie somewhere between the  $P_1$  and  $P_2$  solutions. Using this procedure it is found that the resulting total neutron flux as a function of the spatial variable was a better approximation to the exact distribution than either the  $P_1$  or  $P_2$  approximation yielded. In addition Marchuk et. al. (9) have used a  $P_2$  approximation to work out a series of simple problems. In most of these problems the  $P_2$  approximation was found to represent the system in question more accurately than the corresponding  $P_1$  approximation. Davison (2) has derived the first order error in the critical size in an  $L^{\text{th}}$  order approximation for a series of homogeneous slabs, which mathematically predicts that the critical thickness determined from the even and odd order approximations will counterconverge to the exact result. There is thus considerable evidence that the



even order approximations will be of value in predicting the critical size of a reactor.

In order to solve the Boltzmann neutron transport equation for a critical size, boundary conditions must be applied at the outer boundary of the core region. When a reactor is assumed to be surrounded by a vacuum which is infinite in extent, these conditions are termed the vacuum-interface boundary conditions. The usual vacuum-interface boundary conditions which are applied are Mark's, Marshak's, and replacement of the vacuum with a black medium which is infinite in extent. Pomraning (15,17) has suggested a new set of boundary conditions developed from a variational approach to the Boltzmann neutron transport equation. These new boundary conditions have been found to predict the extrapolation distance in the standard Milne problem more accurately than any of the boundary conditions currently used (15). There appears to be considerable promise in the use of these boundary conditions to find the critical size of a reactor.

The theory, including all four sets of vacuum-interface boundary conditions and computer programs, and the nature of the convergence of the even and odd order spherical harmonics approximations to the exact critical size for various boundary conditions applied to a spherical reactor is the subject matter of this presentation. In particular considerable care is taken in developing a consistent formulation for the theory of the even order approximations.

## 2.0 THEORY OF NEUTRON TRANSPORT

## 2.1 The Spherical Harmonics Approximations

An extensive development of the Boltzmann neutron transport equation can be found in many references (3,12,21). In this work it will be sufficient to state that the general Boltzmann integro-differential equation for neutron transport can be written as<sup>1</sup>

$$\frac{1}{v} \frac{\partial f(\underline{r}, E, \underline{\Omega}, t)}{\partial t} = -\underline{\Omega} \cdot \nabla f(\underline{r}, E, \underline{\Omega}, t) - \{ \Sigma_a(\underline{r}, E, \underline{\Omega}) + \Sigma_s(\underline{r}, E, \underline{\Omega}) \} f(\underline{r}, E, \underline{\Omega}, t) + S(\underline{r}, E, \underline{\Omega}, t) + \int dE' \int d\underline{\Omega}' f(\underline{r}, E', \underline{\Omega}', t) \Sigma_s(\underline{r}, E' \rightarrow E, \underline{\Omega}' \rightarrow \underline{\Omega}) \quad (1)$$

where:  $f(\underline{r}, E, \underline{\Omega}, t) d\underline{r} dE d\underline{\Omega}$  is the number of neutrons in the differential volume element  $d\underline{r}$  about  $\underline{r}$  having energies between  $E$  and  $E + dE$  whose directions lie in the solid angle of phase space  $d\underline{\Omega}$  about  $\underline{\Omega}$ , multiplied by the neutron speed  $v$  ( $v = \sqrt{2E/m}$ );

$\Sigma_s(\underline{r}, E' \rightarrow E, \underline{\Omega}' \rightarrow \underline{\Omega}) dE d\underline{\Omega}$  is the macroscopic cross section for changing the neutron energy from  $E'$  to  $dE$  about  $E$  and the direction of motion from  $\underline{\Omega}'$  to  $d\underline{\Omega}$  about  $\underline{\Omega}$ , due to neutron scattering interactions with stationary nuclei;

$\Sigma_s(\underline{r}, E, \underline{\Omega}) = \int dE' \int d\underline{\Omega}' \Sigma_s(\underline{r}, E' \rightarrow E, \underline{\Omega}' \rightarrow \underline{\Omega})$  is the macroscopic scattering cross section for any type of scattering interaction which causes a neutron to be displaced from its energy,  $E$ , and direction  $\underline{\Omega}$  at  $\underline{r}$ ; and

$\Sigma_a(\underline{r}, E, \underline{\Omega})$  is the macroscopic absorption cross section for all types of neutron interactions with stationary nuclei which do not result in a scattered neutron.

1 The coordinate system, spherical harmonics and much of the nomenclature used in this work are the same as those of Weinberg and Wigner (21).

The term on the left side of Eq. (1) is the time rate of change of the neutron density. The loss of neutrons from the system is represented by the first and second terms on the right side of Eq. (1). The first term represents the leakage from the incremental volume element  $d\underline{r}$  due to uniform straightforward motion of the neutrons whereas the second term accounts for losses of neutrons from  $dE$  about  $E$  and  $d\underline{\Omega}$  about  $\underline{\Omega}$  in energy and phase space due to all types of neutron-nuclei interactions within the incremental volume element  $d\underline{r}$ . The gain of neutrons in the system is represented by the third and fourth terms on the right side of Eq. (1). The third term accounts for all internal and external neutron sources and the fourth term accounts for the gain of neutrons resulting from the scattering of neutrons into  $dE$  about  $E$  and  $d\underline{\Omega}$  about  $\underline{\Omega}$  from any other point in energy and phase space, within the incremental volume element  $d\underline{r}$ .

At this point the assumption of the existence of only one monoenergetic thermal neutron group is considered. Davison (3) and others (5,12,21) have shown that this assumption is valid only for slightly absorbing media in regions far removed from sources and boundaries. However, even when these restrictions do not apply this assumption has yielded results which agree remarkably well with experimental results (21). Thus for simplicity and without a great sacrifice in accuracy the energy-independent single thermal neutron group is used throughout the remainder of this work.

Using the restrictions that the individual media under consideration are homogeneous and isotropic and that the system is monoenergetic and independent of time, the Boltzmann equation reduces to

$$-\underline{\Omega} \cdot \nabla \underline{f}(\underline{r}, \underline{\Omega}) - (\Sigma_a + \Sigma_s) \underline{f}(\underline{r}, \underline{\Omega}) + S(\underline{r}, \underline{\Omega}) + \int d\underline{\Omega}' \underline{f}(\underline{r}, \underline{\Omega}') \Sigma_s(\underline{\Omega}' + \underline{\Omega}) = 0. \quad (2)$$

Next, defining  $\Sigma = \Sigma_a + \Sigma_s$ , assuming isotropic scattering so that

$$\Sigma_s(\underline{\Omega}' + \underline{\Omega}) = \Sigma_s/4\pi, \text{ and an isotropic source which implies that } S(\underline{r}, \underline{\Omega}) = S(\underline{r})/4\pi,$$

Eq. (2) becomes

$$-\underline{\Omega} \cdot \underline{\nabla} f(\underline{r}, \underline{\Omega}) - \Sigma f(\underline{r}, \underline{\Omega}) + \frac{S(\underline{r})}{4\pi} + \frac{\Sigma}{4\pi} \int d\underline{\Omega}' f(\underline{r}, \underline{\Omega}') = 0 . \quad (3)$$

In this treatment only spherical geometry is considered and the coordinate system used is the same as that of Weinberg and Wigner (21). In a system of spherical symmetry the angular flux distribution depends only on two variables:  $r$ , the distance from the origin, and  $\mu$  the cosine of the angle  $\theta$  between the direction of motion  $\underline{\Omega}$  and the extension of the radius  $r$ . Defining a new variable  $s$  which is a distance laid off along  $\underline{\Omega}$ , the directional derivative in Eq. (3) becomes

$$\underline{\Omega} \cdot \underline{\nabla} f(\underline{r}, \underline{\Omega}) = \frac{\partial f(\underline{r}, \underline{\Omega})}{\partial s} = \frac{\partial f}{\partial r} \frac{dr}{ds} + \frac{\partial f}{\partial \mu} \frac{d\mu}{ds} . \quad (4)$$

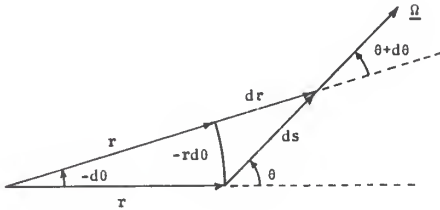


Figure 1. Geometrical interpretation of the variable  $s$ .

Then, as can be seen from Fig. 1,

$$\frac{ds}{dr} = \frac{1}{\cos \theta} = \frac{1}{\mu} ,$$

$$\frac{ds}{d\theta} = \frac{r}{\sin \theta} = - \frac{r}{\sqrt{1-\mu^2}} .$$

With  $\mu = \cos\theta$ ,

$$d\mu = -\sin\theta d\theta = -\sqrt{1-\mu^2} d\theta$$

so that

$$\frac{ds}{d\mu} = \frac{ds}{d\theta} \frac{d\theta}{d\mu} = \frac{r}{1-\mu^2},$$

and the directional derivative in Eq. (4) becomes

$$\underline{\Omega} \cdot \underline{\nabla} f(\underline{r}, \underline{\Omega}) = \mu \frac{\partial f(\underline{r}, \underline{\Omega})}{\partial r} + \frac{(1-\mu^2)}{r} \frac{\partial f(\underline{r}, \underline{\Omega})}{\partial \mu}. \quad (5)$$

Next it is assumed that the only source is an internal fission source<sup>2</sup> that is also isotropic so that

$$S(\underline{r}, \underline{\Omega}) = \frac{S(\underline{r})}{4\pi} = \frac{v\Sigma_f \phi(\underline{r})}{4\pi} = \frac{v\Sigma_f \int d\underline{\Omega}' f(\underline{r}, \underline{\Omega}')}{4\pi} \quad (6)$$

where  $\phi(\underline{r}) = \int d\underline{\Omega}' f(\underline{r}, \underline{\Omega}')$  is the total neutron flux at  $\underline{r}$ . Using the relationships given in Eqs. (5) and (6), Eq. (3) becomes

$$-\mu \frac{\partial f(\underline{r}, \underline{\Omega})}{\partial r} - \frac{(1-\mu^2)}{r} \frac{\partial f(\underline{r}, \underline{\Omega})}{\partial \mu} - \Sigma f(\underline{r}, \underline{\Omega}) + \frac{v\Sigma_f + \Sigma_s}{4\pi} \int d\underline{\Omega}' f(\underline{r}, \underline{\Omega}') = 0. \quad (7)$$

Now,  $d\underline{\Omega}$  is actually  $d(\cos\theta)d\phi = d\mu d\phi$  so that by integrating Eq. (7) over  $\phi$  in the interval  $0 \leq \phi \leq 2\pi$  and defining

$$f(r, \mu) = \int_0^{2\pi} d\phi f(\underline{r}, \underline{\Omega}), \quad (8)$$

and the mean number of secondaries per interaction,  $c$ , as

$$c = \frac{v\Sigma_f + \Sigma_s}{\Sigma},$$

2 In this development the fission neutrons are assumed to be born at thermal energies. In order to obtain better results with the monoenergetic assumption the  $v\Sigma_f$  term should be replaced throughout the development by a corresponding term representing the number of neutrons born in a single fission which eventually reach thermal energies. This term should take into account resonance capture, additional fast fissions and fast leakage. This change will alter the value of  $c$  but will not change any other quantities.

Eq. (7) becomes

$$\nu \frac{\partial f(r, \nu)}{\partial r} + \frac{(1-\nu^2)}{r} \frac{\partial f(r, \nu)}{\partial \nu} + \Sigma f(r, \nu) - \frac{c\Sigma}{2} \int_{-1}^{+1} d\nu' f(r, \nu') = 0. \quad (9)$$

In order to solve this integro-differential equation the angular flux is expanded into an infinite series of Legendre polynomials, i.e.

$$f(r, \nu) = \sum_{\ell} f_{\ell}(r) P_{\ell}(\nu). \quad (10)$$

Substituting this expansion into Eq. (9), multiplying the resulting equation by  $P_m(\nu)$ , integrating over the interval of orthogonality  $-1 \leq \nu \leq +1$ , using the orthogonality relationship

$$\int_{-1}^{+1} d\nu P_{\ell}(\nu) P_m(\nu) = \frac{2}{2\ell+1} \delta_{\ell m},$$

and the recursion relationships

$$(1-\nu^2) \frac{dP_{\ell}(\nu)}{d\nu} = \frac{\ell(\ell+1)}{2\ell+1} \{P_{\ell-1}(\nu) - P_{\ell+1}(\nu)\},$$

$$\nu P_{\ell}(\nu) = \frac{(\ell+1)P_{\ell+1}(\nu) + \ell P_{\ell-1}(\nu)}{2\ell+1}$$

the spherical harmonics component form of the Boltzmann transport equation in spherical geometry becomes

$$\frac{\ell+1}{2\ell+3} \left( \frac{\ell+2}{r} + \frac{d}{dr} \right) f_{\ell+1}(r) + \frac{\ell}{2\ell-1} \left( -\frac{\ell-1}{r} + \frac{d}{dr} \right) f_{\ell-1}(r) + (1-c\delta_{\ell 0})\Sigma f_{\ell}(r) = 0. \quad (11)$$

Equation (11) is an infinite system of differential equations in an infinite number of unknowns. Although the exact solution of this system is impossible, an approximate solution can be found by assuming that

$\left( \frac{\ell+2}{r} + \frac{d}{dr} \right) f_{\ell+1}(r)$  is negligibly small and ignoring all higher order terms.

The resulting approximation will be called the  $P_L$  approximation and will be termed an even or odd order approximation according to the parity of  $L$ .

Increasingly higher orders of approximations should give more accurate descriptions of the angular and total neutron fluxes.

## 2.2 The Spherical Geometry Solution

In order to solve Eq. (11) Weinberg and Wigner (21) propose a solution of the form

$$f_{\ell}(r) = (2\ell+1) \sum_k A_k G_{\ell}(\lambda_k) Q_{\ell}(\Sigma r/\lambda_k) . \quad (12)$$

The  $Q_{\ell}(\Sigma r/\lambda_k)$ 's in Eq. (12) are  $2/\pi$  times the modified spherical Bessel functions of the third kind and are considered in detail in Appendix A. The  $Q_{\ell}(x)$ 's will be termed geometrical functions. Now, substituting the proposed solution, Eq. (12), into Eq. (11) and using the recursion relationships

$$Q_{\ell}(x) = Q_{\ell-2}(x) - \frac{2\ell-1}{x} Q_{\ell-1}(x) ,$$

$$\left(\frac{d}{dx} + \frac{\ell+1}{x}\right) Q_{\ell}(x) = Q_{\ell-1}(x)$$

for the  $Q_{\ell}(x)$  functions, the following set of coupled equations is obtained:

$$(\ell+1)G_{\ell+1}(\lambda_k) + \ell G_{\ell-1}(\lambda_k) - (2\ell+1)(1-c\delta_{k0})\lambda_k G_{\ell}(\lambda_k) = 0 . \quad (13)$$

The recursion relationship of Eq. (13) is similar to those for the Legendre polynomials and the nonsingular part of the Legendre polynomials of the second kind,  $W_{\ell-1}(x)$ , given by Jahnke and Emde (8) as

$$(\ell+1)P_{\ell+1}(x) + \ell P_{\ell-1}(x) - (2\ell+1)xP_{\ell}(x) = 0 ,$$

$$(\ell+1)W_{\ell}(x) + \ell W_{\ell-2}(x) - (2\ell+1)xW_{\ell-1}(x) = 0 .$$

Davison (3) shows that the  $G_{\ell}(\lambda_k)$ 's defined by the recursion relationship of Eq. (13) can be written as a certain linear combination of the Legendre polynomials and the non-singular part of the Legendre polynomials of the second kind, namely:

$$G_{\ell}(\lambda_k) = (-1)^{\ell} \{P_{\ell}(\lambda_k) - c\lambda_k W_{\ell-1}(\lambda_k)\} . \quad (14)$$

With this particular choice of the  $G_{\ell}(\lambda_k)$  functions they are normalized



properly with  $G_0(\lambda_k) = 1$ . Equation (14) defines a polynomial in  $\lambda_k$  of degree  $L$  in which only alternate powers of  $\lambda_k$  appear.

For a  $P_L$  approximation it was previously stated that the term  $(\frac{L+2}{R} + \frac{d}{dR}) f_{L+1}(r)$  should be made negligibly small. Referring to Eq. (12) it is easily seen that the condition

$$G_{L+1}(\lambda_k) = 0 \quad (15)$$

will satisfy this requirement. Equation (15) defines the roots  $\lambda_k$ .

Davison (3) considers the roots of Eq. (15) in detail. For odd order approximations it is shown that the roots always occur in pairs such that one of the pair is the negative of the other. For  $c < 1$  all of the roots are real whereas for  $c > 1$  two of the roots are imaginary and the remaining roots are real. In either case there are  $L+1$  different roots or  $(L+1)/2$  pairs of different roots in an odd order approximation. For even order approximations Davison (3) shows that there is always a zero root. In addition if  $c < \{(L+1)P_L(0)\}^2$  (which is true for most nuclear reactors) for a given even order approximation, the remaining  $L$  roots of Eq. (15) are real or imaginary in pairs just as for the preceding odd order approximation roots. There is thus a correspondence between an odd order approximation and the succeeding even order approximation.

The zero root ( $\lambda_0$ ) in the even order approximations must be considered separately. Following Davison (3)  $\lambda_0$  is assumed to be small and tend toward zero. Then assuming  $R$  is the interface between two media the constant  $A_0$  is assumed to be of the form

$$A_0 = A_0^*/Q_2(\Sigma R/\lambda_0) .$$

Using this expression and taking the limit as  $\lambda_0$  approaches zero of the term in Eq. (12) corresponding to the zero root

$$\begin{aligned} \lim_{\lambda_0 \rightarrow 0} A_0(2\ell+1)G_\ell(\lambda_0)Q_\ell(\Sigma R/\lambda_0) &= A_0^*(2\ell+1) \lim_{\lambda_0 \rightarrow 0} G_\ell(\lambda_0)Q_\ell(\Sigma r/\lambda_0)/Q_\ell(\Sigma R/\lambda_0) \\ &= \begin{cases} A_0^*(2\ell+1)(-1)^\ell P_\ell(0) & , r = R \\ 0 & , r < R \end{cases} \end{aligned}$$

which follows since with  $\lambda_0 = 0$  in Eq. (14),  $G_\ell(0) = (-1)^\ell P_\ell(0)$ . It is clear that this limiting procedure can be carried out only once within a particular region and hence the zero root term for even order approximations is non-zero at only one interface of a particular region. In this work the zero root term will be chosen so that it is nonzero at the right hand interface of a region since it is more common in spherical geometry to think in terms of concentric regions expanding outward from the origin rather than of outer regions contracting inward. Thus in the even order approximations the term due to the zero root is finite at a right hand interface and identically zero elsewhere in the medium. This term introduces a discontinuity in the even order moments at the interface between two media.

Finally the solution of Eq. (11) is, for odd order approximations

$$f_\ell(r) = (2\ell+1) \sum_{k=1}^{L+1} A_k G_\ell(\lambda_k) Q_\ell(\Sigma r/\lambda_k) , \quad (16)$$

and for even order approximations

$$f_\ell(r) = (2\ell+1) A_0^* (-1)^\ell P_\ell(0) \Delta(r-R) + (2\ell+1) \sum_{k=1}^L A_k G_\ell(\lambda_k) Q_\ell(\Sigma r/\lambda_k) \quad (17)$$

where  $\Delta(r-R)$  is a unit pulse function defined by

$$\Delta(r-R) = \begin{cases} 1, & r = R \\ 0, & r \neq R \end{cases} . \quad (18)$$

These even order approximation solutions will be valid at radii up to and including the right hand interfacial boundary since the discontinuity constant,  $A_0^*$ , which arises at the interface is contained in these solutions. The solutions in the next region will be valid at this interface and at radii up

to and including the next right hand interfacial boundary where another discontinuity will occur. Thus although the solution of Eq. (11) for even order approximations may be discontinuous it will be continuously defined and finite for all values of  $r$ .

### 2.3 The General Theory of Boundary Conditions

In terms of the Legendre polynomial expansion of  $f(r, \mu)$  the total neutron flux is given as

$$\phi(r) = \int d\Omega f(r, \mu) = \int_0^{2\pi} d\phi \int_{-1}^{+1} d\mu \sum_{\ell} f_{\ell}(r) P_{\ell}(\mu) = 4\pi f_0(r) . \quad (19)$$

From physical considerations it is known that  $\phi(0)$  must be finite. In order to achieve this condition  $f_0(0)$  must be finite. Considering Eqs. (16) and (17) it is readily seen that this can be accomplished by equating the  $A_k$ 's corresponding to pairs of roots of equal magnitude. From the recursion relationships for the  $G_{\ell}(\lambda_k)$ 's, Eq. (13), it is easily verified that

$$G_{\ell}(-\lambda_k) = (-1)^{\ell} G_{\ell}(\lambda_k) . \quad (20)$$

In order to take advantage of these conditions in a medium which is spherically symmetric about the origin a new set of functions,  $C_{\ell}(x)$ , which are the modified spherical Bessel functions of the first kind, are defined as

$$C_{\ell}(x) = \frac{1}{2} \{ Q_{\ell}(x) + (-1)^{\ell} Q_{\ell}(-x) \} . \quad (21)$$

These new functions are considered in detail in Appendix A. Using these new functions the solution to Eq. (11) in a region which is spherically symmetric about the origin is, for odd order approximations

$$f_{\ell}(r) = (2\ell+1) \sum_{k=1}^{(L+1)/2} A_k G_{\ell}(\lambda_k) C_{\ell}(\lambda_k r) , \quad (22)$$

and for even order approximations

$$f_{\ell}(r) = (2\ell+1) A_0^* (-1)^{\ell} P_{\ell}(0) \Delta(r-R) + (2\ell+1) \sum_{k=1}^{L/2} A_k G_{\ell}(\lambda_k) C_{\ell}(\lambda_k r) . \quad (23)$$

The zero root term in even order approximations does not introduce any difficulties since it is zero at  $r = 0$ . From this finiteness of the

total neutron flux at  $r = 0$  boundary condition,  $[(L+1)/2]$  constants<sup>3</sup> have been eliminated.

Next the boundary conditions which are to be applied at an interface between two media will be considered. Due to the discontinuity of the even order moments at an interfacial boundary in an even order approximation it will be necessary to consider the even and odd order boundary conditions separately. In both even and odd order approximations the general boundary condition which would seem to be the most desirable is to demand continuity of  $f(r, \mu)$  at a boundary located at  $r = R$ . Denoting a second region with a bar this condition mathematically is

$$f(R, \mu) = \bar{f}(R, \mu) ,$$

or

$$\sum_{\ell=0}^L f_{\ell}(R) P_{\ell}(\mu) = \sum_{\ell=0}^L \bar{f}_{\ell}(R) P_{\ell}(\mu) . \quad (24)$$

Multiplying Eq. (24) by  $P_m(\mu)$  and integrating over the period of orthogonality,  $-1 \leq \mu \leq +1$ , this condition reduces to

$$f_{\ell}(R) = \bar{f}_{\ell}(R) \quad \ell = 0, 1, \dots, L . \quad (25)$$

Equation (25) is the boundary condition to be applied at an interfacial boundary in odd order approximations.

Davison (3) points out that in an even order approximation only  $L$  conditions can be satisfied. This is because the constant  $A_0^*$  corresponding to the zero root cannot be determined directly since it exists only at an interfacial boundary between two media which is a point of discontinuity. If the first equation of Eq. (25) is multiplied by  $(2\ell+1)(-1)^{\ell} P_{\ell}(0)$  and subtracted from the other  $L$  equations the zero root term is eliminated and the equations

---

3 Square brackets will be used in this work to denote the bracket operator, i.e.  $[x] =$  the largest integer less than  $x$ .

$$f_{\ell}(R) - (2\ell+1)(-1)^{\ell}P_{\ell}(0)f_0(R) = \overline{f}_{\ell}(R) - (2\ell+1)(-1)^{\ell}P_{\ell}(0)\overline{f}_0(R)$$

$$\ell = 1, 2, \dots, L \quad (26)$$

constitute the L conditions needed to determine the remaining L constants.

When  $\ell$  is odd,  $P_{\ell}(0)$  is zero so Eq. (26) can be reduced to

$$f_{\ell}(R) - (2\ell+1)P_{\ell}(0)f_0(R) = \overline{f}(R) - (2\ell+1)P_{\ell}(0)\overline{f}_0(R)$$

$$\ell = 1, 2, \dots, L. \quad (27)$$

Equation (27) is the boundary condition to be applied at an interfacial boundary between two media in even order approximations. Pomraning (16) has rigorously verified the validity of the use of Eq. (27) for even order approximations using a variational method of solution of the Boltzmann neutron transport equation with the Legendre polynomial expansion of the angular flux as a trial function. The use of either Eq. (25) for odd order approximations or Eq. (27) for even order approximations results in  $2[(L+1)/2]$  conditions at an interfacial boundary between two media which can be used to determine as many constants.

Since Eq. (27) does not prescribe continuity of  $f_0(r)$  it will be expected that in even order approximations the zeroth order moment will be discontinuous at an interface between two media. This discontinuity is due to the zero root which is characteristic of even order approximations. On the other hand, in odd order approximations continuity of  $f_0(r)$  at an interfacial boundary is assured by Eq. (25). By Eq. (19)  $\phi(r)$  is proportional to  $f_0(r)$  so continuity of  $\phi(r)$  is dependent upon continuity of  $f_0(r)$ . With  $\ell = 1$  it is apparent from Eqs. (25) and (27) that  $f_1(r)$  must be continuous at the interface between two media in both even and odd order approximations. Letting  $\ell = 0$  in Eq. (11) it is seen that  $f_1(r)$  is proportional to the derivative of  $f_0(r)$ , and therefore  $\phi(r)$ , with respect to  $r$ . Prescribing continuity of  $f_1(r)$  at an interfacial

boundary requires that the neutron current which is proportional to the derivative of the total neutron flux be continuous across the boundary. Summarizing the conditions listed above,  $\phi(r)$  is continuous across an interfacial boundary between two media for odd order approximations but discontinuous across the boundary for even order approximations whereas the neutron current is continuous across a boundary in both even and odd order approximations. These conditions can be seen graphically for the  $P_1$  and  $P_2$  approximations in Fig. 2.

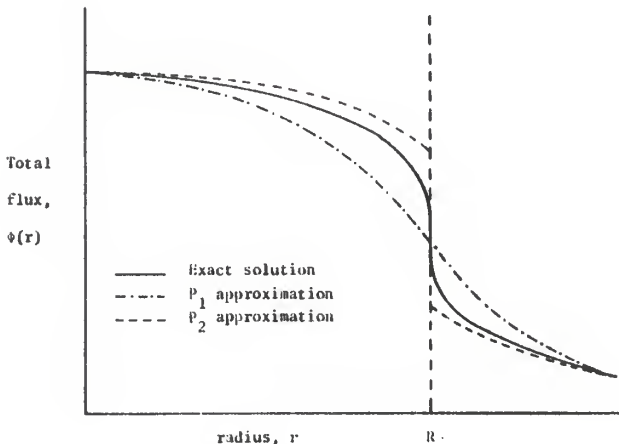


Figure 2. The spatial dependence of the total neutron flux for a two region problem with the interfacial boundary at  $R$ .

From Fig. 2 it is readily apparent that the even and odd order approximations tend to approach the exact solution for the total neutron flux in a

counterconvergent manner i.e. the odd order approximations approach the exact solution from below in the central region while the even order approximations approach the exact solution from above. Thus it is expected that if the central region was that of a reactor core and the peripheral region an infinite reflector the computed critical radii from the even and odd order approximations will be counterconvergent. Davison (2) has derived a formula which predicts this type of counterconvergence in slab geometry for a series of slabs. For values of  $c$  close to unity his formula is

$$R - R_L = \frac{\{3(-1)^{L+1}\}c\eta^2}{96(L+3/2)^2} \left\{ 1 + O\left(\frac{\ln(2L+3)}{L}\right) \right\} \quad (28)$$

where  $R$  is the exact critical radius and  $R_L$  is the critical radius found using the  $L^{\text{th}}$  order approximation. Although this equation was originally derived for slab geometry cases the same counterconvergent trend should appear in spherical geometry for interfaces at which the curvature of the interface is small with respect to the critical radius of the central region. A counterconvergence of the even and odd order approximations will be expected whenever an interface between two media is the dominant boundary. Davison (3) has shown that, at least for slab geometry, the vacuum-interface boundary conditions attributed to Mark are equivalent to replacing the vacuum with an infinite black medium. Since the replacement of the vacuum by an infinite black medium introduces an interfacial boundary between two media, counterconvergence of the even and odd order approximations will also be expected for Mark's vacuum-interface boundary conditions.

Next, the boundary conditions at a right hand vacuum interface will be considered. At a vacuum interface at  $r = R$  the exact boundary condition is

$$f(R, \mu) = 0 \quad \text{for} \quad \mu < 0. \quad (29)$$

This, however, constitutes an infinite number of conditions which cannot



all be exactly satisfied in an approximation of finite order. In an  $L^{\text{th}}$  order approximation in a central region only  $[(L+1)/2]$  conditions can be satisfied by the  $\Lambda_k$ 's in Eqs. (22) and (23). The exact vacuum-interface boundary condition, Eq. (29), is commonly reduced to  $[(L+1)/2]$  conditions in four ways.

First, it is physically plausible that the total number of neutrons entering from the vacuum should be zero. This condition can be written mathematically as

$$\int_{-1}^0 f(R, \mu) \mu d\mu = 0 . \quad (30)$$

Since  $\mu$  is just  $P_1(\mu)$ , for an  $L^{\text{th}}$  order approximation a set of boundary conditions which includes Eq. (30) is

$$\int_{-1}^0 f(R, \mu) P_{2j-1}(\mu) d\mu = 0 \quad j = 1, 2, \dots, [(L+1)/2] \quad (31)$$

or, what is equivalent

$$\int_{-1}^0 f(R, \mu) \mu^{2j-1} d\mu = 0 \quad j = 1, 2, \dots, [(L+1)/2] . \quad (32)$$

These vacuum-interface boundary conditions are known as the Marshak boundary conditions. Choosing the form in Eq. (32), expanding  $f(R, \mu)$  by Eq. (10), and interchanging the order of integration and summation Eq. (32) becomes

$$\sum_{\ell=0}^L f_{\ell}(R) \int_{-1}^0 P_{\ell}(\mu) \mu^{2j-1} d\mu = 0 \quad j = 1, 2, \dots, [(L+1)/2] . \quad (33)$$

Second, Mark (11) has proposed that Eq. (29) be satisfied exactly for  $[(L+1)/2]$  values of  $\mu$ . In particular he chose to use the condition that

$$f(R, \mu_j) = 0 \quad j = 1, 2, \dots, [(L+1)/2] \quad (34)$$

where the  $\mu_j$ 's are defined by

$$P_{L+1}(\mu_j) = 0 \quad , \quad \mu_j < 0 . \quad (35)$$

From the Legendre polynomial expansion, Eq. (10), it is readily apparent that Mark's boundary conditions impose the condition that the term  $P_{L+1}(\mu)f_{L+1}^{(R)}$  be zero and thus that the  $L+1$  order term and assumably all higher order terms in the Legendre polynomial expansion make no significant contribution to the angular flux at the vacuum interface. Expanding  $f(R,\mu)$  by Eq. (10), Eq. (34) becomes

$$\sum_{\ell=0}^L f_{\ell}^{(R)} P_{\ell}(\mu_j) = 0 \quad j = 1, 2, \dots, [(L+1)/2]. \quad (36)$$

Third, the vacuum can be replaced by a fictitious infinite black medium. For slab geometry Mark (11) has shown that this condition is equivalent to Eq. (36). However, it is impossible to prove equivalence of those two sets of boundary conditions for spherical geometry due to the curvature of boundaries and inherent boundedness in one-dimensional spherical geometry. Physically this difference occurs in spherical geometry because the infinite black medium reflector boundary condition takes the curvature at the boundary into account in a much different manner than do Mark's vacuum-interface boundary conditions. In general the infinite black medium surrounding a center region constitutes a two region problem in which  $\zeta = 0$  in the infinite outer or surrounding medium. As before it is to be noted that, although the problem here considers only spherical geometry and Davison's proof of counterconvergence is for slab geometry, the same counterconvergence trend should be found. This should be true for Mark's boundary conditions as well as for the fictitious infinite black reflector boundary conditions.

Fourth, Pomraning (15) has used a variational formulation of the Boltzmann equation and a Legendre polynomial expansion of the angular flux as a trial function to determine a set of mathematically consistent boundary conditions. By setting the first variation of the boundary terms to zero Pomraning found

the boundary conditions which result from the variational calculus to be:

$$\int_{-1}^0 f(R, u) \delta f(R, -u) u du = 0 . \quad (37)$$

These boundary conditions, called variational boundary conditions, are considered in detail in Appendix B. In general they can be put into the form

$$\sum_{\ell=0}^L f_{\ell}(R) b_{\ell j} = 0 \quad j = 1, 2, \dots, [(L+1)/2] . \quad (38)$$

Considering Eqs. (33), (36) and (38) it is readily seen that each of the equations can be forced into the form of Eq. (38). For Marshak's vacuum-interface boundary conditions this is accomplished by setting

$$b_{\ell j} = \int_{-1}^0 P_{\ell}(u) u^{2j-1} du \quad (39)$$

while for Mark's vacuum-interface boundary conditions

$$b_{\ell j} = P_{\ell}(u_j) . \quad (40)$$

Since the variational boundary conditions are developed directly from the mathematics instead of from adaptations of physical considerations to the mathematics as Marshak's and Mark's boundary conditions are, the variational boundary conditions should give the best results for a given order of approximation. For low orders of approximations the Marshak boundary conditions should give better results than Mark's or the infinite black reflector boundary conditions for the same order of approximation since the physically plausible condition of no return current of neutrons from the vacuum is automatically included in Marshak's boundary conditions whereas it is not included in the other boundary conditions.

## 2.4 Formulation of Boundary Conditions

In this section three hypothetical reactor systems will be considered. For each reactor system the appropriate boundary conditions will be imposed. Then the equations representing the appropriate boundary conditions will be forced into a common matrix equation form. Finally the solution of the common matrix equation form will be examined.

A hypothetical reactor consisting of a spherical central core region with  $c > 1$  surrounded by a vacuum infinite in extent will be referred to in this work as a bare spherical reactor. Choosing the coordinate system so that the center of the bare spherical reactor is at the origin, Eqs. (22) and (23) are the appropriate solutions of Eq. (11) for  $r \leq R$ . The vacuum is not capable of supporting a neutron flux and therefore cannot be considered a medium. Since an interfacial boundary between two media does not exist in the system considered here the constant  $A_0^*$  will be assumed to be zero. The consequences of this assumption will be examined later from the results of numerical computations based on this assumption. This assumption allows Eqs. (22) and (23) to be simplified to

$$f_{\ell}(r) = (2\ell+1) \sum_{k=1}^{[(L+1)/2]} A_k G_{\ell}(\lambda_k) C_{\ell}(rR/\lambda_k) .$$

Applying the general vacuum-interface boundary condition, Eq. (38), the set of  $[(L+1)/2]$  linear equations in  $[(L+1)/2]$  unknowns (the  $A_k$ 's) for a bare spherical reactor is

$$\sum_{k=1}^{[(L+1)/2]} A_k \sum_{\ell=0}^L (2\ell+1) G_{\ell}(\lambda_k) C_{\ell}(rR/\lambda_k) b_{\ell j} = 0$$

$$j = 1, 2, \dots, [(L+1)/2] . \quad (41)$$

Or, defining the  $[(L+1)/2]$  by one column matrix  $X$  with elements

$$x_k = A_k \quad (42)$$

and the  $[(L+1)/2]$  by  $[(L+1)/2]$  square matrix  $T$  with elements  $t_{jk}$  such that

$$t_{jk} = \sum_{\ell=0}^L (2\ell+1) G_{\ell}(\lambda_k) C_{\ell}(\Sigma R/\lambda_k) b_{\ell j} \quad (43)$$

Eq. (41) can be rewritten in matrix form as

$$TX = 0. \quad (44)$$

Equation (44) is the general matrix form in which all of the cases to be considered in this work will be written. For a bare spherical reactor Eqs. (42) and (43) define the elements of the  $X$  and  $T$  matrices involved in Eq. (44).

A hypothetical reactor consisting of a spherical central core region with  $c > 1$  surrounded by a black medium ( $c = 0$ ) infinite in extent will be referred to in this work as a bare spherical reactor with an infinite black reflector. Choosing the coordinate system so that the center of the reactor is at the origin, Eqs. (22) and (23) are the solutions of Eq. (11) for  $r \leq R$ . For  $r \geq R$  it is known from physical considerations that as  $r$  approaches infinity the total neutron flux approaches zero i.e.

$$\lim_{r \rightarrow \infty} \phi(r) = \lim_{r \rightarrow \infty} 4\pi r^2 f_0(r) = 0. \quad (45)$$

Thus all of the  $A_k$ 's corresponding to positive roots must be identically zero. Since for the infinite black medium region no right hand boundary exists the  $\bar{A}_0^*$  constant will be zero, i.e. it will never arise at least not for finite  $r$ . Thus for  $r \geq R$  eqs. (16) and (17) reduce to

$$F_{\ell}(r) = (2\ell+1)(-1)^{\ell} \sum_{k=1}^{[(L+1)/2]} \bar{A}_k \bar{G}_{\ell}(\bar{\lambda}_k) Q_{\ell}(-\bar{\Sigma}r/\bar{\lambda}_k) \quad (46)$$

where  $\bar{\lambda}_k$  is assumed to be positive, for both even and odd order approximations. In order to solve for the constants ( $A_k$ 's and  $\bar{A}_k$ 's) in odd order approximations Eq. (25) is applied at the interface at  $r = R$  between the reactor and the black medium so that for a bare spherical reactor with an infinite black reflector,

$$\begin{aligned}
& (2\ell+1) \sum_{k=1}^{[(L+1)/2]} A_k G_\ell(\lambda_k) C_\ell(\varepsilon R/\lambda_k) \\
& - (2\ell+1)(-1)^\ell \sum_{k=1}^{[(L+1)/2]} \bar{A}_k \bar{G}_\ell(\bar{\lambda}_k) Q_\ell(-\bar{\varepsilon} R/\bar{\lambda}_k) = 0 \quad \ell = 0, 1, \dots, L. \quad (47)
\end{aligned}$$

For even order approximations the corresponding condition, Eq. (27), is applied at the interface so that

$$\begin{aligned}
& (2\ell+1) \sum_{k=1}^{[(L+1)/2]} \{G_\ell(\lambda_k) C_\ell(\varepsilon R/\lambda_k) - P_\ell(0) C_\ell(\varepsilon R/\lambda_k)\} A_k \\
& - (2\ell+1) \sum_{k=1}^{[(L+1)/2]} \{(-1)^\ell \bar{G}_\ell(\bar{\lambda}_k) Q_\ell(-\bar{\varepsilon} R/\bar{\lambda}_k) - P_\ell(0) Q_\ell(-\bar{\varepsilon} R/\bar{\lambda}_k)\} \bar{A}_k = 0 \\
& \ell = 1, 2, \dots, L. \quad (48)
\end{aligned}$$

Or, defining the  $2[(L+1)/2]$  by one column matrix  $X$  with elements

$$\begin{aligned}
x_k &= A_k \quad \text{for } k \leq [(L+1)/2], \\
x_k &= \bar{A}_j \quad \text{for } [(L+1)/2] < k \leq 2[(L+1)/2] \quad (49)
\end{aligned}$$

where

$$j = k - [(L+1)/2]$$

and the  $2[(L+1)/2]$  by  $2[(L+1)/2]$  square matrix  $T$  with elements  $t_{\ell k}$  such that, for odd order approximations

$$\begin{aligned}
t_{\ell k} &= (2\ell+1) G_\ell(\lambda_k) C_\ell(\varepsilon R/\lambda_k) \quad \text{for } k \leq [(L+1)/2] \\
& \ell = 0, 1, \dots, L \\
t_{\ell k} &= (2\ell+1)(-1)^\ell \bar{G}_\ell(\bar{\lambda}_j) Q_\ell(-\bar{\varepsilon} R/\bar{\lambda}_j) \quad \text{for } [(L+1)/2] < k \leq 2[(L+1)/2] \\
& \ell = 0, 1, \dots, L \quad (50)
\end{aligned}$$

where

$$j = k - [(L+1)/2]$$

and for even order approximations

$$\begin{aligned}
t_{\ell k} &= (2\ell+1)G_{\ell}(\lambda_k)C_{\ell}(\epsilon R/\lambda_k) - (2\ell+1)P_{\ell}(0)C_0(\epsilon R/\lambda_k) \\
&\quad \text{for } k \leq [(L+1)/2] \\
&\quad \ell = 1, 2, \dots, L \\
t_{\ell k} &= (2\ell+1)(-1)^{\ell} \bar{G}_{\ell}(\bar{\lambda}_j)Q_{\ell}(-\bar{\epsilon}R/\bar{\lambda}_j) - (2\ell+1)P_{\ell}(0)Q_0(-\bar{\epsilon}R/\bar{\lambda}_j) \\
&\quad \text{for } [(L+1)/2] < k \leq 2[(L+1)/2] \\
&\quad \ell = 1, 2, \dots, L
\end{aligned} \tag{51}$$

where

$$j = k - [(L+1)/2]$$

Eqs. (47) and (48) can be written in the same matrix form as Eq. (44). For a bare spherical reactor with an infinite black reflector Eqs. (49) and (50) or (51) define the elements of the X and T matrices for Eq. (44).

A hypothetical reactor consisting of a spherical central core region with  $c > 1$  surrounded by a concentric spherical shell of thickness  $R_0$  in which  $c < 1$  and immersed in a vacuum infinite in extent will be referred to as a reflected reactor. Choosing the coordinate system so that the center of the reflected reactor coincides with the origin, Eqs. (22) and (23) are the solutions of Eq. (11) for  $r \leq R$ . As in the case of the bare spherical reactor the zero root constant in even order approximations associated with the vacuum boundary will be assumed to vanish. Since the zero root terms in even order approximations are taken to be nonzero only at right hand boundaries, the zero root term will vanish entirely from the reflector region solutions. Applying the interfacial boundary condition, for odd order approximations, Eq. (25), and Eq. (27) for even order approximations, at  $r = R$  and the general vacuum-interface boundary condition, Eq. (38), at  $r = R + R_0$  the equations determining the  $A_k$ 's and  $\bar{A}_k$ 's for a reflected reactor are, for odd order approximations

$$\begin{aligned}
(2\ell+1) \sum_{k=1}^{[(L+1)/2]} \Lambda_k G_\ell(\lambda_k) C_\ell(\Sigma R/\lambda_k) \\
- (2\ell+1) \sum_{k=1}^{2[(L+1)/2]} \bar{\Lambda}_k \bar{G}_\ell(\bar{\lambda}_k) Q_\ell(\bar{\Sigma} R/\bar{\lambda}_k) = 0 \\
\ell = 0, 1, \dots, L
\end{aligned} \quad (52)$$

and for even order approximations

$$\begin{aligned}
(2\ell+1) \sum_{k=1}^{[(L+1)/2]} \{G_\ell(\lambda_k) C_\ell(\Sigma R/\lambda_k) - P_\ell(0) C_\ell(\Sigma R/\lambda_k)\} \Lambda_k \\
- (2\ell+1) \sum_{k=1}^{[(L+1)/2]} \{\bar{G}_\ell(\bar{\lambda}_k) Q_\ell(\bar{\Sigma} R/\bar{\lambda}_k) - P_\ell(0) Q_\ell(\bar{\Sigma} R/\bar{\lambda}_k)\} \bar{\Lambda}_k = 0 \\
\ell = 1, 2, \dots, L
\end{aligned} \quad (53)$$

together with

$$\begin{aligned}
2 \sum_{k=1}^{[(L+1)/2]} \frac{1}{\bar{\Lambda}_k} \sum_{\ell=0}^L (2\ell+1) \bar{G}_\ell(\bar{\lambda}_k) Q_\ell(\bar{\Sigma}(R+R_0)/\bar{\lambda}_k) \bar{B}_{\ell j} = 0 \\
j = 1, 2, \dots, [(L+1)/2] .
\end{aligned} \quad (54)$$

Now define the  $3[(L+1)/2]$  by one column matrix  $X$  with elements

$$\begin{aligned}
x_k &= \Lambda_k & \text{for } k \leq [(L+1)/2], \\
x_k &= \bar{\Lambda}_j & \text{for } [(L+1)/2] < k \leq 3[(L+1)/2]
\end{aligned} \quad (55)$$

where

$$j = k - [(L+1)/2]$$

and the  $3[(L+1)/2]$  square matrix  $T$  with elements  $t_{\ell k}$  such that, for odd order approximations

$$\begin{aligned}
t_{\ell k} &= (2\ell+1) G_\ell(\lambda_k) C_\ell(\Sigma R/\lambda_k) & \text{for } k \leq [(L+1)/2] \\
& & \ell = 0, 1, \dots, L \\
t_{\ell k} &= (2\ell+1) \bar{G}_\ell(\bar{\lambda}_j) Q_\ell(\bar{\Sigma} R/\bar{\lambda}_j) & \text{for } [(L+1)/2] < k \leq 3[(L+1)/2] \\
& & \ell = 0, 1, \dots, L
\end{aligned} \quad (56)$$



where

$$j = k - [(L+1)/2]$$

and for even order approximations

$$\begin{aligned} t_{\ell k} &= (2\ell+1)G_{\ell}(\lambda_k)C_{\ell}(ER/\lambda_k) - (2\ell+1)P_{\ell}(0)C_0(ER/\lambda_k) \\ &\qquad\qquad\qquad \text{for } k \leq [(L+1)/2] \\ &\qquad\qquad\qquad \ell = 1, 2, \dots, L \\ t_{\ell k} &= (2\ell+1)\overline{G}_{\ell}(\overline{\lambda}_j)Q_{\ell}(\overline{ER}/\overline{\lambda}_j) - (2\ell+1)P_{\ell}(0)Q_0(\overline{ER}/\overline{\lambda}_j) \\ &\qquad\qquad\qquad \text{for } [(L+1)/2] < k \leq 3[(L+1)/2] \\ &\qquad\qquad\qquad \ell = 1, 2, \dots, L \end{aligned} \quad (57)$$

where

$$j = k - [(L+1)/2] .$$

Then using Eqs. (56) and (57) together with

$$\begin{aligned} t_{\ell k} &= 0 \quad \text{for } k \leq [(L+1)/2] \\ &\qquad\qquad\qquad 2[(L+1)/2] < k \leq 3[(L+1)/2] \end{aligned} \quad (58)$$

and

$$\begin{aligned} t_{\ell k} &= \sum_{m=0}^L (2m+1)\overline{G}_m(\overline{\lambda}_j)Q_m(\overline{E}(R+R_0)/\overline{\lambda}_j)\overline{G}_{mn} \\ &\qquad\qquad\qquad \text{for } [(L+1)/2] < k \leq 3[(L+1)/2] \\ &\qquad\qquad\qquad 2[(L+1)/2] < k \leq 3[(L+1)/2] \end{aligned} \quad (59)$$

where

$$\begin{aligned} j &= k - [(L+1)/2] , \\ n &= \ell - 2[(L+1)/2] \end{aligned}$$

Eqs. (52), (53) and (54) can be written in the same matrix form as Eq. (44).

For a reflected reactor Eqs. (55), (56) or (57), (58) and (59) define the elements of the X and T matrices in Eq. (44).

Since all three of the reactor systems considered have been put into the form of Eq. (44), solution of this type of equation will be considered in detail. From the theory of linear algebra (22) the column matrix X can have a non-trivial solution only if the determinant of T vanishes. Examining the various terms which make up T it is readily apparent that R is the undetermined free quantity which must be varied until

$$|T| = 0 . \quad (60)$$

Since the  $C_k(x)$  functions can be periodic an infinite number of values of R will satisfy Eq. (60). In order for the total neutron flux to be non-negative (a physical necessity) the first or smallest positive value of R which satisfies Eq. (60) is the required value and is commonly known as the "critical" radius of the spherical reactor in question. Equation (60) is known as the criticality equation.

After a "critical" radius has been found the constants composing the column matrix can be determined to within a normalization factor. If the first column is transferred to the other side of the equality and any one of the rows deleted, the resulting matrix equation (one less in rank) may be solved for the remaining  $A_k$ 's and  $\bar{A}_k$ 's in terms of  $A_1$ . Using this procedure  $A_1$  is defined to be equal to one.

### 3.0 DISCUSSION AND RESULTS

#### 3.1 General Discussion

The basic purpose of this study is to examine the rate of convergence of the spherical harmonics method for both bare and reflected spheres using various vacuum-interface boundary conditions. Since an adequate treatment of the problem requires a great number of numerical computations, a computer program is used to carry out the numerical work. The program is written in a general manner so that only one program is required for all of the cases to be considered. The program is written for the IBM 1410 in the FORTRAN language and is compiled in a fourteen digit floating point mantissa length. In the sections of the program which require iteration a relative accuracy of  $10^{-13}$  is employed. Since only six digits are retained in the final results, this accuracy is deemed satisfactory for the size of matrices encountered in the program. A complete description of the computer program is given in Appendix C.

Before considering some practical cases the equations will be analyzed for the important unspecified constants. It is readily apparent from the theory for a bare sphere that  $c$  and  $\Sigma$  are the only unspecified constants. The constant  $\Sigma$  always occurs in a product with the radial variable  $r$  so if radii are measured and reported in mean free paths, only the mean number of secondaries per collision  $c$  needs to be specified for a bare spherical reactor. For reflected spheres  $c$ ,  $\Sigma$ ,  $\bar{c}$ ,  $\bar{\Sigma}$ , and  $R_0$  are the unspecified constants. The constants  $\Sigma$  and  $\bar{\Sigma}$  always occur in products with  $r$  so if radii are measured in mean free paths, only  $\Sigma/\bar{\Sigma}$ ,  $c$ ,  $\bar{c}$  and  $R_0$  are the unspecified constants for a reflected reactor.

In order to fully appreciate the magnitude of certain transport theory constants they will be compared with the more familiar diffusion theory

constants. In particular the thickness of a reflector in diffusion lengths is a very important property in diffusion theory. Glasstone (6) shows that if a reflector is 1.5 to 2.0 diffusion lengths in thickness it may be considered essentially infinite. From diffusion theory the diffusion length,  $\kappa^{-1}$ , is

$$\kappa^{-1} = \sqrt{D/\Sigma_a} = 1/\sqrt{3\Sigma_a\bar{E}} \quad (61)$$

for isotropic scattering. In the  $P_1$  approximation which corresponds to diffusion theory the root of

$$\bar{U}_{L+1}(\bar{\lambda}_k) = \bar{U}_2(\bar{\lambda}_1) = 3(1-\bar{c})\bar{\lambda}_1^2 - 1 = 0$$

is,

$$\bar{\lambda}_1 = 1/\sqrt{3(1-\bar{c})}$$

or, since for a non-multiplying medium  $\bar{c} = \bar{E}_s/\bar{E}$ ,

$$(1-\bar{c}) = \bar{E}_a/\bar{E}$$

so

$$\bar{\lambda}_1 = \bar{E}/\sqrt{3\bar{E}_a\bar{E}} \quad (62)$$

With  $R_0$  being the thickness of the reflector in mean free paths

$$\bar{E}R_0/\bar{\lambda}_1 = R_0\sqrt{3\bar{E}_a\bar{E}} = \bar{\kappa}R_0 \quad (63)$$

is the thickness of the reflector in diffusion lengths. As the order of approximation increases the principal or largest root of Eq. (15) changes slightly but the quantity  $\bar{E}R_0/\bar{\lambda}_1$  still closely approximates the thickness of the reflector in diffusion lengths.

At this point further consideration will be given to Eq. (28) which predicts counterconvergence of the even and odd order approximations for interfacial boundaries, infinite black media reflectors and Mark's vacuum-interface boundary conditions. If the  $O\left\{\frac{kn(2L+3)}{L}\right\}$  terms in Eq. (28) are ignored it is

possible to find a pair of weighting factors which would determine a weighted average critical radius that will approximate the exact critical radius. With  $L$  odd this combination of corresponding even and odd order results can be written mathematically as

$$R = w_L R_L + w_{L+1} R_{L+1} \quad (64)$$

where

$$w_L = \frac{R - R_{L+1}}{R_L - R_{L+1}},$$

$$w_{L+1} = \frac{R_L - R}{R_L - R_{L+1}}.$$

The values of the weighting factors  $w_L$  and  $w_{L+1}$  are worked out readily by using Eq. (28). Ignoring the higher order terms these factors are found to be

$$w_L = \frac{2(2L+3)^2}{2(2L+3)^2 + (2L+5)^2},$$

and

$$w_{L+1} = \frac{(2L+5)^2}{2(2L+3)^2 + (2L+5)^2} \quad (65)$$

A list of the values of these weighting factors for approximations up to order nine may be found in Table I.

Table I  
Weighting Factors for Eq. (64)

$L$	$w_L$	$w_{L+1}$
1	.505051	.494949
3	.572438	.427562
5	.600355	.399645
7	.615548	.384452
9	.625089	.374911

For very large orders of approximations

$$\lim_{L \rightarrow \infty} w_L = 2/3 ,$$

$$\lim_{L \rightarrow \infty} w_{L+1} = 1/3 .$$

Thus for very large orders of approximations it will be expected that the odd order approximations will be about twice as close to the exact answer as their corresponding even order approximations. Although this criterion was originally developed for slab geometry it should apply to the spherical geometry cases considered in this work when the critical radius is large enough so that the curvature of the boundary contributes a small effect.

### 3.2 Results of Numerical Calculations for Bare Spherical Reactors

In order to examine the rate of convergence of the spherical harmonics approximations for various boundary conditions imposed at the surface of a bare sphere three cases will be considered. First a bare spherical reactor with  $c = 1.05$  in the core region is utilized. In this case the value of  $c$  is probably too large for diffusion theory to be exact but not so large that the assumption of the existence of a single thermal neutron group will no longer be valid. This basic intermediate case will be considered in detail and the results from other cases will be compared to the results of this basic case. The second case to be considered will be that of a bare spherical reactor in which  $c = 1.02$ . For this case the value of  $c$  is probably close enough to unity so that diffusion theory should give very good accuracy. As a third case, the extreme of a large value of  $c$ , namely 1.40, will be considered. In order to adequately describe this bare spherical reactor case a multigroup transport theory would be needed since the fast leakage would be so great that the single thermal energy neutron group assumption would not be valid. However for a limiting standpoint, the results for this large value of  $c$  are needed in this work.

Table II is a compilation of the computed results for a bare spherical reactor with  $c = 1.05$ . The exact critical radii given in this table and other tables are taken from results computed by Carlson and Bell (1) using the extrapolated end point method. The per cent error column is the percentage error in an  $L^{\text{th}}$  order approximation which is computed as

$$\text{per cent error} = \frac{R - R_L}{R} \times 100 .$$

The column labeled "inward flux" represents the integral of the computed angular

Table II. Calculated results for a bare spherical reactor in which  $c$  is 1.05. The exact critical radius is 7.2772 mean free paths.

Marshak vacuum-interface boundary conditions			
Approximation	Critical radius	Per cent error	Inward flux
P <sub>1</sub>	7.3976	1.654	$1.895 \times 10^{-3}$
P <sub>2</sub>	7.3201	.590	$1.251 \times 10^{-3}$
P <sub>3</sub>	7.2805	.045	$5.433 \times 10^{-4}$
P <sub>4</sub>	7.2826	.074	$6.973 \times 10^{-4}$
P <sub>5</sub>	7.2784	.016	$3.221 \times 10^{-4}$
P <sub>6</sub>	7.2793	.029	$4.370 \times 10^{-4}$
P <sub>7</sub>	7.2778	.008	$2.216 \times 10^{-4}$
P <sub>8</sub>	7.2783	.015	$3.056 \times 10^{-4}$
P <sub>9</sub>	7.2775	.004	$1.545 \times 10^{-4}$
P <sub>10</sub>	7.2778	.008	$2.019 \times 10^{-4}$

Mark's vacuum-interface boundary conditions					
Approximation	Critical radius	Per cent error	Weighted average	Per cent error	Inward flux
P <sub>1</sub>	7.4979	3.033	7.3682	1.250	$8.644 \times 10^{-4}$
P <sub>2</sub>	7.2359	-.568			$2.140 \times 10^{-3}$
P <sub>3</sub>	7.2875	.142	7.2784	.016	$3.076 \times 10^{-4}$
P <sub>4</sub>	7.2663	-.150			$1.204 \times 10^{-3}$
P <sub>5</sub>	7.2808	.050	7.2776	.005	$1.791 \times 10^{-4}$
P <sub>6</sub>	7.2727	-.062			$7.870 \times 10^{-4}$
P <sub>7</sub>	7.2789	.023	7.2774	.003	$1.241 \times 10^{-4}$
P <sub>8</sub>	7.2749	-.032			$5.650 \times 10^{-4}$
P <sub>9</sub>	7.2781	.012	7.2773	.001	$8.147 \times 10^{-5}$
P <sub>10</sub>	7.2759	-.018			$4.167 \times 10^{-4}$



Table II (continued)

Infinite black reflector boundary conditions					
Approximation	Critical radius	Per cent error	Weighted average	Per cent error	Inward flux
P <sub>1</sub>	7.5436	3.661	7.3716	1.297	4.023 x 10 <sup>-4</sup>
P <sub>2</sub>	7.1960	-1.116			2.569 x 10 <sup>-3</sup>
P <sub>3</sub>	7.2962	.261	7.2791	.026	1.655 x 10 <sup>-4</sup>
P <sub>4</sub>	7.2562	-.289			1.445 x 10 <sup>-3</sup>
P <sub>5</sub>	7.2843	.098	7.2775	.004	6.513 x 10 <sup>-5</sup>
P <sub>6</sub>	7.2672	-.137			9.950 x 10 <sup>-4</sup>
P <sub>7</sub>	7.2810	.052	7.2773	.001	2.949 x 10 <sup>-5</sup>
P <sub>8</sub>	7.2714	-.080			7.567 x 10 <sup>-4</sup>
P <sub>9</sub>	7.2795	.032	7.2772	0	1.760 x 10 <sup>-6</sup>
P <sub>10</sub>	7.2734	-.052			6.033 x 10 <sup>-4</sup>
Variational vacuum-interface boundary conditions					
Approximation	Critical radius	Per cent error			Inward flux
P <sub>1</sub>	7.3519		1.026		2.374 x 10 <sup>-3</sup>
P <sub>2</sub>	7.2003		-1.057		2.522 x 10 <sup>-3</sup>
P <sub>3</sub>	7.2764		-.011		7.010 x 10 <sup>-4</sup>
P <sub>4</sub>	7.2887		.158		1.643 x 10 <sup>-3</sup>

flux at the vacuum interface over all angles representing neutrons returning from the vacuum, i.e.  $\int_{-1}^0 f(R, \mu) d\mu$ , with the normalization such that the total flux at the center,  $\phi(0)$ , is one neutron per square centimeter per second. Since for an exact solution this quantity would be zero, it would seem that this column should contain numbers which would be indicative of the accuracy of the critical radius computed in this approximation. However, upon close examination it is readily apparent that these numbers are not indicative of the accuracy of their corresponding critical radii. Even for a particular boundary condition the inward flux column is not a good indication of the accuracy of the computed critical radii. However, for a particular boundary condition the number in this column corresponding to odd order approximations decreases for increasing orders of approximations. Similarly the even order numbers decrease with increasing orders of approximations but no indication of the relative accuracy of a particular computed critical radius can be found by comparing these numbers for the even and odd order approximations. The basic problem here is that since the critical radii and roots for each of the approximations are different so are the values of the arguments of the geometrical functions and hence the values of the geometrical functions themselves. Since this column has little indicative ability, it will be omitted from the remaining tables of results.

The computed results with Marshak boundary conditions used at the vacuum interface of a bare sphere with  $c = 1.05$  are graphed in Fig. 3. This type of graph where the computed critical radius is plotted against the reciprocal of the order of approximation will be referred to as a convergence graph. Although the graph is composed of discrete points, it is convenient to draw in curves connecting the points representing the even and odd order approximations since this facilitates visualization of the rate of convergence. It is readily

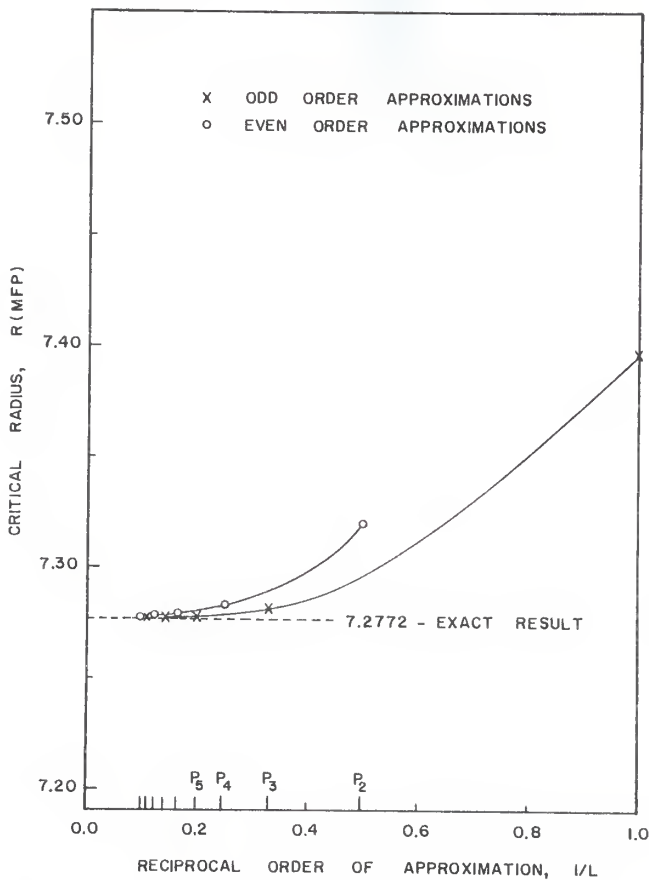


Figure 3. CONVERGENCE GRAPH FOR A BARE SPHERICAL REACTOR IN WHICH  $C$  IS 1.05 USING MARSHAK'S BOUNDARY CONDITIONS.

apparent from Fig. 3 that although the  $P_2$  result is more accurate than the  $P_1$  result, the odd order approximations converge to the exact critical radius more rapidly than their corresponding even order approximations. Both the even and odd order approximations tend to asymptotically approach the exact critical radius from above along separate paths, i.e., the even and odd order approximations are not counterconvergent. Examining the Marshak results in Table II it is readily apparent that as the order of approximation increases the odd order approximations become about twice as accurate as their successive even order approximations. This is the same ratio of accuracy of odd and successive even order approximations as Davison's formula predicts for large orders of approximations, in spite of the fact that when using Marshak's vacuum-interface boundary conditions the even and odd order approximations are not counterconvergent to the exact critical radius.

Figure 4 is a convergence graph for a bare spherical reactor in which  $c = 1.05$  and Mark's boundary conditions are used at the vacuum interface. The weighted average points in Fig. 4 and the weighted average column in the appropriate section of Table II are found by applying Eq. (64) with the weighting factors given in Table I. The expression  $|P_L, P_{L+1}|_{av}$ , in which  $L$  is assumed to be odd, will be used to indicate a weighted average of the critical radii from the  $P_L$  and  $P_{L+1}$  approximations. It is readily apparent that the weighted average values converge to the exact critical radius much more rapidly than do either the even or odd order approximations. The counter-convergence trend which Eq. (28) predicts for Mark's boundary conditions is also shown in Fig. 4. As with the Marshak boundary conditions, the  $P_2$  result is more accurate than the  $P_1$  result, but for higher orders of approximations the odd order results are better than the corresponding even order results. The fact that the weighted average critical radii converge so rapidly to the

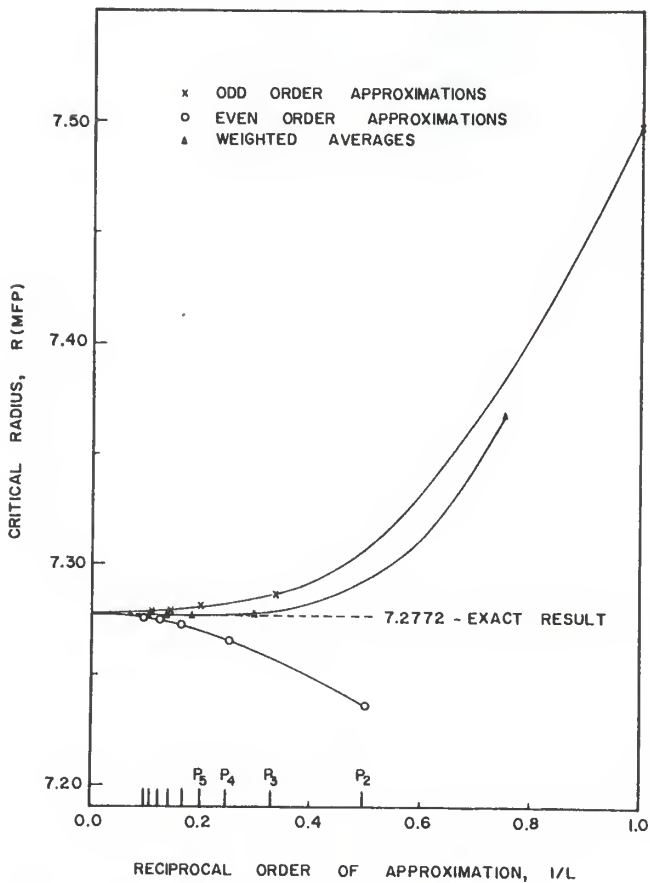


Figure 4. CONVERGENCE GRAPH FOR A BARE SPHERICAL REACTOR IN WHICH  $C$  IS 1.05 USING MARK'S BOUNDARY CONDITIONS.

exact result indicates that Davison's formula predicts the correct trend for this case. Since the  $|P_1, P_2|_{av}$  is not as accurate as might be expected, the  $O\left\{\frac{\ln(2L+3)}{L}\right\}$  term in Eq. (28) is not negligible for these low orders of approximation.

Figure 5 is the convergence graph for a bare spherical reactor with  $c = 1.05$  which is infinitely reflected with a black medium. As with Mark's vacuum-interface boundary conditions, the weighted average critical radii converge to the exact critical radius much more rapidly than do either the even or odd order approximations. For this two region problem the counter-convergence of the even and odd order approximations is again readily apparent. The  $P_2$  result is once again more accurate than the  $P_1$  result although for higher orders of approximations the odd order approximations are more accurate than the corresponding even order approximations. The  $|P_1, P_2|_{av}$  for this case is not as accurate as would be expected so that again it is apparent that the higher order terms in Eq. (28) are not negligible.

The computed results for a bare spherical reactor with  $c = 1.05$  using variational boundary conditions at the vacuum interface are shown in Fig. 6. From the limited results shown it is not possible to deduce the type of convergence which the variational boundary conditions yield. It is readily apparent that the convergence is neither counterconvergent nor asymptotic as is the case for Mark's and Marshak's boundary conditions respectively. In contrast to previous cases the  $P_1$  and  $P_2$  approximations with variational boundary conditions yield critical radii which have about the same magnitude of error but opposite signs. For the variational boundary conditions the  $P_3$  result very closely approximates the exact critical radius and is definitely superior to the  $P_4$  result.

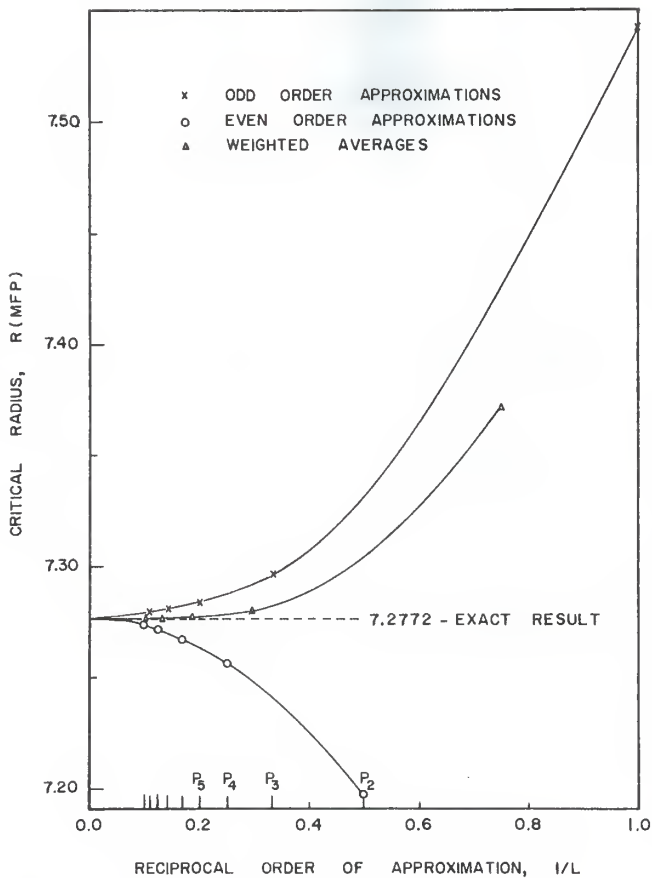


Figure 5. CONVERGENCE GRAPH FOR A BARE SPHERICAL REACTOR IN WHICH  $C$  IS 1.05 USING THE INFINITE BLACK REFLECTOR BOUNDARY CONDITIONS.

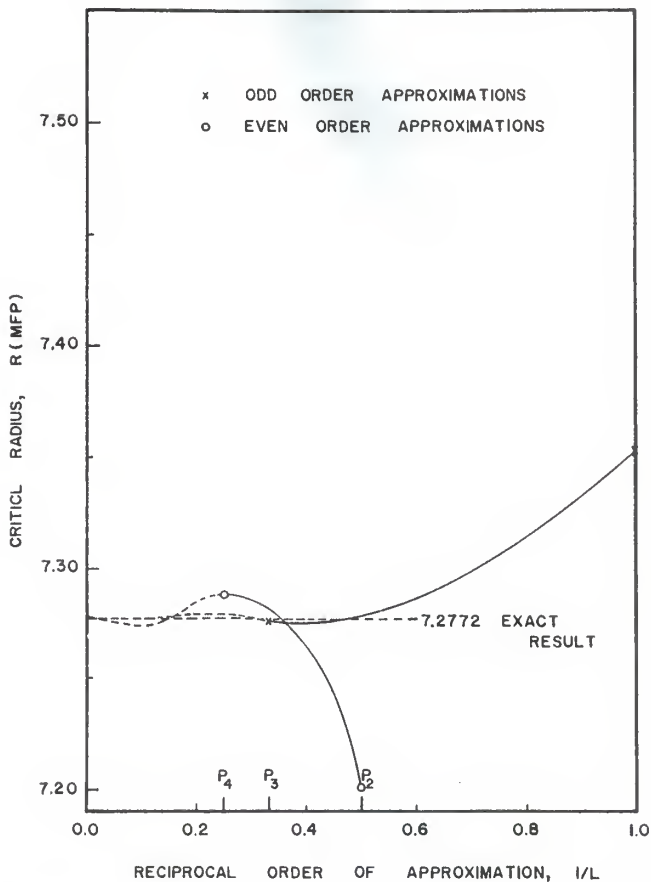


Figure 6. CONVERGENCE GRAPH FOR A BARE SPHERICAL REACTOR IN WHICH  $C$  IS 1.05 USING THE VARIATIONAL BOUNDARY CONDITIONS.



Figure 7 plots the angular flux at the vacuum interface as a function of  $\cos\theta$  for a bare spherical reactor in which  $c = 1.05$  resulting from a  $P_3$  approximation for each of the four vacuum-interface boundary conditions considered. The angular fluxes are normalized such that the total neutron flux at the center,  $\phi(0)$ , is one neutron per square centimeter per second. For an exact solution Eq. (29) shows that in the range  $-1 \leq \mu \leq 0$  the angular flux would be zero. Figure 7 shows that the variational boundary conditions best approximate this condition. It is also apparent from Fig. 7 and Table 1 that the closeness with which the various boundary conditions approximate the exact condition the closer the critical radius is to the exact critical radius. However, the relative accuracy with which a particular boundary condition approximates the exact condition is not directly proportional to the relative accuracy of the computed critical radius. The type of graph shown in Fig. 7 could be employed as a rough guide to find out which critical radius determined from a set of boundary conditions is the most accurate for a particular problem.

Tables III and IV list the computed results for a bare spherical reactor in which the values of  $c$  are 1.02 and 1.40 respectively. As the value of  $c$  deviates from unity by increasing amounts, it seems natural that more and more terms in the Legendre polynomial expansion of the angular flux will be needed to satisfy the exact boundary condition to a preset degree of accuracy. Thus it will be expected that the rate of convergence of the spherical harmonics approximations will be proportional to the relative departure of the value of  $c$  from unity. This trend is readily apparent in the per cent error columns of Tables II, III, and IV.

Some generalizations can be made as to the relative accuracy obtained with various boundary conditions by examining Tables II, III and IV. The

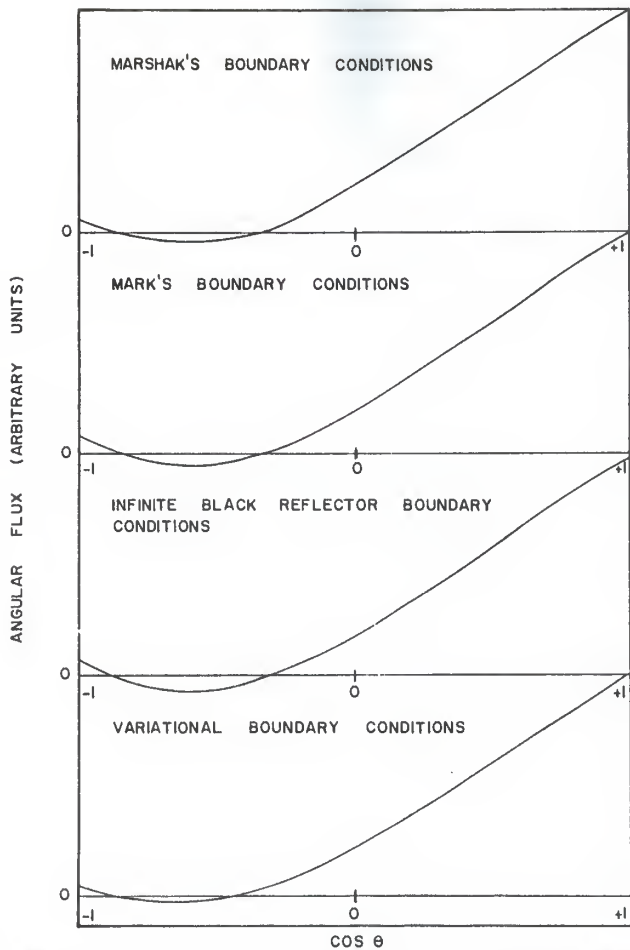


Figure 7. ANGULAR FLUX AT THE VACUUM INTERFACE AS A FUNCTION OF  $\cos \theta$  FOR A  $P_3$  APPROXIMATION.

Table III. Calculated results for a bare spherical reactor in which  $c$  is 1.02. The exact critical radius is 12,0270 mean free paths.

Marshak vacuum-interface boundary conditions		
Approximation	Critical radius	Per cent error
P <sub>1</sub>	12.1269	0.831
P <sub>2</sub>	12.0729	.382
P <sub>3</sub>	12.0312	.035
P <sub>4</sub>	12.0338	.057
P <sub>5</sub>	12.0289	.016
P <sub>6</sub>	12.0301	.026
P <sub>7</sub>	12.0282	.010
P <sub>8</sub>	12.0288	.015
P <sub>9</sub>	12.0279	.007
P <sub>10</sub>	12.0283	.011

Mark's vacuum-interface boundary conditions				
Approximation	Critical radius	Per cent error	Weighted average	Per cent error
P <sub>1</sub>	12.2239	1.637		
P <sub>2</sub>	11.9787	-.402	12.1025	0.628
P <sub>3</sub>	12.0395	.104		
P <sub>4</sub>	12.0138	-.110	12.0285	.012
P <sub>5</sub>	12.0319	.041		
P <sub>6</sub>	12.0214	-.047	12.0277	.006
P <sub>7</sub>	12.0297	.022		
P <sub>8</sub>	12.0242	-.023	12.0276	.005

Table III (continued)

Infinite black reflector boundary conditions				
Approximation	Critical radius	Per cent error	Weighted average	Per cent error
P <sub>1</sub>	12.2520	1.871	12.1060	0.657
P <sub>2</sub>	11.9571	-.581		
P <sub>3</sub>	12.0448	.148	12.0289	.016
P <sub>4</sub>	12.0076	-.161		
P <sub>5</sub>	12.0343	.061	12.0278	.007
P <sub>6</sub>	12.0180	-.075		
P <sub>7</sub>	12.0312	.035	12.0276	.005
P <sub>8</sub>	12.0219	-.042		
P <sub>9</sub>	12.0298	.023	12.0276	.005
P <sub>10</sub>	12.0238	-.027		
Variational vacuum-interface boundary conditions				
Approximation	Critical radius	Per cent error		
P <sub>1</sub>	12.0827	0.463		
P <sub>2</sub>	11.9843	-.355		
P <sub>3</sub>	12.0262	-.007		
P <sub>4</sub>	12.0336	.055		

Table IV. Calculated results for a bare spherical reactor in which  $c$  is 1.40. The exact critical radius is 1.9854 mean free paths.

Marshak vacuum-interface boundary conditions				
Approximation	Critical radius	Per cent error		
P <sub>1</sub>	2.1223	6.895		
P <sub>2</sub>	1.9760	-.473		
P <sub>3</sub>	1.9869	.076		
P <sub>4</sub>	1.9873	.096		
P <sub>5</sub>	1.9860	.030		
P <sub>6</sub>	1.9861	.035		
P <sub>7</sub>	1.9856	.010		
P <sub>8</sub>	1.9856	.010		
P <sub>9</sub>	1.9855	.005		
P <sub>10</sub>	1.9855	.005		
Mark's vacuum-interface boundary conditions				
Approximation	Critical radius	Per cent error	Weighted average	Per cent error
P <sub>1</sub>	2.2224	11.937		
P <sub>2</sub>	1.9590	-1.330	2.0920	5.369
P <sub>3</sub>	1.9898	.222		
P <sub>4</sub>	1.9821	-.166	1.9865	.055
P <sub>5</sub>	1.9867	.065		
P <sub>6</sub>	1.9843	-.055	1.9857	.015
P <sub>7</sub>	1.9859	.025		
P <sub>8</sub>	1.9849	-.025	1.9855	.005
P <sub>9</sub>	1.9856	.010		
P <sub>10</sub>	1.9851	-.015	1.9854	0

Table IV (continued)

Infinite black reflector boundary conditions				
Approximation	Critical radius	Per cent error	Weighted average	Per cent error
P <sub>1</sub>	2.3531	18.520	2.0610	3.808
P <sub>2</sub>	1.7629	-11.207		
P <sub>3</sub>	2.0394	2.720	1.9982	.645
P <sub>4</sub>	1.9430	-2.136		
P <sub>5</sub>	1.9994	.705	1.9873	.096
P <sub>6</sub>	1.9692	-.816		
P <sub>7</sub>	1.9914	.302	1.9857	.015
P <sub>8</sub>	1.9766	-.443		
P <sub>9</sub>	1.9889	.176	1.9855	.005
P <sub>10</sub>	1.9798	-.282		
Variational vacuum-interface boundary conditions				
Approximation	Critical radius	Per cent error		
P <sub>1</sub>	2.0779	4.659		
P <sub>2</sub>	1.7481	-11.952		
P <sub>3</sub>	1.9858	.020		
P <sub>4</sub>	2.0605	3.783		

spherical harmonics approximations are seen to converge much more rapidly for Mark's boundary conditions than for the infinite black reflector boundary conditions. For slab geometry these two sets of boundary conditions are equivalent, but in spherical geometry they are seen to be different although they both counterconverge to the exact critical radius as expected. The difference in spherical geometry is undoubtedly due to the fact that the infinite black reflector boundary conditions take the curvature of the outer edge of the spherical reactor into account in a much different manner than do Mark's boundary conditions. Except for the infinite black reflector boundary conditions, the boundary conditions used in this work are actually derived for slab geometry cases. The fact that these slab geometry boundary conditions yield such good results indicates that these boundary conditions are also applicable in spherical geometry where the curvature of the vacuum interface is not too great.

It was previously stated that the variational boundary conditions would be expected to give the most accurate results since they are developed directly from the mathematics. It is readily apparent in Tables II, III and IV that, at least for the  $P_1$  and  $P_3$  approximations, the variational boundary conditions give the most accurate critical radii for these orders of approximations. No particular set of boundary conditions yields a best critical radius for the  $P_2$  approximation. As expected, Marshak's boundary conditions are seen to be less accurate than the variational boundary conditions. In addition, for a given order of approximation, Mark's or the infinite black reflector boundary conditions are always poorer than Marshak's boundary conditions. However, the weighted average critical radii from Mark's boundary conditions are seen to converge more rapidly to the exact critical radius than the odd order approximations using Marshak's boundary conditions. Except for the  $\{P_1, P_2\}_{av}$ , the

the  $|P_L, P_{L+1}|_{av}$ 's using Mark's or the infinite black reflector boundary conditions are about as accurate as the  $P_{L+2}$  Marshak boundary condition results, e.g., the  $|P_3, P_4|_{av}$  using Mark's boundary conditions is about as accurate as the  $P_5$  Marshak boundary condition result. The critical radii resulting from the use of the  $P_3$  approximation with the variational boundary conditions are about as accurate as the  $|P_5, P_6|_{av}$  from Mark's or the infinite black reflector boundary conditions, or the  $P_7$  Marshak boundary condition results. Thus for the amount of work involved the  $P_3$  approximation with variational boundary conditions applied at the vacuum interface yields the most accurate estimate of the critical radius.



### 3.3 Results of Numerical Calculations for Reflected Spherical Reactors

In order to examine the rate of convergence of the spherical harmonics approximations for a reflected spherical reactor the cases shown in Table V will be considered.

Table V  
Reflected Reactor Cases to be Considered

Case	$\bar{c}$	$\Sigma/\bar{\Sigma}$	$R_0$ (mfp)
1	0.99	1.0	1.0
2	.99	1.0	10.0
3	.50	1.0	2.0
4	.99	2.5	1.0
5	.99	2.5	10.0
6	.50	2.5	2.0

The combinations of  $\bar{\Sigma}R_0$  and  $\bar{c}$  for the six cases are such that for cases 1 and 4 the reflector is about 0.2 diffusion lengths in thickness whereas for cases 2, 3, 5, and 6 the reflector is about 2.0 diffusion lengths in thickness. As previously noted, a reflector which is 1.5 to 2.0 diffusion lengths in thickness is essentially infinite. When a reflector is of such a thickness, it will be referred to in this work as a "thick" reflector. In contrast when the thickness of the reflector is much less than 2.0 diffusion lengths, it will be termed a "thin" reflector. Thus cases 1 and 4 represent "thin" reflectors whereas cases 2, 3, 5, and 6 represent "thick" reflectors. The value of  $c = .99$  represents a reflector which is a good moderator whereas the value of  $c = .50$  represents a reflector which is a breeder blanket or other poor

moderator. The case of a small value of  $c$  for a thin reflector is not considered since for such a case the thickness of the reflector would be about 0.2 mean free paths or less and hence would be extremely thin physically. In cases 1, 2, and 3 the total macroscopic cross section,  $\Sigma$ , is continuous across the core-reflector interface whereas in cases 4, 5, and 6 the total macroscopic cross section is discontinuous across the boundary.

As in the bare spherical reactor cases, 1.05 will be used as the value of  $c$ , the mean number of secondaries, in a basic reflected reactor core to which the results for the values of  $c = 1.02$  and 1.40 will be compared. Whenever a counterconvergent trend is found in the computed results, Eq. (64) will be used to find weighted average critical radii and they will be listed in a weighted average column. Table VI lists the computed results for case 1 with  $c = 1.05$  in the core region. It is readily apparent from the data that the nature of the convergence for each of the vacuum-interface boundary conditions is the same as the convergence with the boundary condition applied to a bare spherical reactor. Thus for a thin reflector and continuity or near continuity of the total macroscopic cross section, and the mean number of secondaries across the core-reflector boundary, the vacuum-interface boundary conditions dominate the convergence pattern. Tables VII and VIII list the computed results for cases 2 and 3 respectively with  $c = 1.05$  in the core region. The convergence pattern in these two cases is seen to reflect the counterconvergent trend expected of an interfacial boundary or Mark's vacuum-interface boundary conditions. Thus for a thick reflector and continuity of the total macroscopic cross section across the core-reflector interface the interfacial boundary dominates the convergence pattern. The computed results for a reflected reactor whose constants are those of case 4 and whose core has a value of  $c$  equal to 1.05 are listed in Table IX. It is readily apparent from the results

Table VI. Calculated results for case 1 (reflected reactor)  
in which  $c$  is 1.05.

Approximation	Marshak's B.C.		Mark's B.C.		Variational B.C.
	Critical radius	Weighted average	Critical radius	Weighted average	Critical radius
$P_1$	6.6192		6.6901		6.5875
$P_2$	6.5114		6.4600	6.5762	6.4274
$P_3$	6.4873		6.4910	6.4858	6.4852
$P_4$	6.4880		6.4788		6.4943
$P_5$	6.4862		6.4876	6.4855	
$P_6$	6.4863		6.4824		

Table VII. Calculated results for case 2 (reflected reactor)  
in which  $c$  is 1.05

Approximation	Marshak's B.C.		Mark's B.C.		Variational B.C.	
	Critical radius	Weighted average	Critical radius	Weighted average	Critical average	Weighted average
$P_1$	5.1896		5.1913		5.1889	
$P_2$	5.0625	5.1267	5.0609	5.1268	5.0611	5.1256
$P_3$	5.0779		5.0780		5.0778	
$P_4$	5.0739	5.0762	5.0736	5.0761	5.0740	5.0762
$P_5$	5.0762		5.0763			
$P_6$	5.0749	5.0757	5.0748	5.0757		

Table VIII. Calculated results for case 3 (reflected reactor)  
in which  $c$  is 1.05.

Approximation	Marshak's B.C.		Mark's B.C.		Variational B.C.	
	Critical radius	Weighted average	Critical radius	Weighted average	Critical radius	Weighted average
$P_1$	7.3215		7.3223		7.3211	
$P_2$	7.0284	7.1764	7.0283	7.1768	7.0271	7.1756
$P_3$	7.0981		7.0983		7.0981	
$P_4$	7.0731	7.0874	7.0733	7.0876	7.0734	7.0875
$P_5$	7.0903		7.0903			
$P_6$	7.0803	7.0863	7.0803	7.0863		

Table IX. Calculated results for case 4 (reflected reactor)  
in which  $c$  is 1.05.

Approximation	Marshak's B.C.		Mark's B.C.		Variational B.C.	
	Critical radius	Weighted average	Critical radius	Weighted average	Critical radius	Weighted average
$P_1$	6.9287		6.9788		6.9062	
$P_2$	6.6506	6.7911	6.6370	6.8096	6.5510	6.7304
$P_3$	6.6967		6.6981		6.6965	
$P_4$	6.6829	6.6908	6.6813	6.6909	6.7025	6.6991
$P_5$	6.6942		6.6946			
$P_6$	6.6877	6.6916	6.6864	6.6913		

for this thin reflector case that the counterconvergent trend imposed by the core-reflector interface is the predominant factor in the convergence pattern although the vacuum-interface boundary conditions have considerably more effect on the convergence pattern than was observed in the two previous thick reflector cases. Thus, for a thin reflector and discontinuity of the total macroscopic cross section at the core-reflector interface the interfacial boundary conditions dominate the convergence pattern although the vacuum-interface boundary conditions may play a significant role in the relative speed of convergence. Tables X and XI list the computed results for cases 5 and 6 for a reflected reactor which has  $c = 1.05$  in the core region. Here as with the other thick reflector cases the core-reflector interface dominates the convergence picture. For thick reflectors the interfacial boundary dominates the convergence pattern so strongly that the vacuum-interface boundary conditions have little or no effect on the convergence. Thus, as would be expected, the convergence trend for a reactor reflected with a thick reflector is always that of counterconvergence. Tables XII and XIII list the computed results for case 5 with the values of  $c$  in the core equal to 1.02 and 1.40 respectively. As with the previous thick reflector cases, the interfacial boundary dominates the convergence pattern. It is readily apparent that when the core region has  $c = 1.40$  the vacuum-interface boundary conditions have little or no effect on the convergence. In general the greater the discontinuity in the value of  $c$  at the core-reflector interface the greater the dominance of the interfacial boundary in the convergence pattern.

In all of the computed results for the reflected reactor cases the weighted average critical radii, whenever noted in the tables, converge more rapidly than the critical radii computed directly from the spherical harmonics

Table X. Calculated results for case 5 (reflected reactor)  
in which  $c$  is 1.05.

Approximation	Marshak's B.C.		Mark's B.C.		Variational B.C.	
	Critical radius	Weighted average	Critical radius	Weighted average	Critical radius	Weighted average
$P_1$	6.1999		6.2008		6.1995	
$P_2$	5.8765	6.0398	5.8757	6.0399	5.8757	6.0392
$P_3$	5.9697		5.9698		5.9697	
$P_4$	5.9416	5.9577	5.9414	5.9577	5.9416	5.9577
$P_5$	5.9580		5.9581			
$P_6$	5.9489	5.9544	5.9488	5.9544		

Table XI. Calculated results for case 6 (reflected reactor)  
in which  $c$  is 1.05.

Approximation	Marshak's B.C.		Mark's B.C.		Variational B.C.	
	Critical radius	Weighted average	Critical radius	Weighted average	Critical radius	Weighted average
$P_1$	7.4274		7.4281		7.4271	
$P_2$	6.9812	7.2066	6.9816	7.2071	6.9792	7.2054
$P_3$	7.1508		7.1511		7.1507	
$P_4$	7.0900	7.1248	7.0905	7.1252	7.0900	7.1247
$P_5$	7.1306		7.1307			
$P_6$	7.1069	7.1211	7.1069	7.1212		

Table XII. Calculated results for case 5 (reflected reactor)  
in which  $c$  is 1.02.

Approximation	Marshak's B.C.		Mark's B.C.		Variational B.C.	
	Critical radius	Weighted average	Critical radius	Weighted average	Critical radius	Weighted average
$P_1$	10.2116		10.2133		10.2109	
$P_2$	9.9998	10.1068	9.9982	10.1068	9.9984	10.1057
$P_3$	10.0359		10.0360		10.0358	
$P_4$	10.0254	10.0314	10.0251	10.0313	10.0254	10.0314
$P_5$	10.0318		10.0319			
$P_6$	10.0281	10.0303	10.0279	10.0303		

Table XIII. Calculated results for case 5 (reflected reactor)  
in which  $c$  is 1.40.

Approximation	Marshak's B.C.		Mark's B.C.		Variational B.C.	
	Critical radius	Weighted average	Critical radius	Weighted average	Critical radius	Weighted average
$P_1$	2.0657		2.0659		2.0657	
$P_2$	.9252	1.5012	.9252	1.5013	.9252	1.5012
$P_3$	1.8000		1.8000		1.8000	
$P_4$	1.5200	1.6803	1.5200	1.6803	1.5200	1.6803
$P_5$	1.7265		1.7265			
$P_6$	1.6187	1.6834	1.6187	1.6834		

approximations except that the  $|P_1, P_2|_{av}$  is usually not any better than the  $P_2$  result. These observations are in agreement with the bare spherical reactor cases for Mark's boundary conditions or the infinite black reflector boundary conditions.

In the cases considered here it is found that the spatial dependence of the total neutron flux is similar to that of Fig. 2. Figure 8 is a plot of the angular flux at the core-reflector interface as a function of  $\cos\theta$  as viewed from both sides of the boundary for a  $P_4$  approximation. It is apparent that there is a discontinuity in the angular flux across the boundary near  $\cos\theta = 0$  but that the dependence of the angular flux on the radial variable is more nearly continuous as  $\cos\theta$  approaches the value of  $\pm 1$ . This means that the normal component of the angular flux is nearly continuous at the interfacial boundary but that the tangential component is discontinuous. This condition arises from the fact that in an even order approximation the expression  $f_{\ell}(R) - P_{\ell}(0)(2\ell+1)f_0(R)$  is matched at the interfacial boundary. This expression can be shown (3) to be equivalent to removing the dependence of  $f(r, \mu)$  on  $r$  for small values of  $\mu(\cos\theta)$ ; thus allowing a discontinuity in  $f(R, \mu)$  for small values of  $\mu$ . The reason why  $f(r, \mu)$  is not continuous across the interface for values of  $\mu$  approaching unity is that a finite instead of infinite order of approximation is being utilized. A similar plot for an odd order approximation has the two curves in Fig. 8 coinciding since continuity of the angular flux at the interfacial boundary in an odd order approximation is required by Eq. (25).

From the preceding discussion of the computed results for reflected reactors three factors appear to be important in the convergence pattern. First, the relative thickness of the reflector in diffusion lengths is important. For thick reflectors the core-reflector interface dominates the



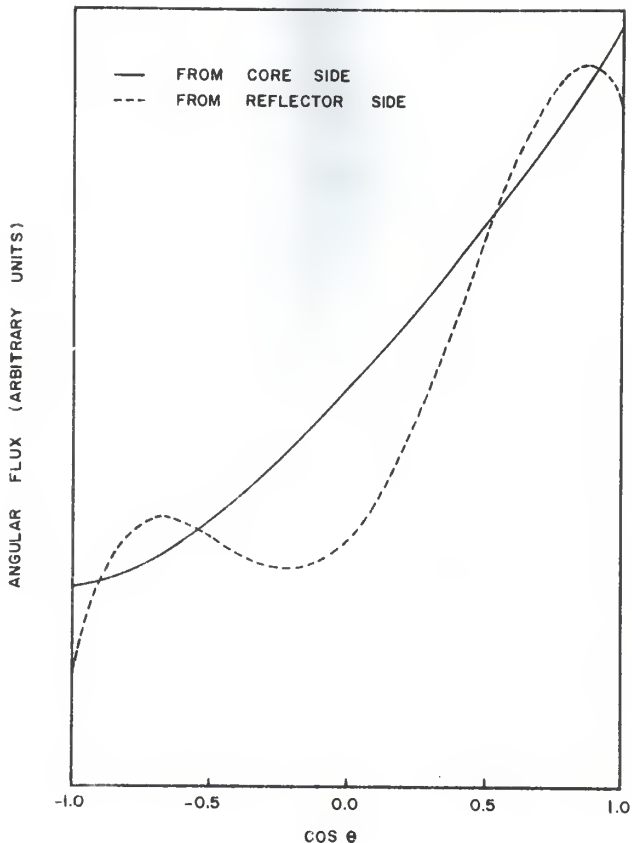


Figure 8. ANGULAR FLUX AS A FUNCTION OF  $\cos \theta$  AT THE CORE-REFLECTOR INTERFACE FOR A  $P_4$  APPROXIMATION.

convergence pattern and produces a counterconvergent trend. The second and third important factors in the convergence pattern are the relative size of the discontinuities in the values of the mean number of secondaries, and the total macroscopic cross section at the core-reflector interface. When a significant discontinuity in either  $c$  or  $\Sigma$  exists at the core-reflector interface the convergence pattern is one of counterconvergence, thus demonstrating that the interfacial boundary is the dominant factor in the convergence pattern for such cases even for a relatively thin reflector.

### 3.4 Conclusions

The  $A_0^*$  constant was assumed to be zero in computing the critical radius of a bare spherical reactor when all of the vacuum-interface boundary conditions except the infinite black reflector boundary conditions were used. The consequences of this assumption will now be considered. Both Mark's vacuum-interface boundary conditions and the infinite black reflector boundary conditions brought about convergence trends which counterconverged in a like manner. Since the infinite black reflector boundary conditions take  $A_0$  into account whereas Mark's boundary conditions do not, the assumption that  $A_0^*$  was zero at a vacuum interface seems entirely justified.

It has been found that in spherical geometry the  $P_2$  approximation is usually superior to the  $P_1$  approximation at least in terms of the prediction of the exact critical radius. For higher orders of approximations the odd order approximations were invariably found to be superior to their corresponding even order approximations. Thus the popular belief that the even order approximations are inferior to the odd order approximations is not entirely justified.

When Davison's formula, which predicts the accuracy of the  $L^{\text{th}}$  order approximation, was rearranged to yield weighting factors, it was seen to predict very accurate weighted average critical radii for the  $P_3$  and higher order approximations. Although Davison's formula was developed for slab geometry it was seen to be quite valid in spherical geometry as well. For the  $P_1$  and  $P_2$  approximations Davison's formula, as used here, was definitely incorrect indicating that for these low order approximations the higher order terms in Eq. (28) cannot be ignored.

In general for a bare spherical reactor the  $P_3$  approximation with variational boundary conditions yielded a critical radius which was about as accurate as a  $|P_5, P_6|_{av}$  using Mark's or the infinite black reflector boundary conditions, or the  $P_7$  result with Marshak's boundary conditions. The  $|P_L, P_{L+1}|_{av}$  for Mark's or the infinite black reflector boundary conditions yielded critical radii which were of the same order of accuracy as a more involved  $P_{L+2}$  approximation using Marshak's boundary conditions. This last observation was found to be invalid for the  $P_1$  and  $P_2$  approximations. For the  $P_1$  approximation the variational boundary conditions always gave the best estimate of the exact critical radius. For the  $P_2$  approximation no particular boundary condition consistently yielded the best estimate of the exact critical radius.

For reflected reactor cases a counterconvergent pattern in the convergence, due to the core-reflector interface, was predominant whenever; a.) the reflector was "thick"; b.) there was a large discontinuity in the value of the total macroscopic cross section,  $\Sigma$ , across the core-reflector interface; and/or c.) there was a large discontinuity in the mean number of secondaries per interaction,  $c$ , across the core-reflector interface. For all but the  $P_1$  and  $P_2$  approximations the weighted average critical radii for reflected reactors, in which the core-reflector interface dominated the convergence pattern, appeared to be closer to the exact critical radius than the results from either the even or odd order approximations.

## 4.0 SUGGESTIONS FOR FURTHER STUDY

In this study only a few representative values of  $c$  are chosen for investigation of the nature of the convergence of the spherical harmonics approximations. For large order of approximations (three or greater) when Davison's formula is used to find the weighting factors in Eq. (65) the weighted average critical radii appear to be very accurate. Unfortunately, the same cannot be said for the  $|P_1, P_2|_{av}$ . A study should be made of the higher order terms in Davison's formula so that it could be improved for low order approximations. Alternatively a study could be made to determine an empirical formula which would predict the values of the weighting factors over a wide range of values of  $c$ . If either of these studies were successful to any substantial degree, only the relatively simple  $P_1$  and  $P_2$  approximations would be needed to obtain a trustworthy critical radius.

The work done here can be extended to the simpler case of slab geometry by noting that the only difference between the slab and spherical geometries is the difference between the  $Q_2(x)$  and  $e^x$  geometrical functions. This extension would only involve some small changes in the computer program described in Appendix C. Also this work should be extended to multigroup approximations. It is possible that many parts of the program described in Appendix C could be used in such a study.

Since the variational boundary conditions were found to be the most accurate of all the boundary conditions considered, it is logical to suggest that they be extended to approximations higher than the  $P_3$  and  $P_4$  approximations used here if accuracies greater than those resulting from the  $P_3$  approximation are required. The odd order variational boundary conditions have been found to be more accurate than the corresponding even order variational boundary

conditions. Therefore the most fruitful results will probably be obtained by using the odd order variational boundary conditions.

## ACKNOWLEDGMENT

This author wishes to express his gratitude to Dr. J. O. Mingle whose original thinking prompted this study. Sincere thanks are extended also to Dr. J. O. Mingle for his advice, helpful suggestions and constructive criticism throughout the course of this study. Sincere appreciation is given to Dr. W. R. Kimel for his encouragement as well as to the Kansas State University Experiment Station, and the Atomic Energy Commission for their financial support. Special thanks must go to the Kansas State University Computing Center staff for their assistance and to the National Science Foundation who through their grant, G-24060, provided the necessary funds for the many hours of computer time utilized.

## LITERATURE CITED

1. Carlson, B. G. and G. I. Bell  
Solution of the Transport Equation by the  $S_N$  Method.  
Proc. 2<sup>nd</sup> Intern. Conf. Peaceful Uses of Atomic Energy, Geneva,  
16 (P/2386), 535, 1958.
2. Davison, B.  
On the Rate of Convergence of the Spherical Harmonics Method (For the  
Plane Case, Isotropic Scattering). Can. J. Phys., 38, 1526, 1960.
3. Davison, B. and J. B. Sykes  
Neutron Transport Theory. London: Oxford University, 1958.
4. Dawson, C.  
Modified  $P_2$  Approximations to the Neutron Transport Equation.  
David Taylor Model Basin, Report 1814, April, 1964.
5. Galanin, A. D.  
Thermal Reactor Theory. New York: Pergamon, 1960.
6. Glasstone, S.  
Principles of Nuclear Reactor Engineering.  
Princeton: Van Nostrand, 1955.
7. Hildebrand, F. B.  
Introduction to Numerical Analysis. New York: McGraw-Hill, 1956.
8. Jahnke, Eugen and Fritz Emde  
Tables of Functions with Formulae and Curves.  
4<sup>th</sup> ed. New York: Dover Publications, 1945.
9. Marchuk, G. I., Sh.S. Nikolaishvili, E. I. Pogudalina, Zh.N. Bel'skava,  
and N. P. Kochubei  
Application of the Spherical Harmonics Method to Transport Theory  
Problems.  $P_2$  Approximation. Theory and Methods of Nuclear Reactor  
Calculations, Edited by G. I. Marchuk. Authorized translation from  
the Russian. Consultants Bureau, New York, 1964.
10. Mark, C.  
The Spherical Harmonics Method, 1.  
Chalk River Project, Atomic Energy of Canada, Ltd., CRT-340 (revised),  
1957.
11. Mark, C.  
The Spherical Harmonics Method, 11.  
Chalk River Project, Atomic Energy of Canada, Ltd., CRT-338 (revised),  
1957.
12. Meghreblian, R. V. and D. K. Holmes  
Reactor Analysis. New York: McGraw-Hill, 1960.



13. Mingle, John O.  
Disadvantage Factors in Slab Geometry by the  $P_2$  Calculation.  
Nuc. Sci. and Eng., 11, 85, 1961.
14. Mingle, John O.  
Convergence Improvement of Disadvantage Factors by the Use of Even Order Spherical Harmonics Approximations. Nuc. Sci. and Eng., 15, 161, 1963.
15. Pomraning, G. C.  
An Improved Free-Surface Boundary Condition for the  $P_3$  Approximation.  
Nuc. Sci. and Eng., 18, 528, 1964.
16. Pomraning, G. C.  
Private Communication.  
General Electric Company, Pleasanton, Calif., Nov. 26, 1963.
17. Pomraning, G. C. and M. Clark, Jr.  
The Variational Method Applied to the Monoenergetic Boltzmann Equation, Part I. Nuc. Sci. and Eng., 16, 147, 1963.
18. Romyantsev, G. Ya.  
Boundary Conditions in the Method of Spherical Harmonics.  
The Soviet Journal of Atomic Energy, 10, 15, Nov., 1961.
19. Watson, G. N.  
Theory of Bessel Functions.  
2<sup>nd</sup> ed, Cambridge: Cambridge University Press, 1962.
20. Wayland, H.  
Differential Equations Applied in Science and Engineering.  
Princeton: Van Nostrand, 1957.
21. Weinberg, A. M. and E. P. Wigner  
The Physical Theory of Neutron Chain Reactors.  
Chicago: University of Chicago, 1958.
22. Wylie, C. R.  
Advanced Engineering Mathematics. New York: McGraw-Hill, 1951.

## APPENDICES

## APPENDIX A

The  $Q_\ell(x)$  and  $C_\ell(x)$  Functions

The  $Q_\ell(x)$  function is defined by Weinberg and Wigner (21) as

$$Q_\ell(x) = -\sqrt{\frac{2}{\pi(-x)}} K_{\ell+1/2}(-x), \quad Q_\ell(-x) = -\sqrt{\frac{2}{\pi x}} K_{\ell+1/2}(x) \quad (\text{A-1})$$

where  $K_{\ell+1/2}(x)$  is a modified Bessel function of the second kind. The  $Q_\ell(x)$  functions are  $2/\pi$  times the modified spherical Bessel functions of the third kind. Watson (19) defines the  $K_{\ell+1/2}(x)$  functions as

$$K_{\ell+1/2}(x) = \sqrt{\frac{\pi}{2x}} e^{-x} \sum_{j=0}^{\ell} \frac{(\ell+j)!}{j!(\ell-j)!(2x)^j}. \quad (\text{A-2})$$

Using Eq. (A-2) in Eq. (A-1) the  $Q_\ell(x)$  functions can be written out more explicitly as

$$Q_\ell(x) = \frac{e^x}{x} \sum_{j=0}^{\ell} \frac{(-1)^j (\ell+j)!}{j!(\ell-j)!(2x)^j}, \quad Q_\ell(-x) = -\frac{e^{-x}}{x} \sum_{j=0}^{\ell} \frac{(\ell+j)!}{j!(\ell-j)!(2x)^j}. \quad (\text{A-3})$$

The first few  $Q_\ell(x)$ 's are

$$Q_0(x) = \frac{e^x}{x}; \quad Q_1(x) = \frac{e^x}{x} \left(1 - \frac{1}{x}\right); \quad Q_2(x) = \frac{e^x}{x} \left(1 - \frac{3}{x} + \frac{3}{x^2}\right).$$

The recursion relationships for the  $Q_\ell(x)$  functions

$$Q_\ell(x) = Q_{\ell-2}(x) - \frac{2\ell-1}{x} Q_{\ell-1}(x), \quad (\text{A-4})$$

and

$$\left(\frac{d}{dx} + \frac{\ell+1}{x}\right) Q_\ell(x) = Q_{\ell-1}(x) \quad (\text{A-5})$$

follow immediately from the properties of Bessel functions.

In this work a new function,  $C_\ell(x)$  was defined as

$$C_\ell(x) = 1/2\{Q_\ell(x) + (-1)^\ell Q_\ell(-x)\}. \quad (\text{A-6})$$

The  $C_\ell(x)$  functions are the modified spherical Bessel functions of the first

kind. Mark (10,11) considers these functions<sup>1</sup> and shows that for small  $x$ ,

$$C_\ell(x) = \frac{x^\ell}{1 \cdot 3 \cdot 5 \cdots (2\ell+1)} (1 + O(x^2)) . \quad (A-7)$$

At this point it is necessary to investigate the finiteness of these functions at  $x = 0$ . Since

$$\lim_{x \rightarrow 0} C_\ell(x) = \lim_{x \rightarrow 0} \frac{x^\ell}{1 \cdot 3 \cdot 5 \cdots (2\ell+1)} (1 + O(x^2)) = C_\ell(0) = \begin{cases} 1, & \ell = 0 \\ 0, & \ell > 0, \end{cases} \quad (A-8)$$

the  $C_\ell(x)$  functions are thus bounded for a zero argument and so the total neutron flux is bounded at  $r = 0$  as is required in section 2.3.

The  $C_\ell(x)$  functions may be written as a combination of  $\sinh(x)$  and  $\cosh(x)$  terms. In this form the  $C_\ell(x)$  functions are, for  $\ell$  even

$$C_\ell(x) = \frac{\sinh(x)}{x} \sum_{j \text{ even}}^{\ell} \frac{(j+\ell)!}{j!(\ell-j)!(2x)^j} - \frac{\cosh(x)}{x} \sum_{j \text{ odd}}^{\ell} \frac{(j+\ell)!}{j!(\ell-j)!(2x)^j} , \quad (A-9)$$

and for  $\ell$  odd

$$C_\ell(x) = \frac{\cosh(x)}{x} \sum_{j \text{ even}}^{\ell} \frac{(j+\ell)!}{j!(\ell-j)!(2x)^j} - \frac{\sinh(x)}{x} \sum_{j \text{ odd}}^{\ell} \frac{(j+\ell)!}{j!(\ell-j)!(2x)^j} . \quad (A-10)$$

The arguments of the  $C_\ell(x)$  functions which are encountered in this work are either entirely real or entirely imaginary. Equations (A-3), (A-9), and (A-10) are appropriate for real arguments. The imaginary arguments arise only in the central core region in which the  $C_\ell(x)$  functions are used. In this region one of the roots  $\lambda_k$  is imaginary. The argument for the  $C_\ell(x)$  functions is  $Er/\lambda_k$ , so the form of the imaginary argument is  $x/i$  or  $-ix$ . For this type of imaginary argument the  $C_\ell(x)$  functions become, for  $\ell$  even

---

1 Mark actually defines a function  $H_k(x)$  which is the same as  $Q_k(x)$  in this development and considers the combination  $H_k(x) + (-1)^k H_k(-x)$  which differs from the  $C_k(x)$  used here only by a factor of two.

$$C_{\ell}(-ix) = \frac{\sin(x)}{x} \sum_{\substack{j=0 \\ j \text{ even}}}^{\ell} \frac{(-1)^{j/2} (\ell+j)!}{j! (\ell-j)! (2x)^j} + \frac{\cos(x)}{x} \sum_{\substack{j=1 \\ j \text{ odd}}}^{\ell} \frac{(-1)^{(j-1)/2} (\ell+j)!}{j! (\ell-j)! (2x)^j}, \quad (\text{A-11})$$

and for  $\ell$  odd

$$C_{\ell}(-ix) = -i \left\{ \frac{\sin(x)}{x} \sum_{\substack{j=1 \\ j \text{ odd}}}^{\ell} \frac{(-1)^{(j-1)/2} (\ell+j)!}{j! (\ell-j)! (2x)^j} - \frac{\cos(x)}{x} \sum_{\substack{j=0 \\ j \text{ even}}}^{\ell} \frac{(-1)^{j/2} (\ell+j)!}{j! (\ell-j)! (2x)^j} \right\} \quad (\text{A-12})$$

where  $x$  is entirely real. The fact that for odd  $\ell$ ,  $C_{\ell}(-ix)$  is imaginary is acceptable since in Eqs. (14), (22), and (23)  $G_{\ell}(\lambda_k)$  is imaginary for odd  $\ell$  and an imaginary root. Since  $-i^2 = +1$ , the product of  $G_{\ell}(i\lambda_k)$  and  $C_{\ell}(\Sigma r/i\lambda_k)$  for odd  $\ell$  will be positive and real.

## APPENDIX B

## Variational Boundary Conditions

Pomraning and Clark (17) have used the variational calculus to develop a set of consistent vacuum-interface boundary conditions. The fundamental equation of the variational boundary conditions at a right hand vacuum-interface boundary is

$$\int_{-1}^0 f(R, \mu) \delta f(R, -\mu) \mu d\mu = 0 . \quad (B-1)$$

In order to arrive at a set of coefficients  $b_{\ell j}$  which can be put into the form

$$\sum_{\ell=0}^L f_{\ell}(R) b_{\ell j} = 0 \quad j = 1, 2, \dots, [(L+1)/2] , \quad (B-2)$$

the angular flux will be expanded with the same Legendre polynomial expansion that Pomraning and Clark used, namely:

$$f(R, \mu) = \sum_{\ell=0}^L \left( \frac{2\ell+1}{2} \right) \phi_{\ell}(R) P_{\ell}(\mu) , \quad (B-3)$$

instead of the expansion

$$f(R, \mu) = \sum_{\ell=0}^L f_{\ell}(R) P_{\ell}(\mu) \quad (B-4)$$

which is used throughout most of this work. From Eqs. (B-3) and (B-4) it is recognized that

$$\phi_{\ell}(R) = \frac{2}{2\ell+1} f_{\ell}(R) . \quad (B-5)$$

Pomraning (16) has noted that in order to solve Eq. (B-1) there must be some linear combination of the moments,  $\phi_{\ell}(R)$ , at the boundary. These linear combinations can be put into the general form

$$\phi_{2[(L+1)/2]-m}(R) + \sum_{\ell=0}^{[(L-1)/2]} R_{\ell m} \phi_{\ell}(R) = 0 \quad \text{for } 1 \leq m \leq [(L+1)/2] . \quad (B-6)$$

For a  $P_1$  approximation this relationship reduces to

$$\phi_1(R) + R_{01}\phi_0(R) = 0 . \quad (B-7)$$

Substituting Eq. (B-3) into Eq. (B-1) and using Eq. (B-7) in the result, Eq. (B-1) for the  $P_1$  approximation becomes

$$\left\{ \frac{1}{8} - \frac{9}{16} R_{01}^2 \right\} \phi_0(R) \delta\phi_0(R) = 0 . \quad (B-8)$$

Since  $\phi_0(R)$  is not zero and  $\delta\phi_0(R)$  is an independent and arbitrary variation Eq. (B-8) can be an equality if and only if the coefficient of  $\phi_0(R)\delta\phi_0(R)$  is set to zero, in which case

$$\begin{aligned} R_{01}^2 &= 2/9 , \\ R_{01} &= \pm \sqrt{2}/3 . \end{aligned} \quad (B-9)$$

Physical considerations demand that the negative sign of Eq. (B-9) be used.

Considering Eqs. (B-5), (B-7), and (B-9) it is readily apparent that the coefficients  $b_{\ell j}$  in Eq. (B-2), for a  $P_1$  approximation, are given by

$$b_{01} = 1 , \quad b_{11} = -\sqrt{2} .$$

For a  $P_2$  approximation an additional equation is necessary. This additional equation comes directly from the spherical harmonics form of the Boltzmann transport equation. Using Eq. (B-3) instead of Eq. (B-4) to expand the angular flux, the spherical harmonics form of the Boltzmann neutron transport equation in slab geometry, subjected to the restrictions used throughout this work, becomes

$$\frac{\ell+1}{2\ell+1} \frac{d}{dx} \phi_{\ell+1}(x) + \frac{\ell}{2\ell+1} \frac{d}{dx} \phi_{\ell-1}(x) + \Sigma(1-c\delta_{\ell 0})\phi_{\ell}(x) = 0 . \quad (B-10)$$

For a  $P_2$  approximation these equations become

$$\frac{d}{dx} \phi_1(x) + \Sigma(1-c)\phi_0(x) = 0 , \quad (B-11)$$

$$\frac{2}{3} \frac{d}{dx} \phi_2(x) + \frac{1}{3} \frac{d}{dx} \phi_0(x) + \Sigma\phi_1(x) = 0 , \quad (B-12)$$

$$\frac{2}{5} \frac{d}{dx} \phi_1(x) + \Sigma \phi_2(x) = 0 . \quad (\text{B-13})$$

From Eqs. (B-1) and (B-13) the elimination of the  $\phi_1(x)$  dependence shows that

$$\phi_2(x) = \frac{2}{5} (1-c) \phi_0(x) . \quad (\text{B-14})$$

This is the required extra relationship. Now, substituting Eq. (B-3) into Eq. (B-1) and using Eqs. (B-7) and (B-14) in the result it is readily verified that the coefficients  $b_{kj}$  for a  $P_2$  approximation are

$$b_{01} = 1, \quad b_{11} = -\sqrt{2}\{1 + (1-c) + (1-c)^2\}^{1/2}, \quad b_{21} = 0 .$$

The  $P_3$  variational boundary conditions have been worked out by Pomraning (15). Using Eqs. (B-6) and (B-3) in Eq. (B-1), defining  $R_{01} = A$ ,  $R_{11} = B$ ,  $R_{02} = C$ , and  $R_{12} = D$  for simplicity and setting to zero the coefficients of  $\phi_0 \delta \phi_0$ ,  $\phi_0 \delta \phi_0$ ,  $\phi_1 \delta \phi_0$  and  $\phi_1 \delta \phi_1$  (where the arguments have been omitted to shorten the expressions) yields four nonlinear equations for the four unknowns, A through D:

$$\frac{1}{8} - \frac{5}{16} C + \frac{25}{32} C^2 - \frac{147}{128} A^2 = 0 , \quad (\text{B-15})$$

$$\frac{1}{4} - \frac{5}{32} D - \frac{1}{2} C + \frac{25}{32} CD + \frac{3}{4} BC + \frac{7}{32} A - \frac{3}{4} AD - \frac{147}{128} AB = 0 , \quad (\text{B-16})$$

$$-\frac{1}{4} - \frac{5}{32} D + \frac{1}{2} C + \frac{25}{32} CD - \frac{3}{4} BC + \frac{7}{32} A + \frac{3}{4} AD - \frac{147}{128} AB = 0 , \quad (\text{B-17})$$

$$-\frac{9}{16} + \frac{7}{16} B + \frac{25}{32} D^2 - \frac{147}{128} B^2 = 0 . \quad (\text{B-18})$$

By appropriately manipulating Eqs. (B-15) through (B-18) it can be shown that they are equivalent to

$$16 - 40C + 100C^2 - 147A^2 = 0 , \quad (\text{B-19})$$

$$20CD - 70AC + 49A - 16D = 0 , \quad (\text{B-20})$$

$$1 - 2C + 3BC - 3AD = 0 , \quad (\text{B-21})$$

$$-72 + 56B + 100D^2 - 147B^2 = 0 . \quad (\text{B-22})$$



At this point the  $P_4$  variational boundary conditions will be considered. As with the  $P_2$  case one extra equation will be required. This extra equation again comes directly from the spherical harmonics equations. It is found to be

$$\phi_4(x) + \frac{20}{27} \phi_2(x) + \frac{8}{27} (1-c) \phi_0(x) = 0 . \quad (B-23)$$

Using Eqs. (B-6), (B-3) and (B-23) in Eq. (B-1), again defining  $R_{01} = A$ ,  $R_{11} = B$ ,  $R_{02} = C$ , and  $R_{12} = D$  for simplicity and setting to zero the coefficients of  $\phi_0 \delta \phi_0$ ,  $\phi_0 \delta \phi_1$ ,  $\phi_1 \delta \phi_0$ , and  $\phi_1 \delta \phi_1$ , yields, after considerable algebraic manipulation, four nonlinear equations for the four unknowns, A through D:

$$\begin{aligned} \frac{1}{8} + \frac{1}{36} (1-c) + \frac{1}{8} (1-c)^2 + \left\{ -\frac{35}{144} + \frac{245}{288} (1-c) \right\} C + \frac{1225}{576} C^2 \\ - \frac{147}{128} A^2 = 0 , \end{aligned} \quad (B-24)$$

$$\begin{aligned} \frac{1}{4} + \left\{ -\frac{35}{288} + \frac{245}{576} (1-c) \right\} D - \frac{1}{2} C + \frac{1225}{576} CD + \frac{161}{108} BC + \frac{7}{32} A \\ - \frac{161}{108} AD - \frac{147}{128} AB + \frac{8}{27} (1-c) B = 0 , \end{aligned} \quad (B-25)$$

$$\begin{aligned} -\frac{1}{4} + \left\{ -\frac{35}{288} + \frac{245}{576} (1-c) \right\} D + \frac{1}{2} C + \frac{1225}{576} CD - \frac{161}{108} BC + \frac{7}{32} A \\ + \frac{161}{108} AD - \frac{147}{128} AB - \frac{8}{27} (1-c) B = D , \end{aligned} \quad (B-26)$$

$$-\frac{9}{16} + \frac{7}{16} B + \frac{1225}{576} D^2 - \frac{147}{128} B^2 = 0 . \quad (B-27)$$

By appropriately manipulating Eqs. (B-24) through (B-27) they can be shown to be equivalent to

$$\begin{aligned} 144 + 32(1-c) + 144(1-c)^2 + \{-280 + 980(1-c)\}C \\ + 2450C^2 - 1323A^2 = 0 , \end{aligned} \quad (B-28)$$

$$\begin{aligned} \{22540 - 490(1-c)\}CD - 30870AC + \{35721 + 8064(1-c)\}A \\ - \{23184 + 9632(1-c) + 75509(1-c)^2\}D = 0 , \end{aligned} \quad (B-29)$$

$$27 - 54C + 161BC - 161AD + 32(1-c)B = 0 , \quad (\text{B-30})$$

$$- 648 + 504B + 2450B^2 - 1323B^2 = 0 . \quad (\text{B-31})$$

Equations (B-28) through (B-31) are in a convenient form for numerical solution. Given a particular value of  $c$ , if a value is assumed for  $C$ , Eq. (B-28) can be solved for  $A$ , then Eq. (B-29) can be solved for  $D$ , and finally Eq. (B-30) can be solved for  $B$ . Equation (B-31) is then used as a consistency check. Equations (B-19) through (B-23) can be solved in exactly the same manner. A computer program is used to compute the values of  $A$ ,  $B$ ,  $C$ , and  $D$ . In iterating to the value of  $C$  which best satisfies the consistency check equation a relative accuracy of  $10^{-13}$  is employed. Since only eight or nine digits are retained in the final results, this accuracy is deemed satisfactory. A list of the calculated values of the constants  $A$ ,  $B$ ,  $C$ , and  $D$  appear in Table B-I. The CMEAN column indicates the value of  $c$  used to find the corresponding constants  $A$ ,  $B$ ,  $C$ , and  $D$ .

The  $P_4$  Marshak boundary conditions when put into the format of Eq. (B-6) yield the following values for  $A$ ,  $B$ ,  $C$ , and  $D$ :

$$A = + \frac{9}{4} ,$$

$$B = - \frac{5}{4} \left\{ 1 + \frac{1}{4} (1-c) \right\} ,$$

$$C = \frac{1}{35} \{ 36 + 4(1-c) \} ,$$

$$D = - \frac{72}{35} .$$

The variational boundary condition constants for the  $P_4$  approximation are seen to be slightly larger in absolute value than the comparable Marshak boundary conditions when  $c = 1.0$ . Using the  $P_4$  variational boundary condition coefficients  $A$ ,  $B$ ,  $C$ , and  $D$  corresponding to  $c = 1.0$ , the Milne problem extrapolation distance is found to be .708554 mean free paths.

Table B-1

CONSTANTS FOR VARIATIONAL BOUNDARY CONDITIONS  
(RIGHT HAND BOUNDARY)

## P 3 APPROXIMATION

A	B	C	D
.53259050	-.86892612	.74494897	-1.52200413

## P 4 APPROXIMATION

CMEAN	A	B	C	D
.00	2.41228043	-3.34191842	1.59843785	-2.64252082
.05	2.35642719	-3.31748672	1.56770363	-2.62488705
.10	2.30118333	-3.29258481	1.53741249	-2.60691839
.15	2.24657098	-3.26720520	1.50758036	-2.58860980
.20	2.19261313	-3.24134083	1.47822382	-2.56995656
.25	2.13933361	-3.21498508	1.44936005	-2.55095430
.30	2.08675713	-3.18813189	1.42100682	-2.53159909
.35	2.03490930	-3.16077590	1.39318254	-2.51188751
.40	1.98381658	-3.13291247	1.36590625	-2.49181671
.45	1.93350634	-3.10453787	1.33919758	-2.47138453
.50	1.88400678	-3.07564938	1.31307676	-2.45058955
.55	1.83534696	-3.04624546	1.28756463	-2.42943124
.60	1.78755677	-3.01632585	1.26268256	-2.40791005
.65	1.74066682	-2.98589179	1.23845245	-2.38602751
.70	1.69470847	-2.95494615	1.21489668	-2.36378638
.75	1.64971370	-2.92349363	1.19203804	-2.34119078
.80	1.60571501	-2.89154096	1.16989967	-2.31824632
.81	1.59703770	-2.88509116	1.16556049	-2.31361617
.82	1.58840181	-2.87862178	1.16125124	-2.30897242
.83	1.57980762	-2.87213292	1.15697212	-2.30431513
.84	1.57125538	-2.86562467	1.15272331	-2.29964438
.85	1.56274537	-2.85909711	1.14850500	-2.29496024
.86	1.55427785	-2.85255035	1.14431738	-2.29026279
.87	1.54585309	-2.84598450	1.14016064	-2.28555211
.88	1.53747135	-2.83939965	1.13603497	-2.28082828
.89	1.52913290	-2.83279592	1.13194056	-2.27609140
.90	1.52083802	-2.82617344	1.12787759	-2.27134155
.91	1.51258696	-2.81953231	1.12384627	-2.26657883
.92	1.50433799	-2.81287266	1.11984676	-2.26180333
.93	1.49621739	-2.80619463	1.11587927	-2.25701515
.94	1.48809942	-2.79949834	1.11194398	-2.25221440
.95	1.48002634	-2.79278394	1.10804108	-2.24740119

CMEAN	A	B	C	D
.96	1.47199843	-2.78605158	1.10417076	-2.24257562
.97	1.46401594	-2.77930139	1.10033320	-2.23773782
.98	1.45607914	-2.77253353	1.09652860	-2.23288789
.99	1.444818831	-2.76574817	1.09275714	-2.22802596
1.00	1.44034369	-2.75894546	1.08901900	-2.22315215
1.01	1.43254557	-2.75212557	1.08531437	-2.21826660
1.02	1.42479419	-2.74528868	1.08164344	-2.21336943
1.03	1.41708983	-2.73843496	1.07800638	-2.20846079
1.04	1.40943274	-2.73156461	1.07440339	-2.20354080
1.05	1.40182318	-2.72467780	1.07083465	-2.19860962
1.06	1.39426141	-2.71777474	1.067330033	-2.19366739
1.07	1.38674770	-2.71085562	1.06380062	-2.18871427
1.08	1.37928229	-2.70392065	1.06033570	-2.18375040
1.09	1.37186545	-2.69697005	1.05690574	-2.17877596
1.10	1.36449742	-2.69000401	1.05351093	-2.17379109
1.11	1.35717846	-2.68302278	1.05015143	-2.16879597
1.12	1.34990882	-2.67602657	1.04682743	-2.16379077
1.13	1.34268875	-2.66901562	1.04353910	-2.15877567
1.14	1.33551849	-2.66199016	1.04028660	-2.15375084
1.15	1.32839830	-2.65495045	1.03707012	-2.14871647
1.16	1.32132841	-2.64789673	1.03388981	-2.14367274
1.17	1.31430906	-2.64082925	1.03074585	-2.13861984
1.18	1.30734050	-2.63374829	1.02763840	-2.13355798
1.19	1.30042296	-2.62665410	1.02456763	-2.12848735
1.20	1.29355667	-2.61954695	1.02153370	-2.12340815
1.25	1.26000204	-2.58382691	1.00692210	-2.09789111
1.30	1.22776225	-2.54782731	.99325449	-2.07219285
1.35	1.19686312	-2.51158873	.98054847	-2.04634346
1.40	1.16732806	-2.47515527	.96881987	-2.02037550
1.45	1.13917774	-2.43857439	.95808245	-1.99432388
1.50	1.11242969	-2.40189670	.94834763	-1.96822571
1.55	1.08709796	-2.36517566	.93962430	-1.94212008
1.60	1.06319282	-2.32846719	.93191850	-1.91604772
1.65	1.04072041	-2.29182922	.92523332	-1.89005070
1.70	1.01968254	-2.25532115	.91956862	-1.86417200
1.75	1.00007647	-2.21900323	.91492102	-1.83845509
1.80	.98189480	-2.18293593	.91128374	-1.81294343
1.85	.96512544	-2.14717924	.90864659	-1.78767998
1.90	.94975159	-2.11179197	.90699607	-1.76270668
1.95	.93575191	-2.07683103	.90631539	-1.73806394
2.00	.92310068	-2.04235081	.90658468	-1.71379019

Employing Eq. (B-5) in Eq. (B-6) it can be shown that for the  $P_3$  and  $P_4$  approximations the coefficients  $b_{kj}$  for the variational boundary conditions are

$$b_{01} = A, b_{11} = B/3, b_{21} = 0, b_{31} = 1/7, b_{41} = 0 ;$$

$$b_{02} = C, b_{12} = D/3, b_{22} = 1/5, b_{32} = 0, b_{42} = 0 .$$

## APPENDIX C

## C.O Description and Explanation of Computer Programs

The group of programs discussed here calculate the critical radius and subsidiary quantities using a  $P_L$  approximation with any one of the appropriate boundary conditions applied at the vacuum interface. The programs are written for the IBM 1410 computer in the FORTRAN 11 language. The program is set up to handle  $P_1$  through  $P_{10}$  approximations for a bare spherical reactor and  $P_1$  through  $P_6$  approximations for a reflected spherical reactor. Since the size of the core storage of the available computer is only 40,000 characters it is necessary to divide the complex program into six phases. In addition each phase is subdivided into a number of subprograms. The following list indicates the order in which the subprograms are arranged within the particular phases:

BOLTZMANN1	BOLTZMANN2	BOLTZMANN3
INPUT	MARSHK	CRITEQ
POLYCO	BCMARS	SETUPA
POLYNO	MARKBC	CRAM
EIGEN	PNP1	DET
SETUPG	VAR1BC	C
ROOT	FOJREQ	CSER
P (short)	NONLIN	Q
FACT	P (long)	ROOT
	FACT	P (short)
		FACT
BOLTZMANN4	BOLTZMANN5	BOLTZMANN6
CRAM	INTOUT	OUTPUT
SOLVE	PHIL	PLOT
RESIDU	C	
	CSER	
	Q	
	P (long)	
	FACT	

Each of the programs in this list will be considered later in this appendix.

The input data is divided into two parts. The proper sequence for loading the first part of the input data is shown in the BOLTZMANN1 program and the INPUT subprogram. The meaning of the symbols used in these programs is given in Table C-I. The second part of the necessary input data is discussed under the PLOT subprogram.

Table C-1  
Input Data

Symbol	Explanation
NCASES	Number of cases to be considered in this computer run
NORDER	Order of approximation, L
NREG	Number of regions to be considered = 1 for bare reactors = 2 for reflected reactors including the infinite black reflector case
NBC	Code number for vacuum-interface boundary condition to be applied = 1 for Marshak's boundary conditions = 2 for Mark's boundary conditions = 3 for variational boundary conditions = 4 for infinite black reflector boundary conditions
ACCR	Relative accuracy to be employed in iterations
IHOLD	= 0 skip extra results and graphs used in program testing = 1 print extra results used in program testing
IHOLD2	= 0 skip graphs used in program testing = 1 print graphs used in program testing
C(1)	Mean number of secondaries, $c$ , in the core region
SIGMA(1)	Total macroscopic cross section, $\Sigma$ , in the core region in $\text{cm}^{-1}$
C(2)	Mean number of secondaries, $\bar{c}$ , in the reflector region
SIGMA(2)	Total macroscopic cross section, $\bar{\Sigma}$ , in the reflector region in $\text{cm}^{-1}$
REFLTH	Reflector thickness, $R_0$ (cm)

A sample page of output is shown in Table C-11. Most of the output is self explanatory. The output shown in Table C-II is punched on cards as well as being printed. Since output occurs in the first and last phases a special card consisting of the number of the case in columns 1-5 and periods in the remaining 75 columns is punched for convenient separation of the cards

Table C-II. Sample page of output

P<sup>2</sup> APPROXIMATION  
OF THE ONE VELOCITY BOLTZMANN TRANSPORT EQUATION BY  
THE SPHERICAL HARMONICS METHOD IN SPHERICAL GEOMETRY.

BAKE CORE  
VARIATIONAL VACUUM INTERFACE BOUNDARY CONDITIONS  
IN THE CORE C = 1.0500 , SIGMA = .1000 /CM.  
THE ACCURACY USED IS 1.0E-07

THE COMPUTED CRITICAL RADIUS IS 72.7644 CM.  
OR, 7.2764 MEAN FREE PATHS.  
THE INTEGRATED INWARD ANGULAR FLUX AT THE  
VACUUM INTERFACE IS 7.010E-04

IN THE CORE

EIGEN VALUES

2.53185E 00 5.17133E-01

G(L,K) MATRIX

1.00000E 00	1.26592E-01	-1.92287E-02	-3.25449E-03
1.00000E 00	2.58566E-02	-5.20057E-01	4.30994E-01

BOUNDARY CONDITION MATRIX

5.32590E-01	-2.89640E-01	0.00000E-00	1.42857E-01
7.44948E-01	-5.07333E-01	2.00000E-01	0.00000E-00

NORMALIZED COEFFICIENTS

7.95775E-02 -1.98469E-08

DATA FOR ANGULAR FLUX PLOT AT THE OUTER BOUNDARY

MU	PHI(MU)	MU	PHI(MU)	MU	PHI(MU)
1.0	2.007E-02	.3	8.797E-03	-.4	2.544E-04
.9	1.858E-02	.2	7.227E-03	-.5	-2.885E-04
.8	1.702E-02	.1	5.736E-03	-.6	-5.940E-04
.7	1.540E-02	.0	4.347E-03	-.7	-6.393E-04
.6	1.374E-02	-.1	3.081E-03	-.8	-4.016E-04
.5	1.208E-02	-.2	1.962E-03	-.9	1.417E-04
.4	1.042E-02	-.3	1.012E-03	-1.0	1.013E-03



belonging to different cases. In Table C-II the EIGEN VALUES are the roots  $\lambda_k$  arranged so that reading from right to left on each successive line the first value encountered is the imaginary root (for a core region) and then the remaining real roots in order of decreasing magnitude. The  $G(L,K)$ ,  $G_\ell(\lambda_k)$ , and BOUNDARY CONDITION,  $b_{\ell j}$ , matrices are arranged so that the second subscript is the row number and  $\ell$  is the column number. If  $\ell$  exceeds 4 then the remainder of a particular row appears on succeeding lines. The NORMALIZED COEFFICIENTS are the  $A_k$ 's and correspond in position to the roots  $\lambda_k$  listed under EIGEN VALUES. The PHI(MU) column in the inward flux section is whichever of  $f(R,\mu)$  or  $f(R+R_0,\mu)$  is representative of the vacuum interface.

Approximately ten minutes is required to compute the results shown in Table C-II if this problem is run with 5 or more cases.

The sense switches do not alter the program when they are in the off position. The changes which occur when they are in the on position are shown in Table C-III.

Table C-III  
Sense Switches

Switch	Phase	Operation when Switch is on
6	BOLTZMANN1	Prints convergence in an iteration loop for testing purposes
6	BOLTZMANN2	Prints convergence in an iteration loop for testing purposes
6	BOLTZMANN3	Prints convergence in an iteration loop for testing purposes
1	BOLTZMANN5	Sets IHOLD in Table C-I to the value of 1
1	BOLTZMANN6	Sets IHOLD2 in Table C-I to the value of 1

#### C.1 BOLTZMANN1 Program

This program is the control program for the first phase. In the first phase the input data is read and the preliminary output is printed. The roots

$\lambda_k$ , the  $G_\ell(\lambda_k)$  matrix and an initial lower bound estimate of the critical radius are computed. The lower bound estimate of the critical radius is obtained by solving a  $P_2$  bare spherical reactor problem.

### C.2 INPUT Subprogram

This subprogram reads all of the input for a particular case to be run and prints the preliminary output data.

### C.3 POLYCO Subprogram

Given a value of  $c$  this subprogram sets up the coefficients of the alternate powers of  $\lambda_k$  in Eq. (15). Using Eq. (14), Eq. (15) can be written as

$$G_{L+1}(\lambda_k) = (-1)^{L+1} \{ P_{L+1}(\lambda_k) - c \lambda_k W_L(\lambda_k) \} = 0 \quad (C-1)$$

The Legendre polynomials  $P_n(x)$ , and the non-singular part of the Legendre polynomials of the second kind,  $W_{n-1}(x)$ , can be written as simple summations (20)

$$P_n(x) = \sum_{i=0}^{[n/2]} \frac{(-1)^i (2n-2i)!}{2^n i! (n-i)! (n-2i)!} x^{n-2i} \quad (C-2)$$

$$W_{n-1}(x) = \sum_{\ell=1}^n \frac{1}{\ell} P_{\ell-1}(x) P_{n-\ell}(x) \quad (C-3)$$

Using Eqs. (C-2) and (C-3) in Eq. (C-1) it is found that the coefficient of  $\lambda_k^{n-2m}$  where  $n$  is  $L+1$  and  $m$  is an index running from 0 to  $[L/2]$  in value is

$$\frac{(-1)^n}{2^n} \left\{ \frac{(-1)^m (2n-2m)!}{m! (n-m)! (n-2m)!} - 2c \sum_{\ell=1}^n \sum_{j=0}^M \sum_{k=0}^N \frac{(-1)^{j+k} (2\ell-2j-2)! (2\ell-2k-2)!}{\ell(\ell-1-j)! (\ell-1-2j)! k! j! (n-\ell-k)! (n-\ell-2k)!} \delta_{m, j+k} \right\}$$

where  $M =$  the lesser of  $(\ell-1)/2$  and  $m$ ,

$N =$  the lesser of  $(k-\ell)/2$  and  $m$ .

This is the expression used in this subprogram to compute the coefficient of

$\lambda_k^{n-2m}$ . The coefficients are arranged for descending alternate powers of  $\lambda_k$  in the column matrix POLY.

#### C.4 POLYNO Subprogram

Given a value of  $\lambda_k$  this subprogram computes the value of  $G_{L+1}(\lambda_k)$  after POLYCO has set up the coefficients of  $\lambda_k$  in POLY. This subprogram is used as an auxilliary subprogram by EIGEN in finding the roots of Eq. (C-1).

#### C.5 EIGEN Subprogram

This subprogram supervises the finding of the roots  $\lambda_k$  of Eq. (C-1). For a core region the signs of alternate coefficients in POLY are changed to find the imaginary root. After the imaginary root has been found the signs of the coefficients in POLY are returned to their original state and the remaining real roots are found. For a reflector region the subprogram finds the real roots immediately. The real roots are stored in order of decreasing magnitude. All roots are stored in EIGENV.

#### C.6 SETUPG Subprogram

This subprogram sets up the  $G_\ell(\lambda_k)$  matrix. The definition that  $G_0(\lambda_k) = 1$  for all  $\lambda_k$  is used for the first row of the matrix. By setting  $\ell = 1$  in Eq. (14) and noting that  $W_0(\lambda_k) = 1$  it is readily apparent that

$$G_1(\lambda_k) = (c-1)\lambda_k .$$

This last equation is used to find the  $G_1(\lambda_k)$ 's. The remaining  $G_\ell(\lambda_k)$ 's are found by applying the recursion relationship for these functions, Eq. (13).

#### C.7 ROOT Subprogram

This subprogram is used to find the zero's of a function  $f(x)$ . The function  $f(x)$  is specified by a subprogram whose name is given as the first

argument of the calling statement. Given two limits between which a zero of  $f(x)$  exists, this subprogram finds that zero to within the relative accuracy specified in the calling statement. The method used in finding the zero's of  $f(x)$  is to apply a first order Newton interpolation formula (22). A complete description of this subprogram is on file at the K.S.U. Computing Center.

#### C.8 P (short) Subprogram

This subprogram computes the value of  $P_n(0)$ . Setting  $x = 0$  in Eq. (C-2) the equation for  $P_n(0)$  is found to be

$$P_n(0) = \begin{cases} 0, & n \text{ odd} \\ \frac{(-1)^{n/2} n!}{2^n \{(n/2)!\}^2}, & n \text{ even} \end{cases} \quad (\text{C-4})$$

#### C.9 FACT Subprogram

Given a positive integer argument,  $n$ , this subprogram finds the value of " $n!$ ". A detailed description of this subprogram is on file in the K.S.U. Computing Center.

#### C.10 BOLTZMANN2 Program

This program is the control program for the second phase. The second phase sets up the vacuum interface boundary condition matrix whose elements are  $b_{ij}$  in the computer variable BC.

#### C.11 MARSHK Subprogram

This subprogram in conjunction with BCMARS sets up the coefficients  $b_{ij}$  in BC corresponding to Marshak's vacuum-interface boundary conditions.

#### C.12 BCMARS Subprogram

This subprogram computes the numerical values of  $b_{ij}$  for Marshak's vacuum-interface boundary conditions for which

$$b_{\ell j} = \int_{-1}^0 P_{\ell}(\mu) \mu^{2j-1} d\mu . \quad (C-5)$$

Employing Eq. (C-2) in Eq. (C-5) and doing the indicated integration analytically Eq. (C-5) becomes

$$b_{\ell j} = (-1)^{\ell+1} \sum_{k=0}^{[\ell/2]} \frac{(-1)^k (2\ell-2k)!}{2^k k! (\ell-k)! (\ell-2k)! (\ell+2j-2k)} . \quad (C-6)$$

Equation (C-6) is used to evaluate the  $b_{\ell j}$ 's for Marshak's boundary conditions except when  $\ell = 0$  in which case

$$b_{0j} = 1/2j$$

is used.

### C.13 MARKBC Subprogram

This subprogram in conjunction with PNP1 sets up the coefficients  $b_{\ell j}$  in BC corresponding to Mark's vacuum-interface boundary conditions. First the roots of

$$P_{L+1}(\mu_j) = 0, \quad \mu_j < 0 \quad (C-7)$$

are found and then the value of  $b_{\ell j}$  is computed from

$$b_{\ell j} = P_{\ell}(\mu_j) . \quad (C-8)$$

Equation (C-8) is used to evaluate the  $b_{\ell j}$  coefficients, which are stored in BC, for Mark's boundary conditions.

### C.15 VARIBC Subprogram

This subprogram supervises the assemblage of the  $b_{\ell j}$  coefficients for the variational vacuum-interface boundary conditions. The variational coefficients  $b_{\ell j}$  are defined in Appendix B. For the  $P_3$  and  $P_4$  approximations it is necessary to solve a set of four nonlinear equations. This subprogram sets up a matrix, CO, of the coefficients in these nonlinear equations and supervises the solving of these equations.

## C.16 FOUREQ Subprogram

This subprogram is an auxilliary subprogram used by VARIBC in finding the solution of the four nonlinear equations for the variational boundary conditions.

## C.17 NONLIN Subprogram

Given a guessed value of C this subprogram solves three of the nonlinear equations representing the variational boundary conditions and uses the fourth equation as a consistency check.

## C.18 P (long) Subprogram

This subprogram computes the values of the Legendre polynomial  $P_n(x)$ . In order to obtain good accuracy for small values of x, Eq. (C-2) is rearranged into the form

$$P_n(x) = \frac{(-1)^n}{2^n} \sum_{k=0}^m \frac{(-1)^k (2n-2m-2k)! x^{n-2m-2k}}{(m-k)! (n-m+k)! (n-2m+2k)!} \quad (C-9)$$

where

$$m = [n/2] .$$

Equation (C-9) is used to compute  $P_n(x)$  except when  $x = 0$  in which case Eq. (C-4) is used. A detailed description of this subprogram is on file at the K.S.U. Computing Center.

## C.19 BOLTZMANN3 Program

This program is the control program for the third phase. The third phase sets up the T matrix in Eq. (44) in the computer variable A and iterates to find a critical radius which satisfies Eq. (60).

### C.20 CRITEQ Subprogram

This subprogram is an auxiliary subprogram used by BOLTZMANN3 in iterating on Eq. (60) to find the critical radius.

### C.21 SETUPA Subprogram

This subprogram sets up the T matrix in the two-dimensional computer variable A for the particular reactor system being considered.

### C.22 CRAM Subprogram

This subprogram performs the first step in a Crout reduction method of solving a matrix equation. The first step in the Crout reduction is to reduce the given Matrix to an upper right triangular matrix. The Crout reduction formulas for this first step are given as (7)

$$a'_{ij} = a_{ij} - \sum_{k=1}^{j-1} a'_{ik} a'_{kj} \quad \text{for } i \geq j,$$

$$a'_{ij} = \frac{1}{a'_{ii}} \left\{ a_{ij} - \sum_{k=1}^{i-1} a'_{ik} a'_{kj} \right\} \quad \text{for } i < j$$

where the primes denote the transformed elements. This subprogram has special provisions which allow imaginary row interchanges so as to maximize the diagonal in the reduction process. A detailed description of this subprogram is on file at the K.S.U. Computing Center.

### C.23 DET Subprogram

This subprogram calculates the determinant of a given matrix after CRAM has reduced the matrix to an upper right triangular matrix. Since the matrix is in the upper right triangular form the determinant of a transformed n by n matrix A' is

$$|A'| = (-1)^{\sum_{i=1}^n} \prod_{i=1}^n a'_{ii}$$

where  $\ell$  is the number of imaginary row interchanges used. A detailed description of this subprogram is on file in the K.S.U. Computing Center.

#### C.24 C Subprogram

This subprogram calculates the values of the  $C_{\ell}(x)$  functions. For real arguments Eq. (A-6) is used whereas for imaginary arguments whichever of Eqs. (A-11) or (A-12) is appropriate is used.

#### C.25 CSER Subprogram

This subprogram evaluates the finite sums in Eqs. (A-11) and (A-12) for the C subprogram.

#### C.26 Q Subprogram

This subprogram computes the values of  $Q_{\ell}(x)$  by using Eq. (A-3). A detailed description of this subprogram is on file in the K.S.U. Computing Center.

#### C.27 BOLTZMANN4 Program

This program is the control program for the fourth phase. The fourth phase having been given the critical radius by the third phase assumes  $A_1$  is one and solves for the remaining  $A_k$  and  $\bar{A}_k$  constants in the column matrix X.

#### C.28 SOLVE Subprogram

This subprogram solves a matrix equation of the form

$$AX = B \quad (C-10)$$

for the column matrix X after CRAM has reduced the matrix A to an upper right triangular matrix. The formulas used in this second step of the Crout reduction are (7)

$$b_i^! = \frac{1}{a_{ii}^!} \left\{ b_i^! - \sum_{k=1}^{i-1} a_{ik}^! b_k^! \right\}$$



and

$$x_i = b_i' - \sum_{k=i+1}^n a_{ik}' x_k$$

where the primes denote transformed quantities. A detailed description of this subprogram is on file in the K.S.U. Computing Center.

#### C.29 RESIDU Subprogram

This subprogram minimizes the error incurred in using the Crout reduction method of solving a matrix equation. After CRAM and SOLVE have been used to find a solution X this subprogram computes the product of the matrix A and the solution X and subtracts the result from the column matrix B in Eq. (C-10). Then CRAM and SOLVE are again used to solve Eq. (C-10) for a new column matrix X. This result is used to reduce the column matrix B in the same manner as before and then it is added to the old column matrix X. Then a new column matrix X is found by solving Eq. (C-10). The iteration is continued until the column matrix X determined after the  $n^{\text{th}}$  iteration is negligible (to within the accuracy of the computer) with respect to the sum of the results of the first  $n-1$  iterations. A detailed description of this subprogram is on file in the K.S.U. Computing Center.

#### C.30 BOLTZMANN'S Program

This program is the control program for the fifth phase. The fifth phase computes all of the data which will be printed in the final output. The amount of data which is computed is governed by the input constant IHOLD or sense switch 1.

## C.31 INTOUT Subprogram

This subprogram computes all of the necessary data for the final output. The amount of computation done is controlled by the input constant IHOLD or sense switch 1.

## C.32 PHIL Subprogram

This subprogram computes the value of  $f_{\ell}(r)$ . If  $r$  represents a point which is in the core region,

$$f_{\ell}(r) = (2\ell+1) \sum_{k=1}^{[(L+1)/2]} A_k G_{\ell}(\lambda_k) C_{\ell}(\epsilon r / \lambda_k) \quad (C-11)$$

whereas if  $r$  represents a point which is in the reflector region,

$$\bar{f}_{\ell}(r) = (2\ell+1) \sum_{k=1}^{2[(L+1)/2]} \bar{A}_k \bar{G}_{\ell}(\bar{\lambda}_k) Q_{\ell}(\bar{\epsilon} r / \bar{\lambda}_k) . \quad (C-12)$$

The  $A_0^*$  terms are omitted from Eqs. (C-11) and (C-12) since they arise only at an interfacial boundary between two media.

## C.33 BOLTZMANN6 Program

This program is the control program for the sixth phase. The sixth phase prints and punches the computed results. In addition graphs of parts of the results may be printed under the control of the input constant IHOLD2 or sense switch 1.

## C.34 OUTPUT Subprogram

This subprogram supervises the printing and punching of the computed results. When graphs are asked for by having IHOLD2 set to one or sense switch 1 on, three graphs are printed for a bare spherical reactor whereas seven graphs are printed for a reflected reactor. For a bare reactor plots are made of the total neutron flux in the core as a function of the spatial

variable, the angular flux at the vacuum interface, and the individual  $f_{\chi}(r)$ 's in the core as a function of the spatial variable. In addition, for a reflected reactor plots are made of the total neutron flux in the reflector as a function of the spatial variable, the individual  $f_{\chi}(r)$ 's in the reflector as a function of the spatial variable, and of the angular flux at the core-reflector interface as viewed from each side of the interface.

### C.35 PLOT Subprogram

This subprogram plots a graph of some of the computed results in the printed output. In order to print titles and axes of graphs, control cards are read in. A list of the control cards used in this work are shown in Table C-IV. A detailed description of this subprogram is on file in the K.S.U. Computing Center.

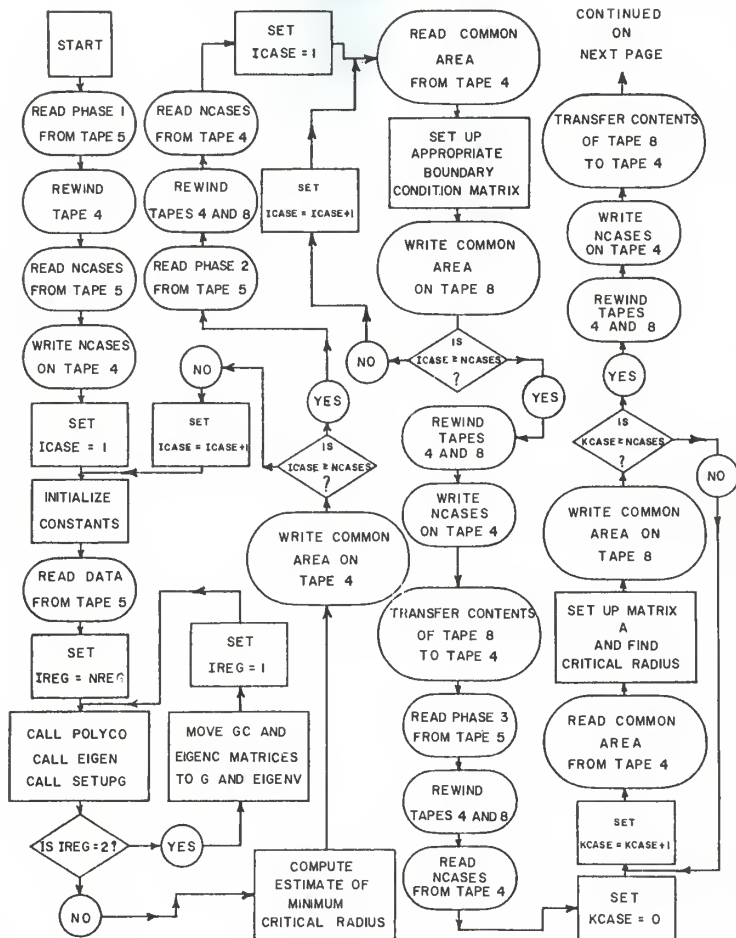
### C.36 Special Machine Language Subprograms

There are three special machine language subprograms which are used in this program. The machine language subprogram CHECK1 is a routine which checks the error indicators and prints appropriate error messages if necessary. EXIT is a machine language routine which terminates program control and gives control to the computer monitor. The machine language subprogram INQUIR checks the inquiry request key on the console of the computer allowing alteration of the sense switch settings. A detailed description of each of these subprograms is on file in the K.S.U. Computing Center.

Table C-IV. Control cards used by PLDT

TOTAL FLUX DISTRIBUTION IN THE CORE AS A FUNCTION OF THE RADIAL DIMENSION	*	FRACTION OF CRITICAL RADIUS	*+--
NORMALIZED FLUX	*	FRACTION OF CRITICAL RADIUS	*+--
TOTAL FLUX DISTRIBUTION IN THE REFLECTOR AS A FUNCTION OF THE RADIAL DIMENSION	*	FRACTION OF DISTANCE FROM R TO ROUT	+--
NORMALIZED FLUX	*	FRACTION OF DISTANCE FROM R TO ROUT	+--
ANGULAR FLUX AT THE VACUUM INTERFACE AS A FUNCTION OF MU	*	MU (COSINE OF THETA)	*+--
ANGULAR FLUX	*	MU (COSINE OF THETA)	*+--
INDIVIDUAL SPATIAL MOMENT DISTRIBUTION IN THE CORE AS A FUNCTION OF R	*	FRACTION OF CRITICAL RADIUS	*+--
INDIVIDUAL SPATIAL MOMENT	0123456789	FRACTION OF CRITICAL RADIUS	*+--
INDIVIDUAL SPATIAL MOMENT DISTRIBUTION IN THE REFLECTOR AS A FUNCTION OF R	*	FRACTION OF DISTANCE FROM R TO ROUT	+--
INDIVIDUAL SPATIAL MOMENT	0123456789	FRACTION OF DISTANCE FROM R TO ROUT	+--
ANGULAR FLUX DISTRIBUTION AT THE INTERFACIAL BOUNDARY FROM THE CORE SIDE	*	MU (COSINE OF THETA)	*+--
ANGULAR FLUX	*	MU (COSINE OF THETA)	*+--
ANGULAR FLUX DISTRIBUTION AT THE INTERFACIAL BOUNDARY FROM THE REFLECTOR SIDE	*	MU (COSINE OF THETA)	*+--
ANGULAR FLUX	*	MU (COSINE OF THETA)	*+--

C.37 Computer Program Logic Diagram





## C.38 Computer Program Listing

```

      BOP BOLTZMANN1      14
C THIS PROGRAM IS THE CONTROL PROGRAM FOR PHASE 1
  DIMENSION POLY(6),EIGENV(5),G(11,5),GC(11,5),C(2),SIGMA(2),EIGENC(
15)
  DIMENSION BC(11,5)
  COMMON POLY,N,EIGENV,G,NREG,NBC,C,SIGMA,REFLTH,EIGENC,GC,ACCUR,HOL
  COMMON HOL2,BC
  REWIND4
  READ INPUT TAPE 5,6,NCASES
6  FORMAT(15)
  WRITE TAPE 4,NCASES
  DO 1001 ICASE=1,NCASES
  TYPE 7,ICASE
7  FORMAT(16X14HPROBLEM NUMBER,I5)
  WRITE OUTPUT TAPE 6,1111,ICASE
1111 FORMAT(2H1$,I5,75H.....)
1.....)
C INITIALIZATIUN OF THE COMMON AREA
  IPROB=1
  NCV2=2
  NP1=5
  POLY(1)=0.0
  REFLTH=0.0
  DO 8 K=1,2
  C(K)=0.0
8  SIGMA(K)=0.0
  DO 9 K=1,NOV2
  EIGENV(K)=0.0
  EIGENC(K)=0.0
  POLY(K+1)=0.0
  DO 9 L=1,NP1
  G(L,K)=0.0
  GC(L,K)=0.0
  BC(L,K)=0.0
  IREG=NOV2+K
9  G(L,IREG)=0.0
  CALL INPUT
C THIS SECTION OF THE PROGRAM SETS UP G(L,K) MATRIX AND FINOS THE
C ROUTS LAMBDA-SUB K.
  DO 19 KREG=1,NREG
  IREG=NREG+1-KREG
  IF(C(IREG)-1.)12,10,12
10  WRITE OUTPUT TAPE 6,11
11  FORMAT(5X32HC = 1,PROBLEM CANNOT BE EXECUTED)
  IPRUB=2
  GC TO 1000
12  IF(N-2*(N/2))16,13,I6
13  IF(C(IREG)-(FLOAT(N+1)*P(N,0.))**2)16,14,14
14  WRITE OUTPUT TAPE 6,15,C(IREG),N
15  FORMAT(5XI6HTHE VALUE OF C =,1PE15.7,3X9HIN THE P ,I3,14H APPROXIM

```

```

IATION,1X45HIS GREATER THAN OR EQUAL TO ((N+1)*P(N,0)**2)
IPROB=2
GO TO 1000
16 CALL POLYCO(N+1,C(IREG),POLY)
   CALLEIGEN(C(IREG))
   CALL SETUPG(C(IREG))
   IF(IREG-1)19,19,17
17 NOV2=(N+1)/2
   NP1=N+1
   DO 18 K=1,NOV2
     EIGENV(K)=EIGENC(K)
     DO 18 L=1,NP1
18 G(L,K)=GC(L,K)
19 CONTINUE
   POLY(1)=HOL
   POLY(2)=HOL2
C   COMPUTE AN ESTIMATE OF THE MINIMUM POSSIBLE CRITICAL RADIUS FROM
C   A P-2 CALCULATION.
   ALAMBD=SQRT((9.-4.*C(1))/(15.*(C(1)-1.)))
   R=1.E+05
   SQRT3=SQRT(3.)
20 RLAST=R
   R=ATAN(1./(1./R-1./SQRT3*(C(1)-1.)*ALAMBD))
   IF(K)30,30,21
30 R=R+3.1415927
   IF(ABS((R-RLAST)/R)-ACCUR)21,20,20
21 GO TO (22,23),NREG
22 R=.9*R
   GO TO 24
23 R=.3*R
24 R=R*ALAMBO/SIGMA(1)
1000 CALL CHECKI
1001 WRITE TAPE 4,IPROB,POLY,N,EIGENV,G,NREG,NBC,C,SIGMA,REFLTH,EIGENC,
   LGC,ACCUR,BC,R
   REWIND 4
   CALL EXIT
   STOP
   END

      BOP INPUT          14
SUBROUTINE INPUT
THIS SUBPROGRAM READS IN THE INPUT DATA
DIMENSION POLY(6),EIGENV(5),G(11,5),GC(11,5),C(2),SIGMA(2),EIGENC(
15)
COMMON POLY,NORDER,EIGENV,G,NKEG,NBC,C,SIGMA,REFLTH,EIGENC,GC,ACCR
COMMON HOLD,HOLD2
READ INPUT TAPES,2,NOROER,NRFG,NBC,ACCR,IHOLD,IHOLD2
2 FORMAT(3I5,E15.8,2I5)
   HOLD=IHOLD
   HOLD2=IHOLD2
   READ INPUT TAPE 5,3,C(1),SIGMA(1)
3 FORMAT(3E15.8)

```



```

      GO TO (5,4),NREG
    4  IF(NBC-4)41,42,41
42  C(2)=0.0
      SIGMA(2)=SIGMA(1)
      GO TO 5
C    THE CONSTANTS FOR THE REFLECTOR ARE NEEDED ONLY IF THIS IS A
C    REFLECTED REACTOR CASE.
    41 READ INPUT TAPE 5,3,C(2),SIGMA(2),REFLTH
C    THIS SECTION PRINTS A STATEMENT OF THE CASE BEING CONSIDERED.
    5  WRITE OUTPUT TAPE 6,6,NURDER
    6  FORMAT(3H-$1,31X1HP,I2,1X13HAPPROXIMATION)
      WRITE OUTPUT TAPE 6,7
    7  FORMAT(3H $ ,15X51HDF THE DNF VELOCITY BOLTZMANN TRANSPORT EQUATIO
      IN BY)
      WRITE OUTPUT TAPE 6,71
    71 FORMAT(3H $ ,15X53HTHE SPHERICAL HARMONICS METHOD IN SPHERICAL GED
      IMETRY.)
      IF(NBC-4)72,8,72
    72 GO TO (8,10),NREG
    8  WRITE OUTPUT TAPE 6,9
    9  FORMAT(3HO$0,20X9HBARE CDRE)
      GO TO 12
    10 WRITE OUTPUT TAPE 6,11
    11 FORMAT(3HO$0,20X14HREFLECTED CDRE)
    12 GO TO (13,15,17,25),NBC
    13 WRITE OUTPUT TAPE 6,14
    14 FORMAT(3H $ ,20X44HMARSHAK VACUUM INTERFACE BOUNDARY CCONDITIDNS)
      GO TO 19
    15 WRITE OUTPUT TAPE 6,16
    16 .FORMAT(3H $ ,20X42HMARKS VACUUM INTERFACE BOUNDARY CNDITIDNS)
      GC TO 19
    17 WRITE OUTPUT TAPE 6,18
    18 FORMAT(3H $ ,20X48HVARIATIONAL VACUUM INTERFACE BOUNDARY CNDITIDN
      IS)
      GO TO 19
    25 WRITE OUTPUT TAPE 6,26
    26 FORMAT(3H $ ,20X40HINFINITELY REFLECTED WITH A BLACK MEDIUM)
    19 WRITE OUTPUT TAPE 6,20,C(1),SIGMA(1)
    20 FORMAT(3H $ ,20X15HIN THE CDPE C =,F7.4,1X9H, SIGMA =,F7.4,1X4H/CM
      1.)
      GO TO (24,21),NREG
    21 IF(NBC-4)27,24,27
    27 WRITE OUTPUT TAPE 6,22,C(2),SIGMA(2)
    22 FORMAT(3H $ ,20X20HIN THE REFLECTOR C =,F7.4,1X9H, SIGMA =,F7.4,1X
      14H/CM.)
      WRITE OUTPUT TAPE 6,23,REFLTH
    23 FORMAT(3H $ ,20X26HTHE REFLECTOR THICKNESS IS,F7.2,1X3HCM.)
    24 WRITE OUTPUT TAPE 6,31,ACCR
    31 FORMAT(3H $ ,20X20HTHE ACCURACY USED IS,1PE8.1)
      RETURN
      END

```

## BOP POLYCO 14

```

SUBROUTINE POLYCO(N,C,POLY)
THIS PROGRAM SETS UP THE COEFFICIENTS OF THE POLYNOMIAL NECESSARY
FOR DETERMINING THE VALUES OF LAMBOA. THE COEFFICIENTS ARE
STORED IN POLY(I).
DIMENSION POLY(1)
NOV2=N/2+1
OOB NM=1,NOV2
M=NM-1
POLY(NM)={{(-1.)**M}*FACT(2*(N-M))/(FACT(M)*FACT(N-M)*FACT(N-2*M))
OO 6 L=1,N
LM1OV2=(L-1)/2+1
NMLOV2=(N-L)/2+1
IF(NM-LM1OV2)1,2,2
1 LM1OV2=NM
2 OO 6 NJ=1,LM1OV2
J=NJ-1
IF(NM-NMLOV2)3,4,4
3 NMLOV2=NM
4 OO 6 NK=1,NMLOV2
K=NK-1
IF(M-K-J)6,5,6
5 POLY(NM)=POLY(NM)-2.*C*FACT(2*(L-1-J))*FACT(2*(N-L-K))*{(-1.)**
(L+J)}/(FACT(J)*FACT(L-1-J)*FACT(L-1-2*J)*FACT(K)*FACT(N-L-K)*FACT
(2N-L-2*K)*FLOAT(L))
6 CONTINUE
B POLY(NM)=POLY(NM)*{(-.5)**N}
RETURN
END

```

## BOP POLYNO 14

```

FUNCTION POLYNO(X)
THIS SUBPROGRAM IS USED AN AUXILLIARY SUBPROGRAM BY EIGEN (N
FINDING THE ROOTS LAMBOA-SUB K.
IT ACTUALLY COMPUTES THE VALUE OF G(L+1,X).
DIMENSION POLY(6)
COMMON POLY,N
NCO= (N+1)/2+1
POLYNO=POLY(NCO)
X2=X*X
FMULT=1.
DO 1 I=2,NCO
NSUB=NCO-I+1
FMULT=FMULT*X2
1 POLYNO=POLYNO+POLY(NSUB)*FMULT
RETURN
END

```

## BOP EIGEN 14

```

SUBROUTINE EIGEN(C)
THIS SUBPROGRAM FINDS THE ROOTS LAMBDA-SUB K
DIMENSION POLY(6),EIGENV(5),G(11,5),GC(11,5),D(2),SIGMA(2),EIGENC(

```

```

15)
COMMON POLY,N,EIGENC,GC,NREG,NBC,O,SIGMA,REFLTH,EIGENV,G,ACCUR
NP1=(N+1)/2+1
C IF THE VALUE OF C IS GREATER THAN 1,FIND THE IMAGINARY ROOT FIRST.
IF(C-1.)1,2,2
1 KIMAG=0
GO TO 3
2 KIMAG=1
DO 11 I=1,NP1
IF(I-2*(I/2))11,10,11
10 POLY(I)=-POLY(I)
11 CONTINUE
3 J=1
9 X=100.
ANS2=POLYNO(X)
DO 5 I=1,205
ANS1=ANS2
IF(I-90)94,94,92
92 IF(I-180)93,93,91
91 DELT=.04
GO TO 95
93 DELT=.1
GO TO 95
94 DELT=1.
95 X=X-DELT
ANS2=POLYNO(X)
IF(SIGN(1.,ANS2)-SIGN(1.,ANS1))4,5,4
F POLYNO
4 EIGENV(J)=ROOT(POLYNO,X+DELT,X,0.0,ACCUR)
J=J+1
IF(KIMAG-1)5,6,6
5 CONTINUE
81 RETURN
6 KIMAG=0
DO 8 I=1,NP1
IF(I-2*(I/2))8,7,8
7 POLY(I)=-POLY(I)
8 CONTINUE
IF(J-NP1)9,81,81
END

BOP SETUPG
14
SUBROUTINE SETUPG(C)
C THIS SUBPROGRAM SETS UP THE FLEMENTS OF THE MATRIX G(L,K)
DIMENSION POLY(6),EIGENV(5),G(11,5),GC(11,5),D(2),SIGMA(2),EIGENC(
15)
COMMON POLY,N,EIGENC,GC,NREG,NBC,O,SIGMA,REFLTH,EIGENV,G,ACCUR
NOV2=(N+1)/2
NP1=N+1
DO 2 K=1,NOV2
G(1,K)=1.
G(2,K)=(C-1.)*EIGENV(K)

```

```

      IF(N-1)2,2,1
1 DO 20 L=3,NP1
  SIGNA=-1.
  IF(C-1.)20,18,18
18 IF(K-1)21,21,20
21 IF(L-1-2*((L-1)/2))20,19,20
19 SIGNA=1.
20 G(L,K)=(FLOAT(2*L-3)*EIGENV(K)*G(L-1,K)*SIGNA-FLOAT(L-2)*G(L-2,K))
  1/FLOAT(L-1)
2 CONTINUE
3 RETURN
END

      BOP ROOT 14
FUNCTION ROOT(DUMMY,RFB,RFC,RFAE,RFRE)
C THIS SUBPROGRAM COMPUTES A ROOT OF A GIVEN FUNCTION.
C DUMMY IS THE NAME OF THE SUBPROGRAM WHICH REPRESENTS THE FUNC.
C RFB IS THE LOWER LIMIT OF THE RANGE IN WHICH THE ROOT IS TO BE
C FOUND.
C RFC IS THE UPPER LIMIT OF THE SAME RANGE.
C RFAE IS THE ABSOLUTE ACCURACY TO BE ITERATED TO.
C RFRE IS THE RELATIVE ACCURACY TO BE ITERATED TO.
C WITH SENSE SWITCH 6 ON THE CONVERGENCE AT EACH TRIAL IS PRINTED.
  JRFS=1
  RFFB=DUMMY(RFB)
  RFFC=DUMMY(RFC)
  IF(RFFC*RFFB)9122,9122,9102
9102 WRITE OUTPUT TAPE 6,200,RFB,RFC
  200 FORMAT(1X76HLIMITS GIVEN TO ROOT FUNCTION GENERATE FUNCTIONAL VALU
  IES WITH THE SAME SIGNS,11H,LIMITS ARE,1PE18.7,4X3HANO,E18.7)
  ROOT=0.0
  RETURN
9122 RFA=RFC
  RFFA=RFFC
9123 IF(ABS(RFFB)-ABS(RFFA))9131,9131,9130
9130 RFB=RFB
  RFB=RFA
  RFA=RFC
  RFFC=RFFB
  RFFB=RFFA
  RFFA=RFFC
9131 RFD=0.5*(RFB-RFA)
  RFT=RFAE+RFRE*ABS(RFB)
  IF(RFFB)9156,9135,9156
9135 ROOT=RFB
  RETURN
9156 IF(1KFK)9137,9157,9137
9157 IRFK=3
9138 RFV=RFD
  GO TO 9140
9137 IF(RFFB-RFFC)9139,913B,9139
9139 RFV=(RFB-RFC)*RFFB/(RFFB-RFFC)

```



```

4 DO 5 I=1,N
  FACT=FACT*FLOAT(I)
5 CONTINUE
2 RETURN
  END

```

```

          BOP BOLTZMANN2          14
C THIS PROGRAM IS THE CONTROL PROGRAM FOR PHASE 2.
  DIMENSION POLY(6),EIGENV(5),C(11,5),GC(11,5),C(2),SIGMA(2),EIGENC(
15),BC(11,5)
  DIMENSION B(10),A(10,10),IP(10)
  COMMON POLY,N,EIGENV,G,NREG,NBC,C,SIGMA,REFLTH,EIGENC,GC,ACCUR,BC,
1R,B,A,IP
  REWIND 4
  REWIND 8
  DO 35 L=1,6
    IP(L)=0
    B(L)=0.0
  DO 35 K=1,6
35 A(L,K)=0.0
  READ TAPE 4,NCASES
  DO 100 ICASE=1,NCASES
  WRITE OUTPUT TAPE 6,7,ICASE
  TYPE 7,ICASE
  7 FORMAT(16X14HPROBLEM NUMBER,I5)
  READ TAPE 4,IPROB,POLY,N,EIGENV,G,NREG,NBC,C,SIGMA,REFLTH,EIGENC,G
  IC,ACCUR,BC,R
  GO TO (8,22),IPROB
C THIS SECTION SUPERVISES SET UP OF THE PROPER BOUNDARY CONDITION
C MATRIX IN BC.
  8 GO TO (20,21,24,22),NBC
20 CALL MARSHK
  GO TO 22
21 CALL MARKBC
  GO TO 22
24 IF(N-4)18,18,19
19 WRITE OUTPUT TAPE 6,17,N
17 FORMAT(1X5HTHE P,13,1XBOHVARIATIONAL BOUNDARY CONDITIONS CANNOT BE
  1 USED AS THEY HAVE NOT BEEN WORKED OUT.)
  IPRUB=2
  GO TO 22
18 CALL VARIBC(C(NREG))
22 CALL CHECKI
100 WRITE TAPE 8,IPROB,POLY,N,EIGENV,G,NREG,NBC,C,SIGMA,REFLTH,EIGENC,
  1GC,ACCUR,BC,R
  REWIND 4
  REWIND 8
  WRITE TAPE 4,NCASES
  DO 101 ICASE=1,NCASES
  READ TAPE 8,IPROB,POLY,N,EIGENV,G,NREG,NBC,C,SIGMA,REFLTH,EIGENC,
  1GC,ACCUR,BC,R
101 WRITE TAPE 4,IPROB,POLY,N,EIGENV,G,NREG,NBC,C,SIGMA,REFLTH,EIGENC,

```

```

IGC, ACCUR, BC, R, B, A, IP
REWIND 4
CALL EXIT
STOP
END

```

```

      BOP  MARSHK          14

```

```

SUBROUTINE MARSHK

```

```

C THIS SUBPROGRAM SETS UP THE COEFFICIENT MATRIX BC WHICH REPRESENTS
C MARSHAKS BOUNDARY CONDITIONS AT A VACUUM INTERFACE.
DIMENSION POLY(6), EIGENV(5), G(11,5), GC(11,5), C(2), SIGMA(2), EIGENC(
15), BC(11,5)
COMMON POLY, N, EIGENV, G, NREG, NBC, C, SIGMA, REFLTH, EIGENC, GC, ACCUR, BC
NOV2=(N+1)/2
NPI=N+1
DO 5 J=1, NOV2
DO 5 LP1=1, NPI
5 BC(LP1, J)=BCMARS(LP1-1, J)
RETURN
END

```

```

      BOP  BCMARS          14

```

```

FUNCTION BCMARS(N, J)

```

```

C THIS SUBPROGRAM COMPUTES THE VALUE OF THE ANALYTICALLY INTEGRATED
C INTEGRAL FROM -1 TO 0 OF P(N, X) TIMES X TO THE 2J-1 POWER FOR
C THE MARSHAK BOUNDARY CONDITIONS AT A VACUUM INTERFACE.
IF(N)1,1,2
1 BCMARS=-1./FLOAT(2*J)
RETURN
2 BCMARS=D.0
MP1=N/2+1
DO 5 KP1=1, MP1
K=KP1-1
5 BCMARS=BCMARS+((-1.)**K*FACT(2*N-2*K))/(2.**N*FACT(K)*FACT(N-K)*FA
IGT(N-2*K)*FLOAT(N+2*J-2*K))
BCMARS=BCMARS*(-1.)**(N+1)
RETURN
END

```

```

      BOP  MARKBC         14

```

```

SUBROUTINE MARKBC

```

```

C THIS SUBPROGRAM SETS UP THE COEFFICIENT MATRIX BC WHICH REPRESENTS
C MARKS BOUNDARY CONDITIONS AT A VACUUM INTERFACE.
DIMENSION POLY(6), EIGENV(5), G(11,5), GC(11,5), C(2), SIGMA(2), EIGENC(
15), BC(11,5)
COMMON POLY, N, EIGENV, G, NREG, NBC, C, SIGMA, REFLTH, EIGENC, GC, ACCUR, BC
NOV2=(N+1)/2
NPI=N+1
K=1
X=-1.0
ANS1=PNPI(X)
DO 5 I=1, 39

```

```

X=X+0.025
ANS2=ANS1
ANS1=PNP1(X)
IF(SIGN(1.,ANS1)-SIGN(1.,ANS2))1,5,1
F PNP1
1 VALUE=ROOT(PNP1,X-0.025,X,0.,ACCUR)
DO 2 J=1,NP1
2 BC(J,K)=P(N-NP1+J,VALUE)
K=K+1
IF(K-NOV2)5,5,3
5 CCNTINUE
3 RETURN
END

      BOP PNP1              14
FUNCTION PNP1(X)
DIMENSION POLY(6)
COMMON POLY,N
C THIS SUBPROGRAM IS USED BY THE MARKBC SUBPROGRAM TO FIND THE ROOTS
C OF THE EQUATION P(N+1,X)=0.
PNP1=P(N+1,X)
RETURN
END

      BOP VARIBC           14
SUBROUTINE VARIBC(CP)
C THIS SUBPROGRAM SUPERVISES THE SET UP OF THE BOUNDARY CONDITION
C MATRIX BC WHICH REPRESENTS THE VARIATIONAL BOUNDARY CONDITIONS.
DIMENSION POLY(6),EIGENV(5),G(11,5),GC(11,5),C(2),SIGMA(2),EIGENC(
15),BC(11,5)
DIMENSION CO(4,4)
COMMON POLY,N,EIGENV,G,NREG,NBC,C,SIGMA,REFLTH,EIGENC,GC,ACCUR,BC,
1R,CG,CPRIME
IF(N-2)1,2,4
1 BC(1,1)=SQRT(2.)/3.
GO TO 3
2 BC(1,1)=SQRT(2.)/3.*SQRT(1.+(1.-CP)*(1.+(1.-CP)))
3 BC(2,1)=-1.0/3.0
RETURN
C THIS SECTION SETS UP THE NECFSSARY COEFFICIENTS TO FIND THE
C P-3 CONSTANTS.
4 BC(4,1)=1.0/7.0
BC(3,2)=1.0/5.0
IF(N-3)5,5,6
5 CO(1,1)=16.
CO(1,2)=-40.
CO(1,3)=100.
CO(1,4)=-147.
CO(2,1)=20.
CO(2,2)=-70.
CO(2,3)=49.
CO(2,4)=-16.

```



```

CO(3,1)=1.
CO(3,2)=-2.
CO(3,3)=3.
CO(3,4)=-3.
CO(4,1)=-72.
CC(4,2)=56.
CO(4,3)=100.
CC(4,4)=-147.
CPRIME=0.0
GO TO 7

```

C THIS SECTION SETS UP THE NECESSARY COEFFICIENTS TO FIND THE  
C P-4 CONSTANTS.

```

6 CO(1,1)=16.*(9.+(1.-CP)*(2.+9.*(1.-CP)))
CO(1,2)=-2.*(140.-490.*(1.-CP))
CO(1,3)=2450.
CO(1,4)=-147.*9.
CO(2,1)=161.*(140.-490.*(1.-CP))+32.*2450.*(1.-CP)
CO(2,2)=-2.*9.*1715.
CO(2,3)=27.*147.*9.+32.*252.*(1.-CP)
CO(2,4)=-161.*144.-301.*32.*(1.-CP)-469.*16.*(1.-CP)**2
CC(3,1)=27.
CO(3,2)=-2.*27.
CO(3,3)=161.
CO(3,4)=-161.
CPRIME=32.*(1.-CP)
CO(4,1)=-648.
CO(4,2)=7.*9.*8.
CO(4,3)=2450.
CO(4,4)=-147.*9.

```

C THIS SECTION SUPERVISES THE FINDING OF THE CONSTANTS A,B,C, AND D  
C FOR THE P-3 AND P-4 APPROXIMATIONS.

```

7 E=.5
DC=.1
10 ANS1=FOUREQ(E)
8 ANS2=ANS1
IF(BC(2,1))13,14,14
13 ITEST=1
GO TO 15
14 ITEST=0
15 E=E+DC
ANS1=FOUREQ(E)
IF(SIGN(1.,ANS1)-SIGN(1.,ANS2))9,11,9
11 IF(E-2.0)8,8,12
12 E=.5
DC=DC/10.
GO TO 10
F FOUREQ
9 IF(ITEST)8,8,16
16 F=ROOT(FOUREQ,E-DC,E,0.0,ACCUR)
CALL NONLIN(F)
IF(BC(2,1))17,18,18
18 CALL NONLIN(E)

```

```

GO TO B
17 BC(2,1)=BC(2,1)/3.0
   BC(2,2)=BC(2,2)/3.0
   RETURN
   END

```

```

          BOP FOUREQ          14
FUNCTION FOUREQ(E)
C THIS SUBPROGRAM IS USED AS AN AUXILLIARY PROGRAM BY VARIBC IN THE
C FINDING IF THE CONSTANTS A,B,C, AND D FOR THE P-3 AND P-4
C APPROXIMATIONS
CALL NONLIN(E)
FOUREQ=E
RETURN
END

```

```

          BOP NONLIN          14
SUBROUTINE NONLIN(E)
C THIS SUBPROGRAM SOLVES THREE OF THE FOUR NONLINEAR EQUATIONS
C AND USES THE FOURTH AS A CONSISTENCY CHECK.
C IN THE USUAL NOTATION A=BC(1,1),B=BC(2,1),C=BC(1,2), AND D=BC(2,2).
DIMENSION POLY(6),EIGENV(5),C(11,5),GC(11,5),C(2),SIGMA(2),EIGENC(
15),BC(11,5)
DIMENSION CO(4,4)
COMMON POLY,N,EIGENV,G,NREG,NBC,C,SIGMA,REFLTH,EIGENC,GC,ACCUR,BC,
1R,CO,CPRIME
BC(1,2)=E
BC(1,1)=SQRT((CO(1,1)+BC(1,2)*(CO(1,2)+BC(1,2)*CO(1,3)))/(-CO(1,4)
1))
BC(2,2)=- (BC(1,1)*(CO(2,3)+BC(1,2)*CO(2,2)))/(CO(2,1)*BC(1,2)+CO(2
1,4))
BC(2,1)=- (CO(3,1)+BC(1,2)*CO(3,2)+CU(3,4)*BC(1,1)*BC(2,2))/(BC(1,2
1)*CO(3,3)+CPRIME)
E=CO(4,1)+BC(2,1)*(CO(4,2)+BC(2,1)*CO(4,4))+BC(2,2)*BC(2,2)*CO(4,3
1)
RETURN
END

```

```

          BOP P          14
FUNCTION P(N,X)
C LEGENDRE POLYNOMIAL FUNCTION CALCULATOR
IF(N)1,2,3
100 FORMAT(1HB,22HNEGATIVE ORDER N FOR P)
1 WRITE OUTPUT TAPE6,100
2 P=1.
RETURN
3 M= N/2
IF(X)5,4,5
4 IF(N-2*M)7,8,7
8 P=(-1.)**M*FACT(N)/((2.**N)*FACT(N-M)*FACT(M))
RETURN
7 P=0.0

```

```

RETURN
5 IF(N-1)2,11,16
16 TERM=(-1.)**M)*FACT(2*N-2*M)*(X**(N-2*M))/(2.**N)*FACT(M)*FACT(N
1-M)
SUM=TERM
DO6K=1,M
TERM=-TERM*FLOAT(M-K+1)*FLOAT(2*(N-M+K)-1)*FLUAT(2*(N-M+K))*(X**2)
1/(FLOAT(N-M+K)*FLOAT(N-2*(M-K)-1)*FLOAT(N-2*(M-K)))
6 SUM=SUM+TERM
P=SUM
RETURN
11 P=X
RETURN
END

      ROP BOLTZMANN3      14
C THIS PROGRAM IS THE CONTROL PROGRAM FOR PHASE 4
DIMENSION POLY(6),EIGENV(5),G(11,5),GC(11,5),C(2),SIGMA(2),EIGENC(
15),BC(11,5),A(10,10),IP(10),V(10),B(10)
COMMON POLY,N,EIGENV,G,NREG,NBC,C,SIGMA,REFLTH,CIGENC,GC,ACCUR,BC,
R,A,IP,V,B,NSUB
REWIND 4
REWIND 8
READ TAPE 4, NCASES
ITIME=1
DO 21 KCASE=1,NCASES
WRITE OUTPUT TAPE 6,3,KCASE
TYPE 3,KCASE
3 FORMAT(16X14HPROBLEM NUMBER,I5)
KTAPE=4
1 READ TAPE KTAPE,IPRUB,POLY,N,EIGENV,G,NREG,NBC,C,SIGMA,REFLTH,EIGE
INC,GC,ACCUR,BC,R,B,A,IP
GO TO (8,22),ITIME
8 GO TO (55,20),IPRUB
2 WRITETAPE KTAPE,IPRUB,POLY,N,EIGENV,G,NREG,NBC,C,SIGMA,REFLTH,EIGE
INC,GC,ACCUR,BC,R,B,A,IP
GO TO (21,23),ITIME
C THIS SECTION SUPERVISES THE SETTING OF THE CRITICALITY
C DETERMINANT TO ZERO THUS FINDING A CRITICAL RADIUS.
55 DR=.2*R
ANS1=CRITEQ(R)
15 ANS2=ANS1
R=R+DR
ANS1=CRITEQ(R)
IF(ANS1*ANS2)16,16,15
F CRITEQ
16 R=ROOT(CRITEQ,R-DR,R,0.,ACCUR)
CALL SETUPA(R)
20 KTAPE =8
GO TO 2
21 CONTINUE
REWIND 4

```

```

REWIND 8
WRITE TAPE 4,NCASES
ITIME=2
DO 23 KCASE=1,NCASES
KTAPE=8
GO TO 1
22 KTAPE=4
GO TO 2
23 CONTINUE
REWIND 4
CALL EXIT
STOP
END

```

BOP CRITEQ 14

```

FUNCTION CRITEQ(R)
THIS SUBPROGRAM IS USED BY BOLTZMANN3 AS AN AUXILLIARY PROGRAM
TO HELP IN FINDING THE CRITICAL RADIUS.
DIMENSION POLY(6),EIGENV(5),G(11,5),GC(11,5),C(2),SIGMA(2),EIGENC(
15),BC(11,5),A(10,10),IP(10),V(10),B(10)
COMMON POLY,N,EIGENV,G,NREG,NBC,C,SIGMA,REFLTH,EIGENC,GC,ACCUR,BC,
I2,A,IP,V,B,NSUB
CALL SETUPA(R)
NOV2=(N+1)/2
IF(NBC-4)16,15,16
15 NSUB=2*NOV2
GO TO 17
16 NSUB=(1+2*(NREG-1))*NOV2
17 CALL CRAM(NSUB,1)
CRITEQ=DET(NSUB)
RETURN
END

```

BOP SETUPA 14

```

SUBROUTINE SETUPA(R)
THIS SUBPROGRAM SETS UP THE CRITICALITY DETERMINANT IN A.
DIMENSION POLY(6),EIGENV(5),G(11,5),GC(11,5),DI(2),SIGMA(2),EIGENC(
15),BC(11,5),A(10,10)
COMMON POLY,N,EIGENV,G,NREG,NBC,D,SIGMA,REFLTH,EIGENC,GC,ACCUR,BC,
IRA,A
DO 24 I=1,10
DO 24 K=1,10
24 A(I,K)=0.0
NP1=N+1
NOV2=NP1/2
NOV=2*NOV2
DO 10 K=1,NOV2
ARG=SIGMA(1)*R/EIGENC(K)
IF(K-1)1,1,2
1 I=1
GO TO 3
2 I=0

```

```

3 TEMP1=C(0,ARG,I)*GC(1,K)
  GO 10 LP1=1,NP1
  TEMP2=C(LP1-1,ARG,I)*GC(LP1,K)*FLOAT(2*LP1-1)
  GO TO (4,6),NREG
C THIS SECTION SETS UP THE MATRIX FOR A BARE SPHERICAL REACTOR.
4 DO 5 NSUB=1,NOV2
5 A(NSUB,K)=A(NSUB,K)+BC(LP1,NSUB)*TEMP2
  GO TO 10
C THIS SECTION SETS UP THE PARTS OF THE MATRIX REPRESENTING THE
C INTERFACIAL BOUNDARY.
6 IF(N-2*(N/2))7,8,7
7 A(LP1,K)=TEMP2
  GO TO 10
8 IF(LP1-1)10,10,9
9 A(LP1-1,K)=TEMP2-P(LP1-1,0.0)*TEMP1*FLOAT(2*LP1-1)
10 CONTINUE
  GO TO (19,11),NREG
11 DO 16 I=1,2
  DO 16 K=1,NOV2
  ARG=(-1.)*I*(I-1)*SIGMA(2)*R/EIGENV(K)
  IF(NBC-4)22,20,22
20 IF(I-1)16,16,21
21 NSUB=K+NOV2
  GO TO 23
22 NSUB=K+NOV2*I
23 TEMP1=Q(0,ARG)*G(1,K)
  GO 15 LP1=1,NP1
  TEMP2=-Q(LP1-1,ARG)*FLOAT(2*LP1-1)*G(LP1,K)*(-1.)*I*(I-1)
  IF(N-2*(N/2))12,13,12
12 A(LP1,NSUB)=TEMP2
  GO TO 15
13 IF(LP1-1)15,15,14
14 A(LP1-1,NSUB)=TEMP2+P(LP1-1,0.0)*TEMP1*FLOAT(2*LP1-1)
15 CONTINUE
16 CONTINUE
  IF(NBC-4)17,19,19
C FOR A REFLECTED REACTOR THIS SECTION SETS UP THE VACUUM
C INTERFACE BOUNDARY CONDITIONS.
17 DO 18 I=1,2
  DO 18 K=1,NOV2
  ARG=(-1.)*I*(I-1)*SIGMA(2)*(R+REFLTH)/EIGENV(K)
  GO 18 LP1=1,NP1
  TEMP2=Q(LP1-1,ARG)*FLOAT(2*LP1-1)*G(LP1,K)*(-1.)*I*(I-1)
  NSUB=NOV2*I+K
  DO 18 L=1,NOV2
  NSUB1=L+NOV
18 A(NSUB1,NSUB)=A(NSUB1,NSUB)+RC(LP1,L)*TEMP2
19 RETURN
  END

```

```

C      CROUT REDUCTION OF AUGMENTED MATRICES
C      THIS PROGRAM PERFORMS A CROUT REDUCTION ON A MATRIX A.
C      WITH I=1, THE CROUT REDUCTION IS PERFORMED WITH ROW INTERCHANGES.
C      WITH I=2, THE CROUT REDUCTION IS PERFORMED WITHOUT ROW CHANGES.
C      DIMENSION POLY(6),EIGENV(5),G(11,5),GC(11,5),C(12),SIGMA(2),EIGENC(
15),BC(11,5),A(10,10),IP(10),V(10),B(10)
COMMON POLY,M,EIGENV,G,NREG,NBC,C,SIGMA,REFLTH,EIGENC,GC,ACCUR,BC,
1R,A,IP,V,B,NSUB
GO TO (2200,2201),I
2200 IDMV=1
      GOTO2202
2201 IDMV=2
C      REDUCTION OF MATRIX
2202 IF(N-1)2223,2223,2224
2223 IP(1)=0
      RETURN
2224 DO 2204 IDK=1,N
      V(IDK)=ABS(A(IDK,1))
      DO2204 IDI=2,N
      IF(V(IDK)-ABS(A(IDK,IDI)))2203,2204,2204
2203 V(IDK)=ABS(A(IDK,IDI))
2204 CONTINUE
      DO 2222 IDK=1,N
      DETR=-1.
      IDK1=IDK-1
      DO2214 IDI=IDK,N
      DETPR=0.0
      IF(IDK-1)2208,2208,2206
2206 DO2207 IDJ=1,IDK1
2207 OETPR=DETPR+A(IDI, IDJ)*A(IDJ, IDK)
2208 A(IDI, IDK)=A(IDI, IDK)-DETPR
      GO TO(2212,2225),IDMV
2212 OETS=ABS(A(IDI, IDK))/V(IDI)
      IF(OETS-DETR)2214,2214,2213
2213 DETR=OETS
      IP(IDK)=IDK-IDI
      GO TO 2214
2225 IP(IDK)=0
2214 CONTINUE
      IDK2=IDK-IP(IDK)
      DETR=A(IDK2, IDK)/V(IDK2)
      IF(ABS(DETR)-1.E-08)2230,2230,2232
2240 FORMAT(1HB,5HP1VOT,13,19HIS LESS THAN 1.E-08)
2241 FORMAT(1HB,5HP1VOT,13,7HIS ZERO)
2230 WRITE OUTPUT TAPE 6,2240, IDK
      IF(A(IDK2, IDK)) 2232,2231,2232
2231 WRITE OUTPUT TAPE 6,2241, IDK
      IF(N-NSUB)2501,2500,2500
2501 CALL EXIT
2232 V(IDK2)=V(IDK)
      V(IDK)=DETR
      DO2222 IDJ=1,N

```

```

      DETR=A(IDK, IDJ)
      IF (IDJ-IDK)2215, 2215, 2216
2215  A(IDK, IDJ)=A(IDK2, IDJ)
      GO TO 2220
2216  DETPR=0.0
      IF (IDK-1)2219, 2219, 2217
2217  DD2218  IDI=1, ICK1
2218  DETPR=DETPR+A(IDK, IDI)*A(IDI, IDJ)
2219  A(IDK, IDJ)=(A(IDK2, IDJ)-DETPR)/A(IDK, IDK)
2220  IF (IP(IDK))2221, 2222, 2222
2221  A(IDK2, IDJ)=DETR
2222  CONTINUE
2500  RETURN
      END

```

```

      BOP DET                      14
      FUNCTION DET(N)
C     AFTER CALLING THE GRAM SUBROUTINE THIS FUNCTION WILL COMPUTE
C     THE DETERMINANT OF THE MATRIX A.
      DIMENSION POLY(6), EIGENV(5), G(11,5), GC(11,5), C(2), SIGMA(2), EIGENC(
15), BC(11,5), A(10,10), IP(10), V(10), B(10)
      COMMON POLY, M, EIGENV, G, NREG, NBC, C, SIGMA, REFLTH, EIGENC, GC, ACCUR, BC,
1R, A, IP, V, B
      DET=1.0
      DO 2229  ICK=1, N
      DET=DET*A(IDK, IDK)
      IF (IP(IDK))2223, 2229, 2229
2223  DET=-DET
2229  CONTINUE
      RETURN
      END

```

```

      BOP C                          14
      FUNCTION C(L,X,I)
C     THIS SUBPROGRAM COMPUTES THE VALUE OF THE FUNCTION C(L,X) FOR BOTH
C     REAL AND NEGATIVE IMAGINARY ARGUMENTS. L IS THE ORDER OF THE
C     FUNCTION AND X IS THE ARGUMENT OF THE FUNCTION. FOR REAL
C     ARGUMENTS I=0, FOR NEGATIVE IMAGINARY ARGUMENTS I=1.
      IF (X)10, 9, 10
9     IF (L)12, 12, 11
11    C=0.0
      RETURN
12    C=1.
      RETURN
10    IF (I)4, 4, 1
4     C=-.5*(Q(L,X)+(-1.)*L*Q(L,-X))
      RETURN
1     IF (L-2*(L/2))2, 3, 2
2     CDFUNC=-CUS(X)
      FUNC=-SIN(X)
      SIGNB=1.
      GO TO 7

```

```

3 CGFUNC=SIN(X)
  FUNC=COS(X)
  SIGNB=-1.
7 C=(COFUNC*CSER(L,X,0)-SIGNB*FUNC*CSER(L,X,1))/X
  RETURN
  END

```

BOP CSER 14

```

C   FUNCTION CSER(L,X,I)
C   THIS SUBPROGRAM COMPUTES THE FUNCTIONAL VALUE OF THE SERIES
C   NECESSARY FOR THE FUNCTION C(L,X). THE ARGUMENTS OF L AND X ARE
C   THE SAME AS IN THE FUNCTION C(L,X,I) SUBPROGRAM. I=0 FOR A
C   STARTING INTEGER OF 0, AND I=1 FOR A STARTING INTEGER OF 1.
  CSER=0.0
  IF(L-I)3,10,10
10 TERM=FACT(L+I)/(FACT(I)*FACT(L-I)*(2.*X)**I)
  CSER=TERM
  IP2=I+2
  IF(L-IP2)3,1,1
1  FMULT=-.25/(X*X)
  DO 2 J=IP2,L,2
  TERM=TERM*FLOAT(L-J+2)*FLOAT(L-J+1)*FLOAT(L+J-1)*FLOAT(L+J)*FMULT/
  1(FLOAT(J-1)*FLOAT(J))
2  CSER=CSER+TERM
3  RETURN
  END

```

BOP Q 14

```

C   FUNCTION Q(L,X)
C   THIS SUBPROGRAM COMPUTES THE VALUE OF THE FUNCTION Q(L,X)
  Q=(EXP(X))/X
  IF(X)7,7,8
7  SIGNA=1.
  X=-X
  GO TO 9
8  SIGNA=-1.
9  POLY=1.
  FMULT=.5*SIGNA/X
  AN=L+1
  ANPLUS=L
  TERM=1.
  N=1
4  TERM=TERM*FMULT*ANPLUS*AN/FLOAT(N)
  POLY=POLY+TERM
  IF(L-N)6,6,5
5  ANPLUS=ANPLUS-1.
  N=N+1
  AN=AN+1.
  GO TO 4
6  Q=Q+POLY
2  RETURN
  END

```



```

      BDP  BOLTZMANN4      14
C   THIS PROGRAM IS THE CONTROL PROGRAM FOR PHASE 4
      DIMENSION POLY(6),EIGENV(5),G(11,5),GC(11,5),C(2),SIGMA(2),EIGENC(
15),BC(11,5),A(10,10),IP(10),V(10),B(10),S(10,10),T(10)
      COMMON POLY,N,EIGENV,G,NREG,NBC,C,SIGMA,REFLTH,EIGENC,GC,ACCUR,BC,
1R,A,IP,V,B,NSUB,S,T
      PI=3.14159265358979324
      REWIND 4
      REWIND 8
      READ TAPE 4, NCASES
      OO 1000 ICASE=1,NCASES
      WRITE OUTPUT TAPE 6,7, ICASE
      TYPE 7, ICASE
17 FORMAT(16X14HPRUBLEM NUMBER,I5)
      READ TAPE 4,IPROB,POLY,N,EIGFNV,G,NREG,NBC,C,SIGMA,REFLTH,EIGENC,G
1C,ACCUR,BC,R,B,A,IP
      GO TO (B,35),IPROB
C   THIS SECTION ASSUMES A1 IS ONE AND COMPUTES THE VALUES OF ALL
C   THE OTHER CONSTANTS,A-SUB K.
18 NOV2=(N+1)/2
      IF(NBC-4)10,9,10
19 NSUB=2*NOV2
      GO TO 11
10 NSUB=(1+2*(NREG-1))*NOV2
11 IF(NSUB-1)12,32,12
12 NSUB1=NSUB-1
      NSUB2=NOV2*NREG
      DO 18 L=1,NSUB1
      IF(L-NSUB2)17,15,15
15 OO 16 K=1,NSUB
16 A(L,K)=A(L+1,K)
17 B(L)=-A(L,1)
      OO 18 K=1,NSUB1
18 A(L,K)=A(L,K+1)
      DO 19 K=1,NSUB1
      T(K)=B(K)
      DO 19 L=1,NSUB1
19 S(L,K)=A(L,K)
      CALL GRAM(NSUB1,1)
      CALL SOLVE(NSUB1)
      CALL RESIDU(NSUB1)
C   THIS SECTION NORMALIZES THE TOTAL NEUTRON FLUX SO THAT AT R = 0
C   IT IS ONE NEUTRON PER SQUARE CENTIMETER PER SECOND.
31 DO 30 K=1,NSUB1
      L=NSUB1+2-K
30 B(L)=B(L-1)
32 B(1)=1.0
      SUM=0.0
      DO 33 K=1,NOV2
33 SUM=SUM+B(K)
      SUM=SUM*4.*PI

```

```

SUM=SUM-5.*ACCUR*SUM
DO 34 K=1,NSUB
34 B(K)=B(K)/SUM
35 CALL CHECK(
1000 WRITETAPE 8, IPROB,POLY,N,EIGENV,G,NREG,NBC,C,SIGMA,REFLTH,EIGENC,G
1C,ACCUR,BC,R,B
REWIND 4
REWIND 8
WRITE TAPE 4, NCASES
DO 36 ICASE=1,NCASES
READ TAPE 8,IPROB,POLY,N,EIGENV,G,NREG,NBC,C,SIGMA,REFLTH,EIGENC,G
1C,ACCUR,BC,R,B
36 WRITETAPE 4,IPROB,POLY,N,EIGENV,G,NREG,NBC,C,SIGMA,REFLTH,EIGENC,G
1C,ACCUR,BC,R,B
REWIND 4
CALL EX(T
STOP
END

```

BOP SOLVE 14

SUBROUTINE SOLVE (N)

```

C AFTER CALLING GRAM THIS SUBROUTINE WILL COMPUTE THE SOLUTION
C VECTOR OF THE MATRIX EQUATION AX=B. BEFORE RETURNING TO THE
C MAIN PROGRAM THE SOLUTION VECTOR (S STORED IN B.
DIMENSION POLY(6),EIGENV(5),G(11,5),GC(11,5),C(2),SIGMA(2),EIGENC(
15),BC(11,5),A(10,10),IP(10),V(10),B(10)
COMMON POLY,M,EIGENV,G,NREG,NBC,C,SIGMA,REFLTH,EIGENC,GC,ACCUR,BC,
1R,A,IP,V,B
DO 2256 IDK = 1,N
IDK1 = IDK - 1
(OK2 = IDK-IP(IDK)
DETR = B(IDK)
DETPR = D.0
(F(IDK-1) 2253, 2253, 2257
2257 DO 2252 IDI = 1, IDK1
2252 DETPR = DETPR+A(OK,IDI)* B(IDI)
2253 B(OK) = (B(OK2) - DETPR) / A(IDK,OK)
(F (IP(IDK)) 2254, 2256, 2256
2254 B(OK2) = DETR
2256 CONTINUE
DO 2263 IDI2 = 1,N
(IDI = N + 1 - IDI2
DETPR = D.0
(IDI = (O( + 1
IF (N - IDI) 2263, 2263, 226I
226I DO 2262 IDJ = IDI1,N
2262 DETPR = DETPR + A(IDI, IDJ)* B(IDJ)
2263 B(IDI) = B(IDI) - DETPR
RETURN
END

```

BOP RESIDU

14

```

SUBROUTINE RESIDU(N)
C   AFTER THE GRAM AND SOLVE SUBROUTINES HAVE BEEN CALLED THIS
C   SUBROUTINE WILL COMPUTE THE RESIDUALS IN THE COEFFICIENT
C   VECTOR T AND ITERATE ON THE ANSWER VECTOR B UNTIL THERE IS
C   NO CHANGE IN B FROM ONE ITERATION TO THE NEXT. THE SUBROUTINE
C   ASSUMES THAT THE ORIGINAL MATRIX IS IN S AND THAT THE ORIGINAL
C   COEFFICIENT VECTOR IS IN T.
  DIMENSION POLY(6),EIGENV(5),G(11,5),GC(11,5),C(2),SIGMA(2),EIGENC(
15),BC(11,5),A(10,10),IP(10),V(10),B(10),S(10,10),T(10)
  COMMON POLY,M,EIGENV,G,NREG,NBC,C,SIGMA,REFLTH,EIGENC,GC,ACCUR,BC,
1R,A,IP,V,B,NSUB,S,T
  DO 1 I=1,N
  V(I)=B(I)
  DO 1 J=1,N
1 T(I)=T(I)-S(I,J)*B(J)
2 DO 3 I=1,N
3 B(I)=T(I)
  CALL SOLVE (N)
  DO 10 I=1,N
  DO 10 J=1,N
10 T(I)=T(I)-S(I,J)*B(J)
  J=0
  DO 5 I=1,N
  B(I)=B(I)+V(I)
  IF(B(I)-V(I))6,5,6
6 J=1
5 V(I)=B(I)
  IF(J) 7,7,2
7 RETURN
  END

      BOP  BOLTZMANN5          14
C   THIS PROGRAM IS THE CONTROL PROGRAM FOR PHASE 5
  DIMENSION POLY(6),EIGENV(5),G(11,5),GC(11,5),C(2),SIGMA(2),EIGENC(
15),BC(11,5),B(10)
  DIMENSION X(100),Y(100)
  COMMON POLY,N,EIGENV,G,NREG,NBC,C,SIGMA,REFLTH,EIGENC,GC,ACCUR,BC,
1R,B,I,PROB
  COMMON X,Y
  REWIND 4
  REWIND 8
  READ TAPE 4,NCASES
  DO 16 ICASE=1,NCASES
  WRITE OUTPUT TAPE 6,7,ICASE
  TYPE 7, ICASE
7 FORMAT(16X14HPROBLEM NUMBER,I5)
  READ TAPE 4,I,PROB,POLY,N,EIGENV,G,NREG,NBC,C,SIGMA,REFLTH,EIGENC,
16,ACCUR,BC,R,B
14 CALL INTOUT
15 CALL CHECKI
16 CONTINUE
  REWIND 4

```

```

REWIND B
WRITE TAPE 4,NCASES
DO 17 ICASE=1,NCASES
READ TAPE B,IPROB,POLY,N,EIGENV,G,NREG,NBC,C,SIGMA,RCFLTH,EIGENC,
IGC,ACCUR,BC,R,B
WRITE TAPE 4,IPROB,POLY,N,EIGENV,G,NREG,NBC,C,SIGMA,REFLTH,EIGENC,
IGC,ACCUR,BC,R,B
GO TO (18,17),IPROB
18 READ TAPE B,X,Y
WRITE TAPE 4,X,Y
READ TAPE 8,NSUB
WRITE TAPE 4,NSUB
IF(NSUB)17,17,20
20 DO 33 K=1,NSUB
READ TAPE B,XMIN,XMAX,YMIN,YMAX,ISCALE,JSCALE,NPTS,NPLOTS,NCOPY,NC
LAROS
WRITE TAPE4,XMIN,XMAX,YMIN,YMAX,ISCALE,JSCALE,NPTS,NPLOTS,NCOPY,NC
LAROS
READ TAPE B,X,Y
33 WRITE TAPE 4,X,Y
17 CONTINUE
REWIND 4
CALL EXIT
STOP
END

```

BOP INTUUT 14

SUBROUTINE INTOUT

```

C THIS SUBROUTINE COMPUTES ALL OF THE NECESSARY DATA FOR THE
C PRINTOUT OF THE FINAL RESULTS.
DIMENSION POLY(6),EIGENV(5),G(11,5),GC(11,5),C(2),SIGMA(2),EIGENC(
15),BC(11,5),B(10)
DIMENSION X(100),Y(100)
COMMON POLY,N,EIGENV,G,NREG,NBC,C,SIGMA,REFLTH,EIGENC,GC,ACCUR,BC,
IR,B,IPROB
COMMON X,Y
GO TO (14,13),IPROB
C THIS SECTION COMPUTES THE DATA FOR A NORMAL PRINT-OUT
14 NP1=N+1
NMAX=100
DO 101 K=1,NMAX
101 Y(K)=0.0
PI=3.14159265358979324
ISCALE=0
JSCALE=0
NCOPY=1
NCAROS=3
IF(NBC-4)55,54,55
54 NREG=1
55 ROUTER=R+FLOAT(NREG-1)*REFLTH
OX=-.1
X(1)=1.0

```

```

      DG 102 K=2,21
102 X(K)=X(K-1)+DX
      DO 19 L=1,NP1
          TEMP=PHIL(L-1,ROUTER,NREG)
          DO 19 K=1,21
19 Y(K)=Y(K)+P(L-1,X(K))*TEMP
          PGLY(3)=Y(11)+Y(21)+4.*Y(20)
          DO 56 K=12,18,2
56 PGLY(3)=POLY(3)+4.*Y(K)+2.*Y(K+1)
          POLY(3)=POLY(3)/30.
13 WRITE TAPE 8,IPROB,POLY,N,EIGENV,G,NREG,N8C,C,SIGMA,REFLTH,EIGENC,
      IGC,ACCUR,RC,R,8
          GO TO (15,26),IPROB
15 WRITE TAPE 8,X,Y
          CALL INQUIR
              IF(SENSE SWITCH 1)50,49
49 IF(POLY(1))50,50,51
      THIS SECTION COMPUTES THE ADDITIONAL DATA NECESSARY FOR TESTING
      PURPOSES
50 NSUB=0
      GO TO 52
51 NSUB=3+(NREG-1)*4
52 WRITE TAPE 8, NSUB
      IF(NSUB)26,26,53
53 DO 100 NFUNC=1,7
          NPERGP=26
          GO TO (18,20,22,23,24,1,2),NFUNC
18 DX=.04
          X(1)=0.0
          GO TO 39
20 GO TO (100,39),NREG
22 X(1)=-I.0
          DX=.08
          ARG=ROUTER
          IREG=NREG
          GO TO 107
23 X(1)=0.0
60 NPERGP=NMAX/NP1
          IF(NPERGP-26)59,59,58
58 NPERGP=26
59 DX=1.0/FLUAT(NPERGP-1)
          GO TO 39
24 GO TO (100,60),NREG
      I GO TO (100,3),NREG
      3 IREG=1
          ARG=R
          X(1)=-I.0
          DX=.08
          GO TO 107
      2 GO TO (100,4),NREG
      4 IREG=2
107 DO 108 K=1,NMAX

```

```

108 Y(K)=0.0
39 DO 104 K=2,NPERGP
104 X(K)=X(K-1)+DX
    IF(NFUNC-2)42,42,41
41 DO 38 L=1,NP1
    TEMP=PHIL(L-1,ARG,IREG)
    DO 38 K=1,NPERGP
109 GC TO (31,32,33,31,32,36,36),NFUNC
38 CCNTINUE
    GO TO 105
42 DO 106 K=1,NPERGP
    GO TO 109
106 CCNTINUE
    GO TO 105
31 ARG=X(K)*R
    IREG=1
    IF(NFUNC-1)57,57,34
32 ARG=R+X(K)*REFLTH
    IREG=2
    IF(NFUNC-2)57,57,34
57 Y(K)=4.*PI*PHIL(0,ARG,IREG)
    GO TO 106
33 Y(K)=Y(K)+P(L-1,X(K))*TEMP
    GOTO 38
34 NSUB=K+(L-1)*NPERGP
    X(NSUB)=X(K)
    Y(NSUB)=PHIL(L-1,ARG,IREG)
    GO TO 38
36 Y(K)=Y(K)+P(L-1,X(K))*TEMP
    GO TO 38
105 IF(NFUNC-4)44,43,43
43 IF(NFUNC-6)47,44,44
47 NPTS=NP1*NPERGP
    NPLOTS=NP1
    GO TO 45
44 NPTS=NPERGP
    NPLOTS=1
45 YMIN=0.0
    YMAX=0.0
    DO 46 K=1,NPTS
    YMIN=MIN1(YMIN,Y(K))
46 YMAX=MAX1(YMAX,Y(K))
    WRITE TAPE 8,X(1),X(NPERGP),YMIN,YMAX,ISCALE,JSCALE,NPTS,NPLOTS,NC
    IOPY,NCARDS
    WRITE TAPE 8,X,Y
100 CONTINUE
26 RETURN
END

```

BOP PHIL

14

FUNCTION PHIL(L,X,IREG)

C THIS SUBPROGRAM COMPUTES THE LTH MOMENT OF THE ANGULAR FLUX AT X.

```

    DIMENSION POLY(6),EIGENV(5),G(11,5),GC(11,5),D(2),SIGMA(2),EIGENC(
    15),BC(11,5),B(10)
    CCMCN POLY,N,EIGENV,G,NREG,NBC,D,SIGMA,REFLTH,EIGENC,GC,ACCUR,BC,
    IR,B
    NCV2=(N+1)/2
    PHIL=0.0
    GO TO (1,5),1REG
1   DO 4 K=1,NOV2
      IF(K-1)2,2,3
2   I=1
    GO TO 4
3   I=0
4   PHIL=PHIL+B(K)*GC(L+1,K)*FLOAT(2*L+1)*C(L,SIGMA(1))*X/EIGENC(K),I
    RETURN
5   DO 6 I=1,2
      DO 6 K=1,NOV2
        NSUB=K+NOV2-I
6   PHIL=PHIL+B(NSUB)*G(L+1,K)*FLOAT(2*L+1)*Q(L,((-1.0)**(I-1))*SIGMA(2
    1)*X/EIGENV(K))*((-1.0)**(L*(I-1)))
    RETURN
    END

```

BOP BOLTZMANN6 14

```

C   THIS PROGRAM IS THE CONTROL PROGRAM FOR PHASE 6
    DIMENSION POLY(6),EIGENV(5),G(11,5),GC(11,5),C(2),SIGMA(2),EIGENC(
    15),BC(11,5),D(10)
    CCMCN POLY,N,EIGENV,G,NREG,NBC,C,SIGMA,REFLTH,EIGENC,GC,ACCUR,BC,
    IR,B
    REWIND 4
    READ TAPE 4,NCASES
    DO 104 ICASE=1,NCASES
      TYPE 5,ICASE
5   FCRMAT(16X14HPRUBLEM NUMBER,I5)
      WRITE OUTPUT TAPE 6,1111,ICASE
1111 FCRMAT(2H1%,I5,75H.....)
      1.....)
      READ TAPE 4,IPROB,POLY,N,EIGENV,G,NREG,NBC,C,SIGMA,RCFLTH,EIGENC,
      IGC,ACCUR,BC,R,B
      GO TO (103,100),IPROB
100 DO 101 K=1,14
101 READ INPUT TAPE 5,6
      6 FORMAT(8DX)
      GO TO 104
103 CALL OUTPUT
104 CONTINUE
      REWIND 4
      CALL EXIT
      STOP
    END

```

BOP OUTPUT

14

SUBROUTINE OUTPUT

```

C   THIS SUBROUTINE PRINTS OUT AND PUNCHES CARDS FOR ALL PERTINANT
C   CALCULATED DATA
    DIMENSION POLY(6),EIGENV(5),C(11,5),GC(11,5),C(2),SIGMA(2),EIGENC(
15),BC(11,5),B(10)
    DIMENSION X(100),Y(100)
    DIMENSION YP(11),IP(11)
    COMMON POLY,N,EIGENV,G,NREG,NBC,C,SIGMA,REFLTH,EIGENC,GC,ACCUR,BC,
1R,B
    COMMON X,Y
C   THIS SECTION PRINTS AND PUNCHES THE NORMAL DATA
    NP1=N+1
    NOV2=(N+1)/2
    X(1)=SIGMA(1)*R
    WRITE OUTPUT TAPE 6,1,R,X(1)
1  FORMAT(3H0$0,20X31HTHE COMPUTED CRITICAL RADIUS IS,F9.4,1X3HCM./3H
1 $ ,22X31HUR,F9.4,1X16HMEAN FREE PATHS.)
    WRITE OUTPUT TAPE 6,121,POLY(3)
121 FORMAT(3H $ ,20X41HTHE INTEGRATED INWARD ANGULAR FLUX AT THE/3H $
1,22X19HVACUUM INTERFACE IS,2X1PE10.3)
    WRITE OUTPUT TAPE 6,2
2  FORMAT(3H-$-,13X11HIN THE COPE)
    WRITE OUTPUT TAPE 6,3
3  FORMAT(3H0$0,15X12HEIGEN VALUES)
    WRITE OUTPUT TAPE 6,4,(EIGENC(K),K=1,NOV2)
4  FORMAT(3H $ ,17X1PE12.5,2XE17.5,2XE12.5,2XE12.5)
    WRITE OUTPUT TAPE 6,5
5  FORMAT(3H0$0,15X13HG(L,K) MATRIX)
    DO 6 L=1,NOV2
6  WRITE OUTPUT TAPE 6,4,(GC(K,L),K=1,NP1)
    GO TO (7,10),NREG
7  IF(NBC-4)120,10,120
120 WRITE OUTPUT TAPE 6,8
8  FORMAT(3H0$0,15X25HBOUNDARY CONDITION MATRIX)
    DO 9 L=1,NOV2
9  WRITE OUTPUT TAPE 6,4,(BC(K,L),K=1,NP1)
10 WRITE OUTPUT TAPE 6,11
11 FORMAT(3H0$0,15X23HNORMALIZED COEFFICIENTS)
    WRITE OUTPUT TAPE 6,4,(B(K),K=1,NOV2)
    GO TO (16,12),NREG
12 WRITE OUTPUT TAPE 6,13
13 FORMAT(3H-$-,13X16HIN THE REFLECTOR)
    WRITE OUTPUT TAPE 6,3
    WRITE OUTPUT TAPE 6,4,(EIGENV(K),K=1,NOV2)
    WRITE OUTPUT TAPE 6,5
    DO 14 L=1,NOV2
14 WRITE OUTPUT TAPE 6,4,(G(K,L),K=1,NP1)
    WRITE OUTPUT TAPE 6,8
    DO 15 L=1,NOV2
15 WRITE OUTPUT TAPE 6,4,(BC(K,L),K=1,NP1)
    NOV=NOV2+1
    NSUB=3*NOV2
    WRITE OUTPUT TAPE 6,11

```



```

WRITE OUTPUT TAPE 6,4,(8(K),K=NOV,NSUB)
16 WRITE OUTPUT TAPE 6,17
17 FORMAT(3H-5-,13X48HDATA FOR ANGULAR FLUX PLOT AT THE OUTER BOUNDAR
1Y)
WRITE OUTPUT TAPE 6,18
18 FORMAT(3H0$0,17X,3(2HMU,4X7HPHI(MU),6X))
READ TAPE 4,X,Y
DO 20 K=1,7
20 WRITE OUTPUT TAPE 6,21,(X(L),Y(L),L=K,21,7)
21 FORMAT(3H $ ,15X,3(OPF4.1,2X,1PE10.3,3X))
READ TAPE 4, NTIMES
IF(NTIMES)106,106,105
105 CALL INQUIR
IF(SENSE SWITCH 1)108,109
108 POLY(2)=0.0
C THIS SECTION PRINTS THE EXTRA DATA USED FOR TESTING PURPOSES
109 DO 50 M=1,7
IF(NTIMES-3)61,61,73
61 IF(M-2)71,72,71
71 IF(M-5)73,72,72
72 IF(POLY(2))50,50,110
110 DO 63 K=1,2
63 READ INPUT TAPE 5,64
64 FORMAT(80X)
GO TO 50
73 READ TAPE 4,XMIN,XMAX,YMIN,YMAX,[SCALE,JSCALE,NPTS,NPLOTS,NCOPY,NC
1ARDS
READ TAPE 4,X,Y
GO TO (80,24,38,81,40,96,99),M
80 WRITE OUTPUT TAPE 6,90
90 FORMAT(1H1,30X73HTOTAL FLUX DISTRIBUTION IN THE CORE AS A FUNCTION
1 OF THE RADIAL DIMENSION///)
WRITE OUTPUT TAPE 6,22
22 FORMAT(15X1HR,16X6HPHI(K)//)
DO 23 K=1,NPTS
23 WRITE OUTPUT TAPE 6,28,X(K),Y(K)
GO TO 74
24 WRITE OUTPUT TAPE 6,91
91 FORMAT(1H1,26X78HTOTAL FLUX DISTRIBUTION IN THE REFLECTOR AS A FUN
1CTION OF THE RADIAL DIMENSION///)
WRITE OUTPUT TAPE 6,22
DO 36 K=1,NPTS
36 WRITE OUTPUT TAPE 6,28,X(K),Y(K)
GO TO 74
38 WRITE OUTPUT TAPE 6,92
92 FORMAT(1H1,37X56HANGULAR FLUX AT THE VACUUM INTERFACE AS A FUNCTIO
1N OF MU///)
WRITE OUTPUT TAPE 6,25
25 FORMAT(13X2HMU,12X14HPHI(ROUTER,MU)//)
DO 26 K=1,NPTS
26 WRITE OUTPUT TAPE 6,28,X(K),Y(K)
28 FORMAT(11XOPF6.3,12X1PE10.3)

```

```

      GC TO 74
81 00 34 K=1,NP1
34 IP(K)=K-1
      WRITE OUTPUT TAPE 6,93
93 FORMAT(1H1,30X69HINDIVIDUOAL SPATIAL MOMENT OISTRIBUTION IN THE COR
      IE AS A FUNCTION OF R///)
95 WRITE OUTPUT TAPE 6,33,(IP(K),K=1,NP1)
33 FORMAT(7X6HR ,L =,1X,11(13,8X)///)
      NPERGP=NPTS/NPLUTS
      00 31 K=1,NPERGP
      00 30 L=1,NP1
      NSUB=K+(L-1)*NPERGP
30 YP(L)=Y(NSUB)
31 WRITE OUTPUT TAPE 6,32,X(K),(YP(L),L=1,NP1)
32 FORMAT(5X,F5.2,11(1X1PE10.3))
      GO TO 74
40 WRITE OUTPUT TAPE 6,94
94 FORMAT(1H1,29X74HINDIVIDUOAL SPATIAL MOMENT OISTRIBUTION IN THE REF
      LECTOR AS A FUNCTION OF R///)
      GO TU 95
96 WRITE OUTPUT TAPE 6,97
97 FORMAT(1H1,30X72HANGULAR FLUX OISTRIBUTION AT THE INTERFACIAL BOUN
      LOARY FROM THE CORE SIDE///)
101 WRITE OUTPUT TAPE 6,41
41 FORMAT(13X2HMU,15X9HPHI(R,MU)///)
      DO 111 K=1,NPTS
111 WRITE OUTPUT TAPE 6,28,X(K),Y(K)
      GO TO 74
99 WRITE OUTPUT TAPE 6,100
100 FORMAT(1H1,28X77HANGULAR FLUX OISTRIBUTION AT THE INTERFACIAL BOUN
      LOARY FROM THE REFLECTOR SIOE///)
      GO TU 101
74 IF(POLY(2))107,50,107
C   THIS SECTION PRINTS THE GRAPHS IF THEY ARE CALLED FOR
107 CALL PLOT(X,Y,XMIN,XMAX,YMIN,YMAX,ISCALE,JSCALE,NPTS,NPLOTS,NCOPY,
      INCARDS)
50 CONTINUE
106 RETURN
      ENO

```

BOP PLOT 14

```

C   THIS SUBPROGRAM PLOTS THE GRAPHS
      SUBROUTINE PLOT(X,Y,XMIN,XMAX,YMIN,YMAX,LX,LY,NPT,NPLOT,NCOPY,NCO)
      DIMENSION X(1),Y(1),SX(10),TITLE(8),TAB(4),L(135),NCH(10),MOP(30)
      NCO=NCO+1
      GOTQ(1,80,82,80),NCO
80 READ INPUT TAPES,81,(TITLE(IT),IT=1,8)
81 FORMAT(8A10)
      IF(4-NCO)1,82,1
82 READ INPUT TAPES,83,(MOP(I),(=1,30),(NCH(I),I=1,10),(TAB(I),I=1,4),
      INO,NP,NM,NB)
83 FORMAT(40A1,4A9,4A1)

```

```
1 Q= 2.302585
  IF(NPLOT-1)2,2,3
2 NPN=NPT
  GO TO 4
3 NPN=NPT/NPLOT
4 IF(LX)5,5,7
5 CX=120./(XMAX-XMIN)
  SX(1)=XMIN
  SX(6)=XMAX
  Z=XMIN
  DO6K=2,5
  Z=(XMAX-XMIN)/5.+Z
6 SX(K)=Z
  GO TO 11
7 CX=120/LX
  NX=(LOG(XMIN))/Q
  LLX=LX+1
  DO10K=1,LLX
10 SX(K)=10.**(NX+K-1)
11 IF(LY)12,12,13
12 CY=50./(YMAX-YMIN)
  GO TO 16
13 CY=50/LY
  KY=CY
  NY=(LOG(YMIN))/Q
16 IF(LX)17,17,21
17 DO20I=1,NPT
  IF(XMIN)18,19,19
18 M=CX*X(I)+.5-CX*XMIN
  GOTU20
19 M=CX*X(I)+.5
20 X(I)=M
  GOTU23
21 DO22I=1,NPT
  M=CX*(LOG(X(I)/XMIN)/Q)+.5
22 X(I)=M
23 IF(LY)24,24,28
24 DO27I=1,NPT
  IF(YMIN)25,26,26
25 M=CY*Y(I)+.5-CY*YMIN
  GO TO 27
26 M=CY*Y(I)+.5
27 Y(I)=M
  GO TO 30
28 DO 29I=1,NPT
  M=CY*(LOG(Y(I)/YMIN)/Q)+.5
29 Y(I)=M
30 DO 79 NN=1,NCOPY
  M1=1
  T1=40.
  LYY=LY
  TT=50.
```

```
WRITEOUTPUTTAPE6,31,(TITLE(IT),IT=1,8)
31 FORMAT(1H126X8A10)
DC61 KK=1,51
N=1
NNN=NPN
JED=1
T=51-KK
0032J=1,132
32 L(J)=NB
L(132)=NO
L(12)=ND
IF(LY)33,33,38
33 L(12)=NP
IF(T-TT)34,34,40
34 SCALE=T/CY
L(132)=NP
IF(YMIN)35,36,36
35 SCALE=T/CY+YMIN
36 N=0
TT=TT-5.
IF(T)37,37,40
37 SCALE=YMIN
GOTO40
38 SS=KY*LYY
IF(T-SS)39,39,40
39 SCALE=10.**(NY+LYY)
N=0
LYY=LYY-1
L(12)=NP
L(132)=NP
40 IF(50.-T)43,44,43
43 IF(T)50,44,50
44 OC45J=13,132
45 L(J)=NM
IF(LX)46,46,48
46 DO47J=12,132,12
47 L(J)=NP
IF(50.-T)50,41,50
41 L(132)=NO
GOTO50
48 KX=120/LX
OO 49 J=12,132,KX
49 L(J)=NP
IF(50.-T)50,42,50
42 L(132)=NO
50 O053LM=1,NPLOT
OG52I=JED,NNN
IF(Y(I)-T)52,51,52
51 J=X(I)+12.
IF(J-12)52,85,84
84 IF(J-132)85,85,52
85 L(J)=NCH(LM)
```

```

52 CONTINUE
   JED=NNN+1
   NNN=NNN+NPN
53 CCNTINUE
   IF(T1-T)56,54,56
54 IF(10.-T)55,56,56
55 L(2)=MOP(M1)
   M1=M1+1
   T1=T1-1.
56 IF(N)57,57,59
57 WRITEOUTPUTTAPE6,58,L(2),SCALE,(L(J),J=11,132)
58 FORMAT(1H A1,E8.2,122A1)
   GOTU61
59 WRITEOUTPUTTAPE6,60,(L(J),J=1,132)
60 FORMAT(132A1)
61 CCNTINUE
   IF(LX)64,62,64
62 WRITEOUTPUTTAPE6,63,(SX(K),K=1,6)
63 FCRMAT(7XE9.3,15XE9.3,15XC9.?,15XE9.3,15XE9.3,11XE9.3)
   GO TU 77
64 GO TO (65,67,69,71,73,75),LX
65 WRITE OUTPUTTAPE6,66,(SX(K),K=1,LLX)
66 FORMAT(7XE9.3,107XE9.3)
   GO TO 77
67 WRITE OUTPUTTAPE6,68,(SX(K),K=1,LLX)
68 FORMAT(7XE9.3,52XC9.3,46XC9.?)
   GO TO 77
69 WRITE OUTPUTTAPE6,70,(SX(K),K=1,LLX)
70 FORMAT(7XE9.3,31XC9.3,31XE9.?,27XE9.3)
   GO TO 77
71 WRITE OUTPUTTAPE6,72,(SX(K),K=1,LLX)
72 FORMAT(7XE9.3,21XE9.3,21XE9.?,21XC9.3,17XE9.3)
   GO TO 77
73 WRITE OUTPUTTAPE6,74,(SX(K),K=1,LLX)
74 FORMAT(7XE9.3,15XC9.3,15XC9.?,15XE9.3,15XE9.3,11XE9.3)
   GO TU 77
75 WRITE OUTPUTTAPE6,76,(SX(K),K=1,LLX)
76 FORMAT(7XE9.3,11XE9.3,11XC9.?,11XC9.3,11XE9.3,11XE9.3,7XE9.3)
77 WRITEOUTPUTTAPE6,78,(TAB()),I=1,4)
78 FCRMAT(48X4A9)
79 CONTINUE
   RETURN
   END

```

THE SPHERICAL HARMONICS METHOD  
FOR CRITICAL SPHERES

by

JAMES DONALD CALLEN

B. S., Kansas State University, 1962

---

AN ABSTRACT OF  
A MASTER'S THESIS

submitted in partial fulfillment of the

requirements for the degree

MASTER OF SCIENCE

Department of Nuclear Engineering

KANSAS STATE UNIVERSITY  
Manhattan, Kansas

1964

## ABSTRACT

A study was made of the convergence of the spherical harmonics approximations of both even and odd orders to the monoenergetic Boltzmann neutron transport equation for a nuclear reactor. The theory and computer programs required for determining the critical radii of bare and reflected spherical reactors were developed. Considerable care was taken in the development of the theory for the even order approximations in order to obtain consistent results. Four types of boundary conditions were employed at the vacuum interface of the reactor system, namely: Marshak's, Mark's, replacement of the vacuum with an infinite black medium, and a set of boundary conditions derived from a variational formulation of the Boltzmann equation.

The nature of the convergence of the spherical harmonics approximations for a bare spherical reactor was found to be dependent on the boundary conditions applied. The critical radii which resulted from using Marshak's boundary conditions converged asymptotically from above along separate paths for the even and odd order approximations. For Mark's and the infinite black reflector boundary conditions the even order approximations converged asymptotically from below while the odd order approximations converged asymptotically from above, i.e., they counterconverged to the exact result. No conclusions could be drawn concerning the nature of the convergence when variational boundary conditions were employed. Whenever one or more of three special conditions were satisfied in a given reflected reactor system, the computed critical radii were found to counterconverge to the exact result. The odd order approximations were found to be superior to the even order approximations for all but the lowest orders of approximations. The  $P_2$  approximation almost always yielded results better than those given by a  $P_1$  approximation.

When the critical radii resulting from the spherical harmonics approximations were found to counterconverge to the exact result a particular weighted average of the even and odd order results was computed. This weighted average was found to yield a considerably more accurate estimate of the critical radius than either of the individual results when approximations of order three or greater were utilized. The odd order approximations using variational boundary conditions were found to yield the best results for a given order of approximation. Although many more cases need to be examined, the results obtained here strongly indicate that the even order approximations are of considerable value.